JOURNAL OF THE

Electrochemical Society

l. 104, No. 11 November 1957

ELECTRODE GLC DIVISION

GREAT LAKES CARBON CORPORATION

18 EAST 48TH STREET, NEW YORK 17, N.Y. · OFFICES IN PRINCIPAL CITIES

Journal of the
Electrochemical Society

NOVEMBER 1957 **VOL. 104 • NO. 11**

CONTENTS

Published monthly by The Electrochemical Society, Inc., from Manchester, N. H., **Executive Offices, Editorial Office** and **Circulation Dept.** at 1860 Broadway, New York 23, N. Y., **Advertising Office** at 545 Fifth Ave., New York, N. Y., combining the JOURNAL and TRANSACTIONS OF THE ELECTROCHEMICAL SOCIETY. Statements and opinions given in articles and papers in the JOURNAL OF THE ELECTROCHEMICAL SOCIETY are those of the contributors, and The Electrochemical Society assumes no responsibility for them. Nondeductible subscription to members $5.00; subscription to nonmembers $18.00. Single copies $1.25 to members, $1.75 to nonmembers. Copyright 1957 by The Electrochemical Society, Inc. Entered as second-class matter at the Post Office at Manchester, N. H., under the act of August 24, 1912.

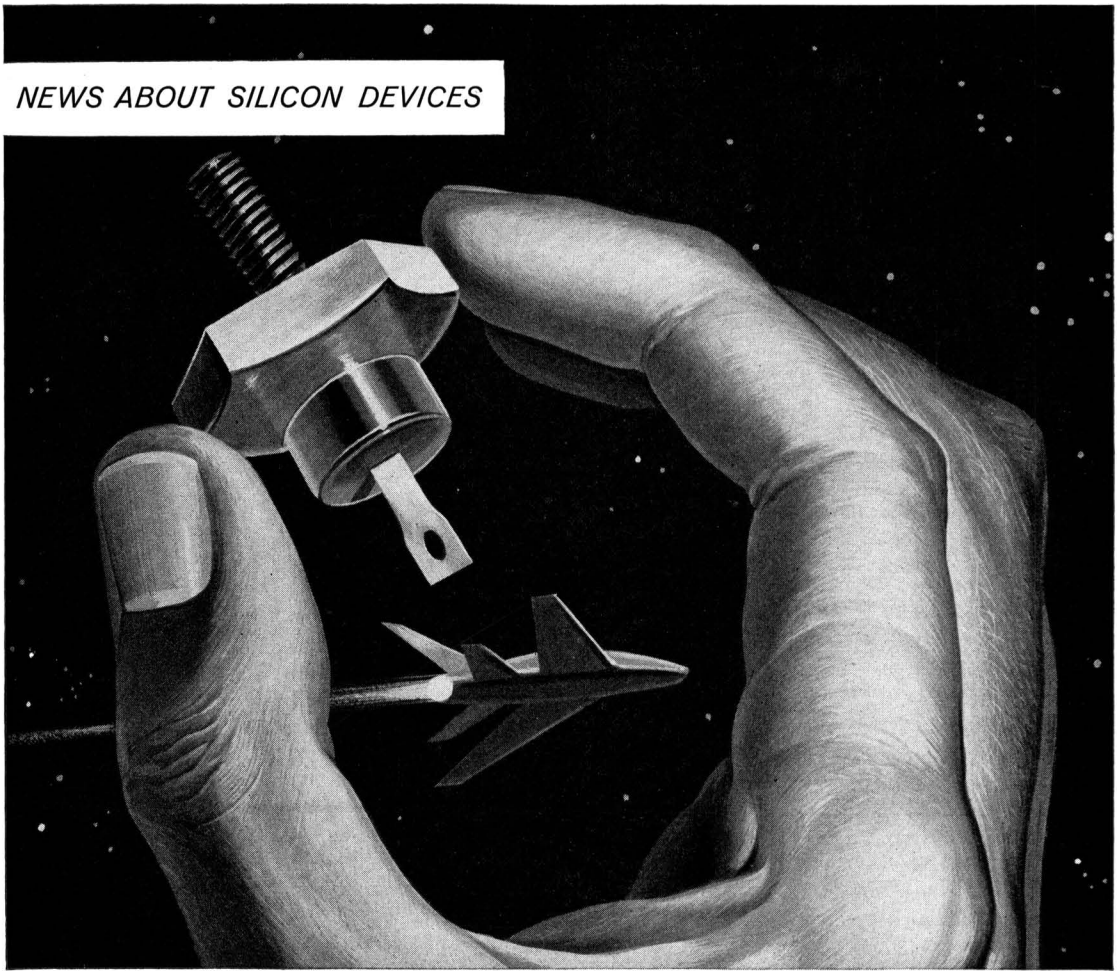

SILICON RECTIFIERS are finding increasing use at elevated temperatures in aircraft and missile applications by providing more power per pound.

Now... design improvements made possible with components of Du Pont Hyperpure Silicon

Today silicon rectifiers make possible a vast improvement in jet-age aircraft generators—the use of engine oil as a coolant instead of less-efficient ram air. Silicon rectifiers take the place of oil-sensitive brushes, commutator and slip rings . . . are completely unaffected by 150°C. engine oil. Result: a *brushless* generator of less weight and size than ordinary generators.

Silicon devices can similarly help you miniaturize—improve design and performance. Silicon rectifiers have excellent stability . . . can operate continuously at —65 to 200°C. They're up to 99% efficient—reverse leakages are only a fraction of those of other semiconductors. Both transistors and rectifiers of silicon can pack *more* capacity into *less* of your equipment space.

Note to device manufacturers:
You can produce high-quality silicon transistors and rectifiers with Du Pont Hyperpure Silicon now available in three grades for maximum efficiency and ease of use... purity range of 3 to 11 atoms of boron per billion... available in 3 forms, needles, densified, cut-rod. Technical information is available on crystal growing from Du Pont... pioneer producer of semiconductor-grade silicon.

NEW BOOKLET ON DU PONT HYPERPURE SILICON
You'll find our new, illustrated booklet about Hyperpure Silicon helpful and interesting—it describes the manufacture, properties and uses of Du Pont Hyperpure Silicon. Just drop us a card for your copy. E. I. du Pont de Nemours & Co. (Inc.), Silicon N-2496-JE-11, Wilmington 98, Delaware.

PIGMENTS DEPARTMENT

DU PONT
REG. U. S. PAT. OFF.

BETTER THINGS FOR BETTER LIVING
...*THROUGH CHEMISTRY*

Editorial

Gmelins Handbook

DURING the last few years this JOURNAL has published reviews of several volumes of *Gmelins Handbuch der Anorganischen Chemie,* and has listed other volumes by title. It is difficult to write adequate reviews of such reference works, even for men of much experience in the various fields. Often a glance at the Table of Contents, or the Index, is worth more than a lengthy review. We take this opportunity to tell a little of the ambitious Gmelin project, and of the time, care, and patience which go into the preparation of the volumes.

The first edition was published in 1817 by Leopold Gmelin, who edited the *Handbuch* through five editions until his death in 1852. The current eighth edition was started in 1921 under the auspices of the German Chemical Society. At the end of World War II there was considerable doubt as to whether publication could be continued. Both German and American scientists bent every effort to obtain financial support, and since 1946 the continued preparation has been in the hands of the Gmelin Institute, with subsidies from chemical industry and the West German Government.

Up to 1957 a total of 146 parts of the eighth edition, including the Supplement volumes, with over 35,000 pages, had been published. It is expected to take another 12 to 15 years to complete the eighth edition, with the addition of some 24,000 pages of new material. It has been intended to cover the literature uniformly in each field up to 1950, but this rule is violated in the more rapidly moving fields. In addition, the Gmelin Information Service has been organized to supply literature reviews of later material in any field covered by the Handbook.

A staff of 100 is employed in preparation of the Handbook material, of whom some 40 are scientists and specialists in particular fields. The average yearly output of each scientist is about 60 published pages; this gives an idea of the care which goes into the evaluation and processing of material, and of why the cost is so high. The Institute has not attempted to bring down the price of the volumes to the level of the individual chemist. The latest volumes are listed at: Calcium, 420 pages, $55.68; Zinc, 1025 pages, $138.00; Platinum, 638 pages, $90.00.

Since the Handbook is widely sold and used in the United States, Great Britain, and other English-speaking countries, future volumes are to have headings and indexes in both German and English. This is perhaps a doubtful tribute to the foreign-language training of English-speaking scientists, who would no doubt prefer to have the headings and indexes in German and the text in English. Perhaps some day all scientific literature will be published in a common international, easy-to-learn language. [*See* Editorial, *This Journal* **104,** 215*C* (1957), and *Science,* **126,** 55, 64 (1957)].

—*CVK*

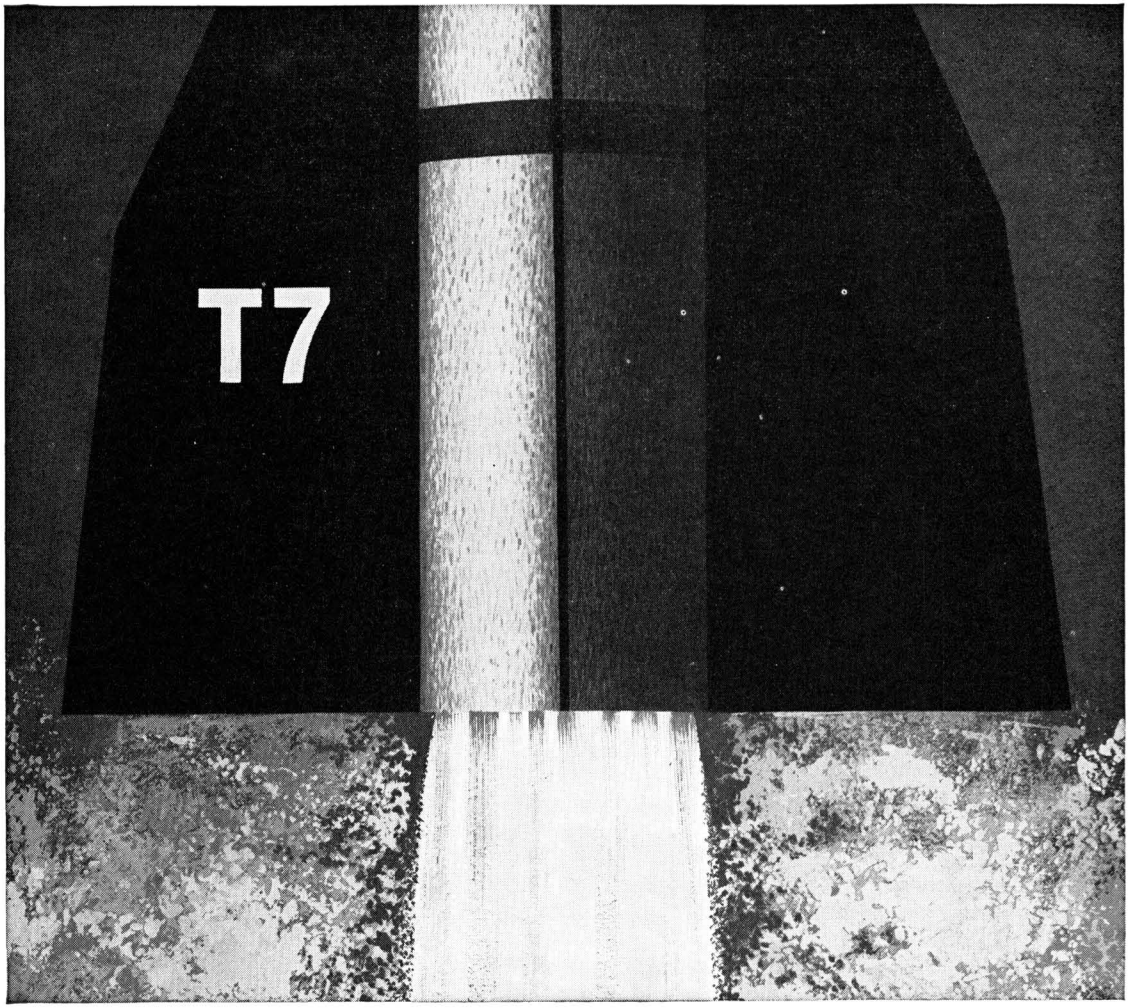

New punch for missile propellants

High heat of reaction, other characteristics point to magnesium for high-energy fuels

Magnesium, in its finely divided form, may well be suitable for new types of rocket fuels. It has long been known that a tremendous amount of chemical energy is locked within the metal. Upon further examination, finely divided magnesium has many significant characteristics that are important to the development of an efficient fuel:

High heat of reaction
Chemically reactive
High energy per unit volume
High theoretical flame temp.
Can be dispersed in various media

Products of combustion are: inert, relatively non-abrasive and present no toxicity problem
Inexhaustible raw material supply

Magnesium's heat of reaction, for example, compares to that of other fuel materials as follows: magnesium, 14,200 B.T.U. per lb. of oxygen required for combustion; aluminum, 13,370; lithium, 10,980; boron, 9,670 (all at 1800°K). This plus magnesium's high theoretical flame temperature indicates that magnesium is especially adaptable for short-range applications where high initial thrust is desirable.

In addition, magnesium can also be considered as an intermediate in the manufacture of other metallic and organometallic fuels.

For information about finely divided magnesium, contact your nearest Dow sales office or write THE DOW CHEMICAL COMPANY, Midland, Michigan, Department MA1438QQ-2.

YOU CAN DEPEND ON DOW

Physicists! Chemists! Electrical Engineers!

Here's a CHECKLIST FOR YOUR FUTURE!

Model 2N174—industry's highest power transistor, product of Delco Radio research and development.

Are you interested in:

- ☐ A progressive research, development and manufacturing program?
- ☐ A good starting salary?
- ☐ An excellent company potential?
- ☐ A top-rated company reputation?
- ☐ Challenging opportunities?
- ☐ Pleasant living for all the family?
- ☐ Regular salary increases?
- ☐ A permanent position?

If you've checked five or more of the above boxes affirmatively, you owe it to yourself to ask about the many opportunities in the expanding semiconductor program at Delco Radio Division of General Motors. Write—Personnel Director, Dept. B or call GLadstone 2-8211.

GM GENERAL MOTORS **DELCO RADIO** DIVISION OF GENERAL MOTORS KOKOMO, INDIANA

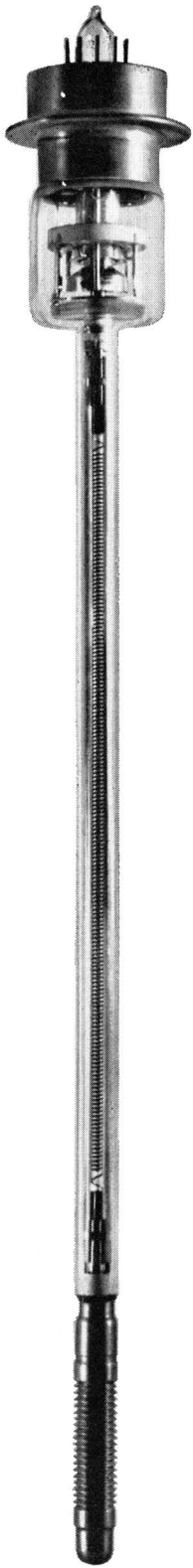

A GREAT AMPLIFIER TUBE IS PERFECTED FOR TELEPHONY

A new transcontinental microwave system capable of carrying four times as much information as any previous microwave system is under development at Bell Laboratories. A master key to this development is a new traveling-wave tube of large frequency bandwidth.

The traveling-wave amplifying principle was discovered in England by Dr. Rudolf Kompfner, who is now at Bell Laboratories; the fundamental theory was largely developed by Labs scientist Dr. John Pierce. Subsequently the tube has been utilized in various ways both here and abroad. At the Laboratories it has been perfected to meet the exacting performance standards of long distance telephony. And now for the first time a traveling-wave tube will go into large-scale production for use in our nation's telephone systems.

The new amplifier's tremendous bandwidth greatly simplifies the practical problem of operating and maintaining microwave communications. For example, in the proposed transcontinental system, as many as 16 different one-way radio channels will be used to transmit a capacity load of more than 11,000 conversations or 12 television programs and 2500 conversations. Formerly it would have been necessary to tune several amplifier tubes to match each channel. In contrast, a single traveling-wave tube can supply all the amplification needed for a channel. Tubes can be interchanged with only very minor adjustments.

The new amplifier is another example of how Bell Laboratories research creates new devices and new systems for telephony.

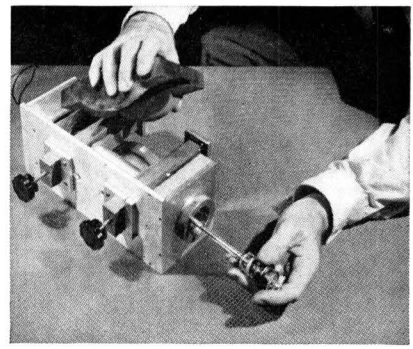

Left: A traveling-wave tube. *Right:* Tube being placed in position between the permanent magnets which focus the electron beam. The tube supplies uniform and distortionless amplification of FM signals over a 500 Mc band. It will be used to deliver an output of five watts.

BELL TELEPHONE LABORATORIES

WORLD CENTER OF COMMUNICATIONS RESEARCH AND DEVELOPMENT

Electrochemical Polarization

III. Further Aspects of the Shape of Polarization Curves

Milton Stern

Metals Research Laboratories, Electro Metallurgical Company,
A Division of Union Carbide Corporation, Niagara Falls, New York

ABSTRACT

The shape of electrochemical polarization curves is discussed for ideal systems containing more than two oxidation-reduction reactions. Situations are described where measured Tafel parameters have no direct relationship to the parameters of any of the oxidation-reduction reactions. The analysis, while containing several simplifying assumptions, shows the complexity of polarization measurements and indicates the care which must be taken if such measurements are to be interpreted quantitatively.

Polarization measurements have been used for many years in studies of corrosion, electrodeposition, and battery performance. In spite of the wide use of such measurements, considerable uncertainty in their interpretation still appears to exist.

Stern and Geary (1) have presented a theoretical analysis of the shape of polarization curves for both reversible electrodes and corroding electrodes and have described some of the reasons for observed deviations from Tafel behavior. They warned against the indiscriminate introduction of breaks in polarization measurements and listed several of the pitfalls which exist in the interpretation of such measurements. Experimental verification of the equations which they presented has been obtained (2). The methods described have proved useful in studies of pit propagation in stainless steels (3) and anodic polarization of iron (4).

This discussion is an extension of the analysis by Stern and Geary which describes more complex systems including those where three oxidation-reduction reactions are operative. Some examples are presented where concentration polarization plays a role in determining the steady-state electrode potential.

Basic Principle of the Method

The method which Stern and Geary (1) describe is based on the principle that the steady-state potential of an electrode is that potential at which the sum of the rates of all the oxidation reactions is equal to the sum of the rates of all the reduction reactions. This value of potential may be called the corrosion potential or the mixed potential and occurs when

$$\Sigma\ \overleftarrow{i_m},\ \overleftarrow{i_y},\ \overleftarrow{i_z} \ldots = \Sigma\ \vec{i}_m,\ \vec{i}_y,\ \vec{i}_z \ldots \qquad \text{(I)}$$

where $\overleftarrow{i_m}$, $\overleftarrow{i_y}$, $\overleftarrow{i_z}$ are the currents equivalent to the rates of oxidation of the M, Y, and Z oxidation-reduction systems, and $\vec{i}_m$, $\vec{i}_y$, and $\vec{i}_z$ are the currents equivalent to the rates of reduction for these systems. When current is applied from an external source, the applied current, $\vec{i}_z$, (cathodic current) is equal to the difference between the current equivalent to the total rate of all the reduction reactions and the current equivalent to the total rate of all the oxidation reactions.

$$\vec{i}_z = \Sigma\ \vec{i}_m,\ \vec{i}_y,\ \vec{i}_z \ldots - \Sigma\ \overleftarrow{i_m},\ \overleftarrow{i_y},\ \overleftarrow{i_z} \ldots \qquad \text{(II)}$$

Since a similar expression exists for anodic polarization, only cathodic polarization is discussed here. If equations are available which describe the relationships between potential and the individual oxidation and reduction currents, then an expression can be derived which describes the variation of the potential of a system as a function of applied current.

System with Two Oxidation-Reduction Reactions

Consider a system with two possible oxidation-reduction reactions Z and M, the rates of which are controlled by activation polarization so that at the reversible potential of the Z reaction the equilibrium $Z^+ + e \rightleftarrows Z$ exists, while at the reversible potential of the M reaction the equilibrium $M^+ + e \rightleftarrows M$ occurs. At equilibrium, the rate of the individual oxidation and reduction reactions is equal so that $\vec{i}_z = \overleftarrow{i_z} = i_{oz}$ and $\vec{i}_m = \overleftarrow{i_m} = i_{om}$ where i_{oz} and i_{om} are the exchange currents for the Z and M reaction, respectively. The current equivalent to the total rate of each of the individual oxidation or reduction reactions may be expressed in the following form (5), using $\vec{i}_z$ as an example.

$$\eta = -\beta_z \log \frac{\vec{i}_z}{i_{oz}} \qquad \text{(III)}$$

where β_z is a constant (the Tafel slope) and η is the overvoltage or the difference between the potential of an electrode at which z is being reduced and the equilibrium potential. Similar equations exist for the dependence of $\overleftarrow{i_z}$, $\overleftarrow{i_m}$, and $\vec{i}_m$ on potential. To aid in visualizing the shape of an experimental polar-

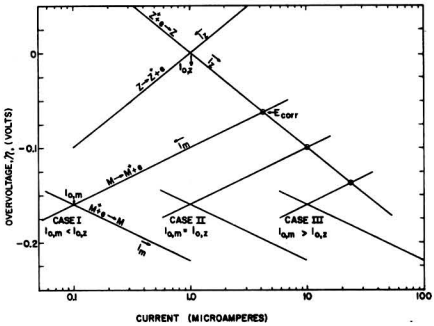

Fig. 1. Electrochemical system with two oxidation-reduction reactions. Illustration of Cases I, II, and III.

ization curve resulting from such a mixed electrode system, it is convenient to assign values to the Tafel constants for each oxidation-reduction system in order to show the effect of changes in these parameters. To express potentials of the various oxidation-reduction systems on the same scale, the equilibrium potential of the Z oxidation-reduction system will be used as a reference, and the equilibrium potential of the M oxidation-reduction system will be given a value of 0.160 v more active than the reversible potential of the Z oxidation-reduction potential.

Three cases will be considered: Case I where i_{om} is smaller than i_{oz}, Case II where i_{om} equals i_{oz}, and Case III where i_{om} is greater than i_{oz}. The following parameters will be held constant at their indicated values ($\beta_z = 0.100$ v, $\beta_m = 0.060$ v, $i_{oz} = 1.0$ μa) and i_{om} will be assigned values of 0.1 μa for Case I, 1.0 μa for Case II, and 10 μa for Case III. Fig. 1 illustrates the three cases described, the circles indicating the mixed or corrosion potential in each case. This is the potential at which $\vec{i}_z + \vec{i}_m = \overleftarrow{i}_z + \overleftarrow{i}_m$.

Case I.—This situation has already been described quantitatively using the same polarization parameters used here (1). The overvoltage as a function of applied cathodic current, $\vec{i}_z$, may be expressed by the following equation.

$$\eta = -\beta_z \log \frac{\vec{i}_z + \overleftarrow{i}_z + \overleftarrow{i}_m - \vec{i}_m}{i_{oz}} \qquad \text{(IV)}$$

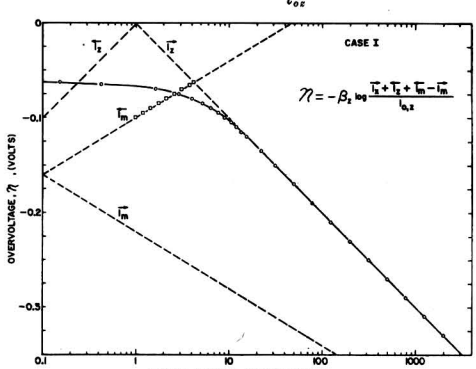

Fig. 2. Overvoltage as a function of applied cathodic current for Case I ($i_{om} < i_{oz}$) showing region where anodic curve can be calculated from cathodic data.

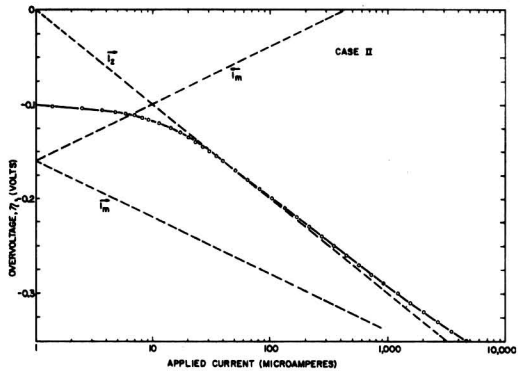

Fig. 3. Overvoltage as a function of applied cathodic current for Case II ($i_{om} = i_{oz}$).

This is derived by substituting Eq. (II) into Eq. (III). A plot of η vs. $\vec{i}_z$ yields a curve which shows deviation from Tafel behavior at low values of $\vec{i}_z$. At higher values of applied current, $\vec{i}_z$ approaches $\vec{i}_z$ and the resulting curve shows Tafel behavior with a β value equal to β_z and an extrapolated exchange current value equal to i_{oz}.

Under these conditions, it is possible to obtain experimental values for the Tafel constants of the Z reaction. It is important to note that a determination of β_z and i_{oz} permits calculation of $\overleftarrow{i}_m$ as a function of potential in the region close to the corrosion potential.[1] This is a measure of the local anodic polarization in a corroding system. Thus, cathodic polarization measurements under conditions indicated in Case I permit a determination of the local anodic polarization curve of the system in the potential region more active than the steady-state potential. This is illustrated in Fig. 2[2] which shows the expected shape of a cathodic polarization curve for the conditions defined in Case I. The region where Eq. (IV) can be used to calculate the local anodic polarization curve is also shown on Fig. 2.

Case II.—When i_{om} is increased so that polarized potentials are reached where $\vec{i}_m$ is significant in comparison to $\vec{i}_z$, the resulting measured polarization curve will not exhibit true Tafel behavior. This situation is illustrated in Fig. 3. Note that the curve of overvoltage vs. applied current follows $\vec{i}_z$ for a short potential interval but then deviates from straight line behavior. Experimental observations under conditions of Case II would yield data suffi-

[1] This calculation is possible since an experimental determination of η vs. $\vec{i}_z$ yields values for β_z and i_{oz}. From these constants $\vec{i}_z$ is known as a function of η. If the corrosion potential is sufficiently removed from the reversible potentials, the rate of metal plating, $\vec{i}_m$, and the rate of oxidation, $\overleftarrow{i}_z$, are negligible. Thus sufficient information is available to apply Eq. (IV) to calculate $\overleftarrow{i}_m$ as a function of η.

[2] Points shown on this curve and all subsequent figures are not experimental. They are calculated from the derived equations and are included to illustrate the need for considerable data to define accurately the shape of a polarization curve.

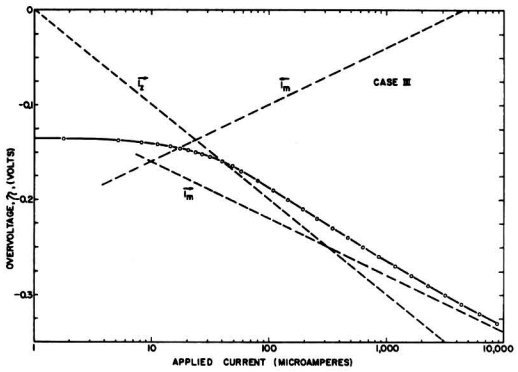

Fig. 4. Overvoltage as a function of applied cathodic current for Case III ($i_{om} > i_{ox}$).

ciently "Tafel-like" in behavior to generally be considered satisfactory. However, such data would yield inaccurate values for β_z and i_{oz}, both measured values being slightly low.

Case III.—When i_{om} is considerably larger than i_{oz}, the resulting curve of overvoltage vs. applied current shows some interesting characteristics. Fig. 4 shows that a "Tafel-like" region is still observed but Tafel constants determined from such data are completely inaccurate and have no direct connection with the Tafel constants of either oxidation-reduction system. Thus, cathodic polarization measurements alone do not permit direct measurement of β_z and i_{oz} under the conditions of Case III. However, three methods are available which yield values for these constants, but the techniques are more tedious and inaccurate than the direct method of measurement illustrated in Case I.

One may measure by chemical means the rate at which Z^+ is reduced at various potentials during cathodic polarization. For example, if reduction of Z^+ represents the rate at which hydrogen ions are reduced to form hydrogen gas, then measurement of the rate of hydrogen evolution as a function of overvoltage during cathodic polarization will yield data from which the Tafel constants can be calculated. The second method is also indirect. Under the conditions stipulated for Case III, anodic polarization measurements yield accurate values for β_m and i_{om}. These data can then be used in the anodic polarization analog to Eq. (IV) to calculate $\vec{i}_z$ as a function of overvoltage on the noble side of the corrosion potential. This is the reverse of what was done in Fig. 2 to calculate the local anodic polarization curve from cathodic polarization data.

The third method is based on polarization measurements at potentials close to the corrosion potential. It has been shown that such data show a linear dependence of overvoltage on applied current (1). The equation which relates the change in potential with applied current is

$$\left(\frac{d\epsilon}{di_x}\right)_{\epsilon \to 0} = \frac{\beta_z \beta_m}{(2.3)(i_{corr})(\beta_m + \beta_z)} \qquad (V)$$

where e is the difference between the polarized potential and the corrosion potential. Note that i_{corr} is

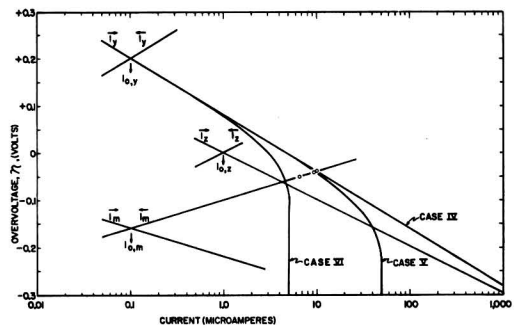

Fig. 5. Electrochemical system with three oxidation-reduction reactions. Illustration of Cases IV, V, and VI.

equivalent to $\overleftarrow{i}_m$ at the corrosion potential. The slope of the linear region, $d\epsilon/di_x$, is the same for both cathodic and anodic polarization. Thus, an anodic polarization measurement yields values for $d\epsilon/di_x$, β_m, and i_{corr}, and permits calculation of β_z using Eq. (V). The second and third methods described above have been used (4) to show that the anodic polarization curve for Fe in HCl is not remarkably steep as was postulated previously (6) from indirect observations.

System with Three Oxidation-Reduction Reactions

The method described above for determining potential as a function of applied current can be used also for a system with three redox reactions. Three examples will be shown for a system containing redox reactions M, Z, and Y where the Tafel parameters of all three are held constant and a limiting diffusion current for reduction of Y is introduced. The constants assigned for this situation are $\beta_m = 0.060$ v, $\beta_z = 0.100$ v, $\beta_y = 0.120$ v, $i_{om} = 0.1$ μa, $i_{oz} = 1.0$ μa, $i_{oy} = 0.1$ μa with the reversible potential of the M redox system more active by 0.160 v and the reversible potential of the Y redox system more noble by 0.200 v than the reversible potential of the Z redox system. The three situations to be considered for this system differ by introducing a limiting diffusion current for reduction of Y with values of $I_{L,y}$ equal to infinity (Case IV), 50 μa (Case V), and 5 μa (Case VI).

Cases IV, V, and VI are illustrated graphically in Fig. 5. The circles indicate the corrosion potential and corrosion current for each set of conditions.

It is worth emphasizing here that Eq. (II) is used in conjunction with the Tafel constants assigned to each redox reaction to determine the relationship between overvoltage and applied current. Thus,

$$\vec{i}_x = \vec{i}_z + \vec{i}_y + \vec{i}_m - \overleftarrow{i}_z - \overleftarrow{i}_y - \overleftarrow{i}_m \qquad (VI)$$

Since the current equivalent to each of the individual oxidation or reduction reactions is known as a function of potential from the Tafel equation [Eq. (III)], $\vec{i}_x$ may be calculated as a function of potential.

For the cases where a limiting diffusion current exists, the value of $\vec{i}_y$ at any overvoltage value is determined from the relation

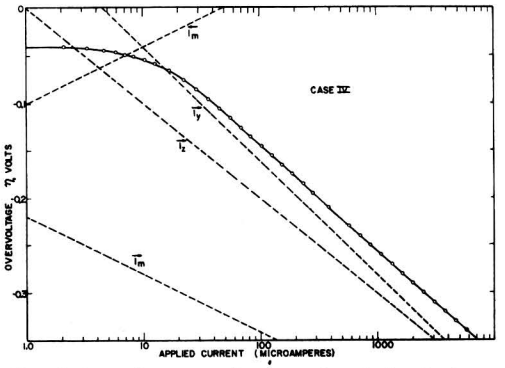

Fig. 6. Overvoltage as a function of applied cathodic current for Case IV.

$$\eta = 0.200 - \beta_y \log \frac{\vec{i}_y}{i_{oy}} + 0.059 \log \frac{I_{Ly} - \vec{i}_y}{I_{Ly}} \qquad \text{(VII)}$$

Case IV.—Potential as a function of applied current for Case IV is shown in Fig. 6. Here as in Case III, a "Tafel-like" relation is observed but β calculated from such a curve is a compromise between β_z and β_y. The exchange current obtained from such data would be markedly different from the real value of i_{oy}.

Case V.—When I_{Ly} equals 50 μa, the plot of potential vs. applied current (Fig. 7) does not show any recognizable diffusion wave. Instead two Tafel-like regions are observed. The first region, from −0.08 to −0.22 v, does not even approximate the Tafel parameters of any of the redox systems. The second Tafel-like region does, however, closely parallel the Tafel parameters of the *X* redox system.

Case VI.—An interesting situation arises when I_{Ly} equals 5 μa. Under these conditions, the mixed or corrosion potential does not approximate the intersection of any of the individual Tafel lines. The corrosion potential is determined by the condition set by Eq. (I) or when

$$\vec{i}_m + \vec{i}_z + \vec{i}_y = \overleftarrow{i}_m + \overleftarrow{i}_z + \overleftarrow{i}_y \qquad \text{(VIII)}$$

In the potential region of interest, $\vec{i}_m$, $\overleftarrow{i}_z$, and $\overleftarrow{i}_y$ are negligible so that $\vec{i}_z + \vec{i}_y = \overleftarrow{i}_m$ at the mixed potential.

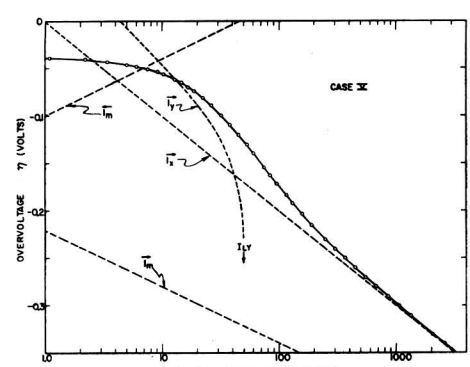

Fig. 7. Overvoltage as a function of applied cathodic current for Case V.

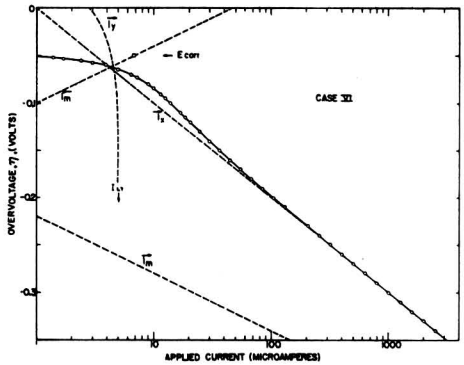

Fig. 8. Overvoltage as a function of applied cathodic current for Case VI.

In the examples illustrated previously, $\vec{i}_z$ was also negligible at the mixed potential so that this potential was approximated by the condition where $\vec{i}_y = \overleftarrow{i}_m$. This is the potential at which the overvoltage curves for $\vec{i}_y$ and $\overleftarrow{i}_m$ cross. Case VI also shows two Tafel-like regions, one of which is false and the other of which will yield valid parameters for the *Z* redox system.

It is interesting to note that no indication of a limiting diffusion current is obtained in Fig. 7 and 8. A limiting diffusion current will be evident, however, on a plot of overvoltage vs. applied current if I_{Ly} is increased further or if the reversible potential of the Y redox system is made more noble. This will be illustrated by changing the conditions indicated in Cases IV, V, and VI so that the reversible potential of the Y redox system is 0.45 v more noble than the *Z* redox system, and considering two cases where I_{Ly} equals 1000 μa and 80 μa. Cases VII and VIII are illustrated in Fig. 9, the circles indicating the corrosion potential in each case.

Case VII.—Fig. 10 illustrates the polarization curve which would be obtained for Case VII. No activation overvoltage parameters can be measured, and the curve represents the typical concentration polarization curve often observed.

Case VIII.—Under these conditions, the corrosion rate is determined by the limiting diffusion current,

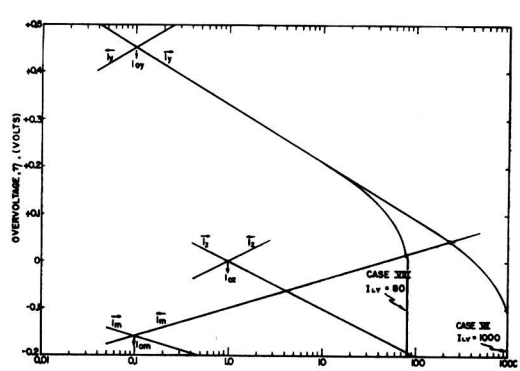

Fig. 9. Electrochemical system with three oxidation-reduction reactions. Illustration of Cases VII and VIII.

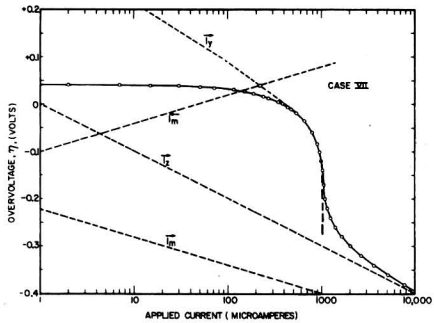

Fig. 10. Overvoltage as a function of applied cathodic current for Case VII.

I_{L_Y}. This was not the situation in Case VII where the corrosion potential occurs in the activation polarization region of the Y reduction system. Thus, physical changes in the system which increase the limiting diffusion current, such as stirring effects, markedly affect the corrosion potential and corrosion rate in Case VIII but have no effect in Case VII except to move the position of the diffusion wave in Fig. 10 further to the right. Fig. 11 shows the polarization curve which is obtained for Case VIII.

Discussion

Even though several simplifying assumptions have been made, this analysis shows the complexity of polarization measurements and indicates the care which must be taken if such measurements are to be interpreted quantitatively. The chemistry of the system must be understood, and the number and magnitude of the rates of oxidation or reduction occurring during polarization should be known.

The primary assumption in this treatment considers that the Tafel parameters remain constant during polarization. This is undoubtedly the case in some real systems, since this is the basis on which all experimental observations of Tafel constants depend. It is important to remember, however, that many situations exist where such an assumption is not valid, certain passivity phenomena being typical. One obvious way to study and recognize systems where the Tafel parameters change is to realize first what the behavior would be if the parameters remain constant and then observe deviations from such behavior.

The treatment does not consider several other complicating factors which influence the shape of polarization curves. Such factors include systems where the electrode surface contains regions with different overvoltage parameters for the same reaction; where anode-cathode area ratios change as a function of potential; and where corrosion product films, which are formed during polarization, change the nature of the surface. Changes in anode-cathode area ratio or film formation appear to give rise to a time effect during polarization which also has not been considered here.

Since it has been shown that ideal systems can produce polarization data which may be difficult to interpret, complicating factors such as those described above would result in a system which is beyond quantitative description with the present knowledge of electrode processes. However, concepts obtained from this treatment of ideal systems provide a guide to an understanding of important practical systems. This can be illustrated in the following manner. Individuals working in the cathodic protection field are constantly concerned with minimum current requirements for complete protection; the potential necessary to achieve protection; and the correlation between "breaks" in polarization curves and the metal equilibrium potential. It has already been shown that "breaks" in polarization curves cannot be expected to have a direct connection to the equilibrium anode potential. If the anodic polarization of metal is activation controlled, the corrosion rate decreases logarithmically as the potential is made more active. Case VIII described above is analogous to the situation which exists when Fe corrodes in sea water under conditions of natural convection. In this case, the corrosion rate of Fe is determined by the limiting diffusion current of oxygen. Iron solution is represented by $\overleftarrow{i_m}$, hydrogen evolution by $\overrightarrow{i_z}$, and oxygen reduction by $\overrightarrow{i_y}$. The per cent change in corrosion rate as a function of potential and applied current for Case VIII is illustrated in Fig. 12. Note the rapid decrease in corrosion rate as the potential is made more cathodic. The rate of decrease of corrosion rate is actually a function of β_m. A larger value of β_m would require that the metal be polarized to a more ca-

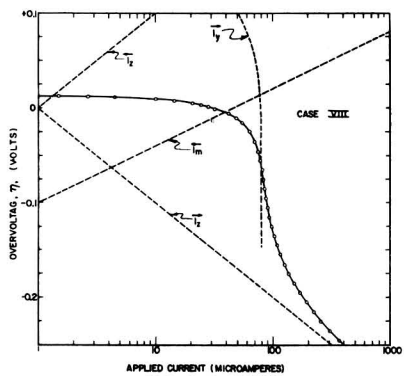

Fig. 11. Overvoltage as a function of applied cathodic current for Case VIII.

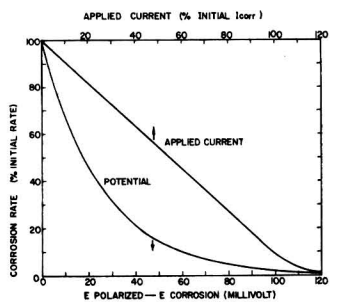

Fig. 12. Per cent change in corrosion rate as a function of potential and applied current for Case VIII.

thodic potential to achieve a corrosion rate of one tenth its steady-state value. It is also interesting to note that the decrease in corrosion rate is directly proportional to the applied cathodic current up to applied current values approximating the initial corrosion current. This situation occurs only for conditions where the corrosion rate is determined by a cathodic limiting diffusion current (Case VIII). This can be shown by considering the general Eq. (II) for these conditions.

$$\vec{i}_x = \vec{i}_y + \vec{i}_z + \vec{i}_m - \overleftarrow{i}_y - \overleftarrow{i}_z - \overleftarrow{i}_m \qquad \text{(IX)}$$

In the potential region of interest, $\vec{i}_z$, $\vec{i}_m$, $\overleftarrow{i}_y$, and $\overleftarrow{i}_z$ can be considered negligible and $\vec{i}_y$ approximates the constant I_{Ly}. Thus, $\vec{i}_x = K - \overleftarrow{i}_m$, and, therefore, the corrosion rate, $\overleftarrow{i}_m$, approximates a linear function of the applied cathodic current, $\vec{i}_x$.

Although this analysis contains calculated polarization curves, an effort was made to select conditions which parallel many found in practice in order to provide a clearer understanding of the effect which many variables have on electrode behavior.

Acknowledgment

The author would like to acknowledge the cooperation of A. L. Geary who carried out several of the calculations used here and supplied valuable discussion.

Manuscript received Dec. 26, 1956. This paper was prepared for delivery before the Buffalo Meeting, Oct. 6-10, 1957.

Any discussion of this paper will appear in a Discussion Section to be published in the June 1958 JOURNAL.

REFERENCES

1. M. Stern and A. L. Geary, *This Journal*, **104**, 56 (1957).
2. M. Stern, *ibid.*, **104**, 559 (1957).
3. M. Stern, *ibid.*, **104**, 600 (1957).
4. M. Stern and R. M. Roth, *ibid.*, **104**, 390 (1957).
5. J. O'M. Bockris, "Modern Aspects of Electrochemistry," Academic Press Inc., New York (1954).
6. M. Stern, *This Journal*, **102**, 609 (1955).

Some Testing Cells for the Study of Electroplating Devices

J. K. Skwirzynski and M. Huttly

Marconi's Wireless Telegraph Company Limited, Baddow Research Laboratories, West Hanningfield Road, Great Baddow, Chelmsford, Essex, England

ABSTRACT

The complete theoretical treatment is given for two kinds of cells, both of which are shown to yield a reasonably linear primary current density distribution along the cathode, calculated under the assumption of negligible polarization. The actual value of these current densities can be ascertained directly from the total current fed into the cell. The first cell is very similar to that proposed by Hull, i.e., trapezoidal in shape, the angle of the slanting side being 45°. The electrodes can be placed either along the parallel sides of the cell or, as first suggested by Hull, along the other two sides, when a singularity of the current density appears on the slanting electrode. In both cases the current density may be arranged to be very nearly linear over almost two thirds of the length of the cathode.

The second cell is triangular in shape; the cathode is placed along the base of a 45° isosceles triangle whereas the anode occupies a part of one of the other sides. The current density distribution along the cathode has almost a triangular shape with good linearity.

Both cells are easy to construct and normalized graphs of the current density allow for straightforward comparison with experimental results.

A plating test designed to detect sources of trouble, such as improper chemical concentrations, impurities, contaminations from the atmosphere, etc., should be designed so as to exhibit simultaneously the results of plating over a range of current densities. Furthermore such a display of the effects of varying and determinable current densities may be used to decide on optimum conditions for the operation of newly formulated baths (1).

A well-known testing device is the Hull cell (2). It consists of a small trapezoidal cell, whose plan view is shown in Fig. 1a and 1b. The parallel sides are insulators, the side, AB, perpendicular to these is the anode, and the fourth side, OC, inclined to the parallel sides is the cathode, on which the deposition is studied. Because of the inclination of the cathode with respect to the anode, the current density on the former varies uniformly and actually reaches a very high value (theoretically an infinity) at the end of the cathode nearest to the anode. The actual Hull cell (2) has fixed dimensions, holding 267 cc; the angle AOC (Fig. 1a and 1b) is about 38°40′.

Recently Gilmont and Walton (3) proposed another cell consisting of two plane walls inclined at 45° and two others shaped as hyperbolae. One of the plane sides is the cathode and one of the curved ones

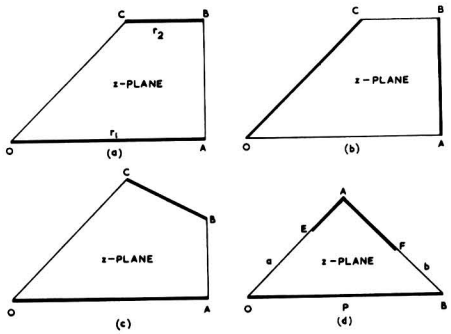

Fig. 1. Plan views of the cells in the z-plane

is the anode. The current density along the cathode is stated to vary linearly with the distance along it and therefore could be calculated exactly. The authors show that the hyperbolic shape of the anode is the necessary condition for a linear variation of the current density.

It would seem that the geometry of an ideal cell should have these properties: (*a*) be easy to construct; (*b*) be equally suitable for large and for small baths; (*c*) yield linear current density along the cathode which can be correlated with the total current fed into the baths; (*d*) have no "infinities" of current which will cause excessive polarization. (This last requirement is not always necessary as occasionally it may be required to observe the effects of very dense currents, e.g., when investigating the deposition on sharp corners.) The Hull and the Gilmont and Walton cells each satisfy some but not all of these requirements.

Thus it is proposed here to investigate a type of a versatile cell which it is hoped would satisfy the points mentioned above. A simple tank should be built of plane walls, typical shapes being shown in Fig. 1 where the electrodes are indicated by thick lines. Assuming uniform electrolyte and infinite extension in the direction perpendicular to the plane of the paper, the tanks shown can only be investigated analytically if the angles between individual walls are multiples of $\pi/6$ or $\pi/4$. Fig. 1a and 1b show two possible electrode positions for a tank of a Hull type. This case is investigated fully below for both electrode configurations; the ratio of the side lengths OA and BC is of course arbitrary, so that the side of the cell can be varied at will. Fig. 1c shows a different configuration whose analysis, although theoretically possible, presents great computational difficulties, e.g., computation of elliptic functions with complex moduli; this case is not considered here. Fig. 1d shows a triangular tank which is considered here for an isosceles case when angles BOA and ABO are both 45°. The second electrode EAF can be either as shown, with sides EA and AF of arbitrary length or it can consist of a single side, say AE. This case is also considered here, in particular when AE = ½AB.

The three cases 1a, b, and d yield almost linear portions of the current density distribution curves. Cases 1a and 1d have no current singularities when OA and OB are respectively cathodes. Case 1b yields a singularity at C on the cathode OC.

The two cases are considered separately, that of the trapezium and the triangle, pointing out only the more important and essential mathematical steps.

1. General Considerations

Assume that the electrolytic conduction in one of the cells shown in Fig. 1 is essentially a two-dimensional one, i.e., that the cell extends infinitely at right angles to its plane cross section shown. In practice, to obtain good agreement with the theoretical predictions, the height of the cell should be at least as big as its lateral dimensions and the investigations should be limited to the medium portion of the plated electrode [*see* Ref. (2), Fig. 3]. Assuming further that the electrolyte is homogeneous, obeys Ohm's Law, that the electrodes are at the same potential throughout this area, and that the polarization, if any, is the same over the electrode surface [*see* Ref. (3)], the current density on an electrode is given by:

$$\tilde{C} = \kappa \left.\frac{\partial V}{\partial n}\right|_s \qquad [1]$$

where n denotes direction normal to the electrode in question and the suffix s denotes the co-ordinates of that electrode in the two-dimensional representation in the complex $z = x + iy$ plane (Fig. 1a). Then $V = V(x,y)$ can be considered as the imaginary part of the complex function

$$w = U + iV = f(z) = f(x + iy) \qquad [2]$$

and

$$\tilde{C} = \kappa \left|\frac{\partial w}{\partial z}\right| \qquad [3]$$

anywhere in the complex z-plane (4).

In order to find the function w for the particular cell in Fig. 1 the z-plane is transformed conformally until the inside of the cell assumes the shape of a rectangle with two electrodes forming the two opposite sides of this rectangle (Fig. 2b) in the new w-plane. Then obviously w is the required function since the lines of current flow and the equipotentials now form the usual cartesian grid. The suitable transformation in this case, or several of them if necessary, is the well-known Schwarz-Christoffel transformation.

2. The Trapezoidal Cell Mathematical Analysis

Consider a trapezium OABC in the complex z-plane as shown in Fig. 1a, whose parallel sides are r_1 and r_2, respectively; the angle AOC is 45°; then:

$$z = \int_0^u \frac{du}{\sqrt{u(1-u^2)(1-k^2u^2)}} \qquad [4]$$

transforms the inside of the trapezium in the z-plane to the first quadrant of the u-plane (Fig. 2a), the corresponding points being

$$\begin{aligned} &O: z = 0 \rightarrow u = 0 \\ &A: z = r_1 \rightarrow u = 1 \\ &B: z = r_1 + i(r_1 - r_2) \rightarrow u = 1/k \\ &C: z = (1+i)(r_1 - r_2) \rightarrow u = \infty \text{ and } i\infty \end{aligned}$$

$k < 1$ is as yet an arbitrary real number. The quad-

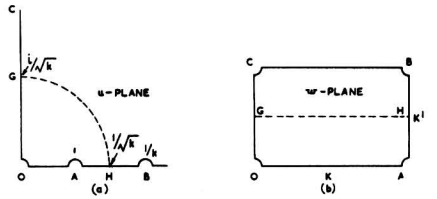

Fig. 2. (a) Trapeziums of Fig. 1a and 1b transformed to the u-plane; (b) the same in the w-plane.

rant in the u-plane can now be transformed to the inside of a rectangle in the w-plane by:

$$u = sn(w,k) \qquad [5]$$

where sn is the Jacobi's elliptic function of modulus k. Then, from [4] and the well-known properties of sn:

$$z = \int_0^w \frac{dw}{\sqrt{sn(w,k)}} \qquad [6]$$

The vertices of the trapezium are now transformed in the w-plane to:

$$\begin{aligned} O &: w = 0 \\ A &: w = K \\ B &: w = K + iK' \\ C &: w = iK' \end{aligned}$$

where K and K' are the complete elliptic integrals of the first kind with complimentary moduli k and $k' = \sqrt{1-k^2}$, respectively. The rectangle in the w-plane is shown in Fig. 2b. From [3] and [6], the current density becomes:

$$\tilde{C} = \kappa \left| \frac{dw}{dz} \right| = \kappa \left| sn(w,k) \right|^{1/2} = \kappa \left| u \right|^{1/2} \qquad [7]$$

One requires the current density in the z-plane, i.e., the plane of the trapezium, and this can be obtained only by expressing u as a function of z, i.e., by inverting the integral expression [4]. The integral [4] can be evaluated by using a substitution given by Cayley (5). Let:

$$\sqrt{u} = \frac{(\lambda + \lambda')\zeta}{\sqrt{1-\lambda^2\zeta^2} + \sqrt{1-\lambda'^2\zeta^2}} \qquad [8]$$

where

$$\lambda = (1 + \sqrt{k})/\sqrt{2(1+k)} \qquad [9]$$

and

$$\lambda' = \sqrt{1-\lambda^2} \qquad [10]$$

Then:

$$z = \frac{1}{\sqrt{2(1+k)}} \left[F(\sin^{-1}\zeta, \lambda) + F(\sin^{-1}\zeta, \lambda') \right] \qquad [11]$$

where F is the elliptic integral of the first kind of moduli λ and λ' respectively and ζ is the new variable which defines by means of [8] and [11] u as a function of z or vice versa. It is interesting to study the contour in the ζ-plane corresponding to the contours OABC in the z-plane (Fig. 1a) and the boundaries OABC of the first quadrant in the u-plane (Fig. 2a). This contour is shown in Fig. 3 [*see* also Ref. (6)]. The three sides of the trapezium and the real axis in the u-plane have been transformed to a

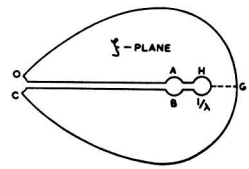

Fig. 3. Trapeziums in Fig. 1a and 1b transformed to the ζ-plane.

cut from the origin to a point H where $\zeta = 1/\lambda$. The boundary OC has become now a part of a lemniscate. Let any point on this lemniscate be denoted as $a + ib$ in the complex ζ-plane. It is easy to show then that:

$$(a^2 + b^2)^2 = 2(a^2 - b^2) \qquad [12]$$

In order to find the current density along any boundary of the trapezium, it is now necessary to evaluate z as a function of given ζ by [11] and then by means of [8] obtain the corresponding $\tilde{C}$ from [7]. Before proceeding with the construction of the current density curves, it is necessary to correlate the parameters λ and k with the actual dimensions of the cell.

In equation [11], let:

$$\begin{aligned} F(\sin^{-1}\zeta, \lambda) &= v \\ F(\sin^{-1}\zeta, \lambda') &= v' \end{aligned} \qquad [13]$$

so that [11] becomes:

$$\sqrt{2(1+k)}\, z = v + v' \qquad [14]$$

Eq. [13] can be considered as defining a transformation from the ζ-plane to the v- and v'-planes, respectively. It can be shown easily that corresponding to lemniscate contour OABC in the ζ-plane; the contours in the v- and v'-planes are as shown in Fig. 4a and 4b. Here L and L' are the complete elliptic integrals of the first kind with moduli λ and λ', respectively. Consider the vertex B. Then in the z-plane (Fig. 1a)

$$z_B = r_1 + i(r_1 - r_2)$$

and in the v- and v'-planes:

$$\begin{aligned} v_B &= L + 2iL' \\ v'_B &= L' \end{aligned}$$

Hence, from [14]

$$\sqrt{2(1+k)}\,[r_1 + i(r_1 - r_2)] = L + L' + 2iL'$$

Comparing the real and the imaginary parts and dividing:

$$\frac{r_1}{r_2} = \frac{L + L'}{L - L'} \qquad [15]$$

Thus, given the ratio of the parallel sides of the trapezium, one can determine the ratio L'/L, which in turn defines uniquely the modulus λ by means of the Jacobi's Nome:

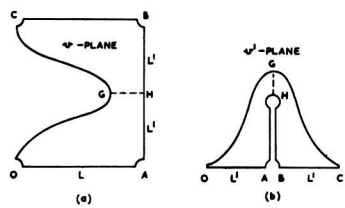

Fig. 4. Auxiliary v- and v'-planes

$$q(\lambda) = \exp\left(-\frac{\pi L'}{L}\right) \qquad [16]$$

The q-function is tabulated extensively (7,8). Having determined λ, the corresponding value of k can be evaluated from [9].

This completes the analysis of a trapezium cell. Now consider, in turn, two possible electrode configurations as depicted in Fig. 1a and 1b.

3. The Trapezoidal Cell First Electrode Position

Assume that the cell is constructed as in Fig. 1a while OA is the cathode. To evaluate the current density along this electrode it is observed that corresponding to the variation of z along OA in Fig. 1a:

$$O \leqq z \leqq r_1$$

the quantity ζ varies:

$$O \leqq \zeta \leqq 1 \quad (see\ Fig.\ 3)$$

Thus for a given ratio r_1/r_2 λ is evaluated by [15] and [16] and hence the values of z are correlated with those of ζ along OA in both planes, respectively. The values of ζ so obtained are then used to compute corresponding values of u from [8]. Then, from [7] current density values are obtained. In order to normalize these values with respect to the total current fed into the cell, it is observed that the total area under a current density curve is:

$$\int_0^{z_1} \sqrt{u}\, dz = \int_0^K dw = K(k)$$

where $z_1 = \max z$ obtained from [11]. In order to insure unit area under the current density curve over the normalized range of z $(O \leqq z \leqq 1)$, one multiplies all the ordinates by z_1/K and divides all the abscissas by z_1. If the height of the electrolyte in the cell is h and A amps are fed into the cell, then $CA/hr_1 = \tilde{C}$ gives the actual current density on the cathode in amp/cm^2. The curves of C are plotted in Fig. 5 for $S = r_1/r_2$ ranging from 1.1 to ∞. It will be observed that for $S = 2$ (i.e., $r_1 = 2r_2$) the current density is almost linear over two thirds of the cathode length. A useful feature of such a cell is that the primary current here does not reach excessively high values at it does in the Hull cell, where polarization errors may become serious; on the other hand this tank is simpler to construct than the hyperbolical Gilmont and Walton cell.

A sample cell was constructed with $S = 2$. The side OA was approximately 8 in. long and the depth of the electrolyte was approximately 1.5 in. The Cu was deposited from an acid Cu electrolyte, peeled off and its thickness at about 0.5 in. from the bottom of the bath was measured at eight equidistant points.[1] In Fig. 5 the suitably normalized micrometer readings are shown. The agreement between the predicted and the practical results seems to be good.

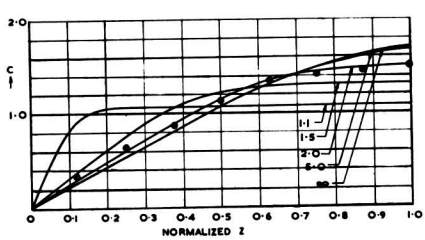

Fig. 5. Normalized current density curves for a cell shown in Fig. 1a. The numbers associated with the curves indicate the corresponding values of $S = r_1/r_2$. The points on the curve for $S = 2$ are experimental (see above).

4. The Trapezoidal Cell Second Electrode Position

Now consider a cell with electrodes situated as in Fig. 1b while OC is the cathode. This arrangement is the same as in the Hull cell and a current density singularity at C is expected. It will be found that this singularity is integrable so as to yield a finite value for the total current, as required.

In this case the evaluation of z corresponding to a given ζ is more involved since the contour OC becomes a lemniscate in the ζ-plane so that

$$\zeta = a + ib \qquad [17]$$

is a complex number whose real and imaginary parts are related by [12].

For a complex angular argument, the elliptic integral of the first kind can be expressed as [*see* Ref. (8) p. 12, Eq. 115.01]

$$F(\theta + i\Psi, \lambda) = F(B, \lambda) + iF(A, \lambda') \qquad [18]$$

where both B and A are real and given by:

$$\cosh \Psi \sin \theta = \frac{\sin B \sqrt{1 - \lambda'^2 \sin^2 A}}{1 - \sin^2 A (1 - \lambda^2 \sin^2 B)}$$

$$\cos \theta \sinh \Psi = \frac{\cos B \cos A \sin A \sqrt{1 - \lambda^2 \sin^2 B}}{1 - \sin^2 A (1 - \lambda^2 \sin^2 B)} \qquad [19]$$

In the present case, from [11]

$$\sin^{-1} \zeta = \theta + i\Psi$$

so that

$$\zeta = a + ib = \sin \theta \cosh \Psi + i \cos \theta \sinh \Psi \qquad [20]$$

The quantities A and B in [19] cannot be found directly from this equation in terms of a and b which define the lemniscate; however using the Eq. [12] of the lemniscate and considering A and B corresponding to the modulus λ as well as A' and B' corresponding to λ', both of which are to be found for the same ζ in [11], one can find a simple relation between A and B:

$$\sin^2 B = \frac{\sin^2 A}{1 + (2\lambda^2 - 1) \sin^2 A} \qquad [21]$$

Furthermore, on the lemniscate:

$$A = B'$$
$$B = A' \qquad [22]$$

Thus [11] can be written:

$$z = \frac{(1 + i)}{\sqrt{2(1 + k)}} [F(B, \lambda) + F(A, \lambda')] \qquad [23]$$

which is of required form since OC is inclined at 45° in the z-plane. Changing A from O to π, one obtains B from [21] and hence z corresponding to

[1] The acid Cu bath was chosen ($CuSO_4$-150 g/l; H_2SO_4-25 g/l) because the polarization in such a bath is low. The total current fed into the cell during 26 hr was 2 amp.

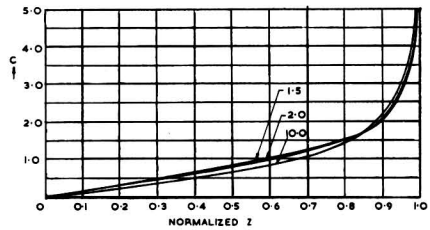

Fig. 6. Normalized current density curves for a cell shown in Fig. 1b. The numbers associated with the curves indicate the corresponding values of $S = r_1/r_2$.

given ζ on the lemniscate as defined by [19] and [20]. Hence the current density curves can be plotted as explained in the previous section. In this case, however, the total area under a curve for given S is equal to K', in analogy to K in the previous section.

The normalized current density curves are plotted in Fig. 6 for $S = 1.5$, 2, and 10. The curves are almost coincident and show reasonable linearity over about two thirds of the cathode length.

5. Triangular Cell
Mathematical Analysis

Consider a right angled isosceles triangle in the complex z-plane as shown in Fig. 1d. Then the inside of the triangle can be transformed into the upper half t-plane (Fig. 7a) by

$$z = z_o + \int_o^t \frac{dr}{2r^{1/2}(r^2-1)^{3/4}} \qquad [24]$$

The corresponding points are

$$O: z = 0 \rightarrow t = 1$$
$$A: z = \tfrac{1}{2} p (1+i) \rightarrow t = 0$$
$$B: z = p \rightarrow t = -1$$
$$E: z = z_E \rightarrow t = n$$
$$F: z = z_F \rightarrow t = -m$$

The half t-plane can now be transformed into the inside of a rectangle in the w-plane by

$$\sqrt{\frac{(1+m)(1+t)}{(1-m)(1-t)}} = sn(w,k) \qquad [25]$$

where

$$\sqrt{\frac{(1-m)(1-n)}{(1+m)(1+n)}} = k \qquad [26]$$

and where

$$z_o = \frac{(1+i)}{\sqrt{2}} K\left(\frac{1}{\sqrt{2}}\right)$$

The vertices of the rectangle (Fig. 7b) are

$$O: w = iK'$$
$$B: w = 0$$
$$E: w = K + iK'$$
$$F: w = K$$

K and K' are complete elliptic integrals of the first kind with moduli k and k', respectively. From [3], [24], and [25] the current density is given by:

$$\tilde{C} = \kappa \left|\frac{dw}{dz}\right| = \kappa \left|\frac{(1+m)(1+n)t(t^2-1)^{1/2}}{(t+m)(t-n)}\right|^{1/2} \qquad [27]$$

Since the current density is required in the z-plane using [24], t must be expressed as a function of z. The integral can be evaluated by using the substitution given in Ref. (9) (case IV), i.e.,

$$\zeta^2 = \frac{t^2}{t^2-1} \qquad [28]$$

Then ζ is given as a Weierstrassian elliptic function of z.

$$\zeta = \mathcal{P}z \qquad [29]$$

defined by

$$\left(\frac{d}{dz}\mathcal{P}z\right)^2 = 4(\mathcal{P}z - e_1)(\mathcal{P}z - e_2)(\mathcal{P}z - e_3)$$

where

$$e_1 = 1,\ e_2 = 0,\ \text{and}\ e_3 = -1.$$

Since e_1, e_2, and e_3 are real, [29] can be expressed as a Jacobi elliptic function of real modulus

$$sn(\sqrt{2}\,z, \lambda) = \sqrt{\frac{2}{\zeta+1}} \qquad [30]$$

where

$$\lambda^2 = \frac{e_2 - e_3}{e_1 - e_3} = \frac{1}{2} \qquad [31]$$

Treating the other triangles given in Ref. (9) in a similar manner, the Jacobi elliptic functions arrived at have a complex moduli and, since Weierstrassian elliptic functions are not extensively tabulated, the problem becomes numerically intractable.

The contour in the ζ-plane which corresponds to the triangle in the z-plane is as shown in Fig. 8. The side OB of the triangle forms a cut in the ζ-plane from $\zeta = \infty$ to the branch point at $\zeta = 1$; the side OA is the negative imaginary axis and the side AB is the positive imaginary axis. In order to evaluate the current density along any boundary of the triangle, z can now be related to t through [28] and [30]. In [27] m and n still remain unknown and must be related to the positions of F and E, respectively. It can be shown that along OA

$$\zeta = -2i \frac{cn^2(|z|,\lambda)}{1 - cn^4(|z|,\lambda)} \qquad [32]$$

where $\lambda = \dfrac{1}{\sqrt{2}}$, as given in [31].

Since at the point E in the t-plane $t = n$, then using [28]

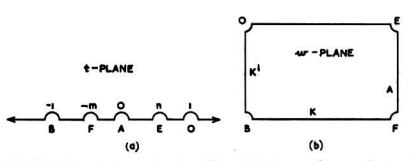

Fig. 7. (a) The triangle in Fig. 1d transformed to the t-plane; (b) the same in the w-plane.

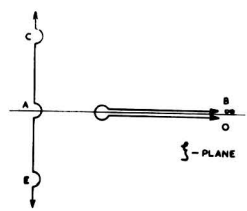

Fig. 8. The triangle in Fig. 1d transformed to the ζ-plane

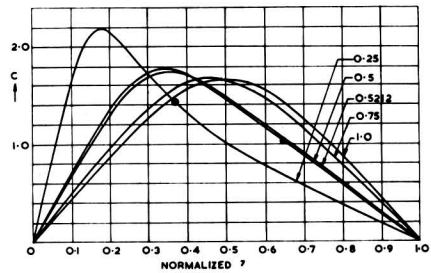

Fig. 9. Normalized current density curves for a cell shown in Fig. 1d when the cathode is along EA only. The numbers associated with the curves indicate the corresponding values of $\sqrt{2}a/p$. The points on the curves for $\sqrt{2}a/p = 0.25$ and 0.5 show the position of the points of inflection.

$$n = \frac{2cn^2\,(a,\lambda)}{1 + cn^4\,(a,\lambda)} \qquad [33]$$

where $a = OE$

Similarly,

$$m = \frac{2cn^2\,(b,\lambda)}{1 + cn^4\,(b,\lambda)} \qquad [34]$$

where $b = FB$

6. Triangular Cell Special Electrode Position

The current density curves shown in Fig. 9 are for a 45° triangular, isosceles cell discussed above when the anode is along OB in Fig. 1d and the cathode is along EA where E can be practically anywhere between O and A. The curves are normalized as before to unit area, the normalizing constant being again $K'(k)$, similarly as in section 4, where now k is given by [26], [33], and [34]. A current density singularity is observed at E, but this singularity is integrable giving a finite value for the total current. No singularity occurs on the cathode OB and the current density curves there are roughly triangular in shape with good linearity between their maximum $z = z_{max}$ and the normalized $z = 1$. When the anode occupies the whole of AO (i.e., $a = 0$ as defined in [33]), this maximum is at $z = 0$ and as E moves along OA toward A the maximum moves along the z-axis until for a point cathode at A (i.e., $a = p/\sqrt{2}$) it occurs at $z_{max} = 0.5$ and the current density curve is symmetrical as expected. For a less than some value, say a_i, the curves have a point of inflection between z_{max} and $z = 1$; such point of inflection destroys the linearity somewhat (*see* Fig. 9 for $a = 0.25$). It is therefore advisable in practice to construct a cell with an $a < a_i$ and in order to have large range of linearity at the same time, the best value is

$$a = a_i = 0.52120\,p/\sqrt{2} \qquad [35]$$

For the ease of construction, it is suggested to take:

$$a = p/2\sqrt{2} \qquad [36]$$

when good linearity is observed. Thus in the last case the slope between $z = 1$ and $z = 0.5$ does not vary by more than 8%. Moreover, the area under the current density curve in Fig. 9 for $\sqrt{2}\,a/p = \frac{1}{2}$ is 0.3695 between $z = 0.5$ and $z = 1$, whereas the area of the corresponding right-angled triangle, between the same limits (the slope of the hypotenuse of this triangle is equal to that of the curve at $z = 1$), is 0.3693.

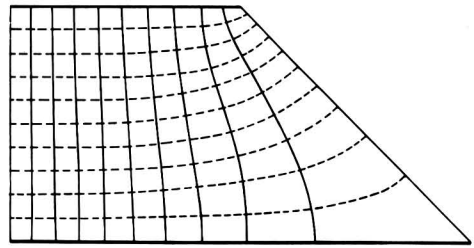

Fig. 10. Equipotentials (broken lines) and the current flow lines (full lines) of a cell shown in Fig. 1a.

Hence, if the total current fed into each cell is A, then 0.3695 A is distributed linearly over that half of the cathode which is further from the anode, while the length of the latter is $1/2\sqrt{2}$ of the total cathode length.

No experiments were made on the triangular cell, which is described here as an interesting alternative to the trapezium one. It seems however that it is more convenient to use practically, since (because of the triangular shape of the primary current distribution; *see* Fig. 9) there are two determinable points on the cathode where the current density is the same. This property could be profitably used for the experimental testing of the deposition, e.g., for deciding the level in the bath at which the actual deposition can be related proportionally to the primary current density.

7. Conclusion

Fig. 10 and 11 show the current flow lines (full lines) and the equipotentials (broken lines) of the two cells discussed in Sections 3 and 6. In both cases the electrodes are marked by thick lines. Reversing the positions of the electrodes and the insulators one interchanges the meaning of the equipotentials and the current lines, so that, in particular, Fig. 10 shows the conditions in one cell discussed in Section 4 (the Hull type cell) when the insulators are marked by thick segments, the current flow lines by broken lines, and the equipotentials by full lines.

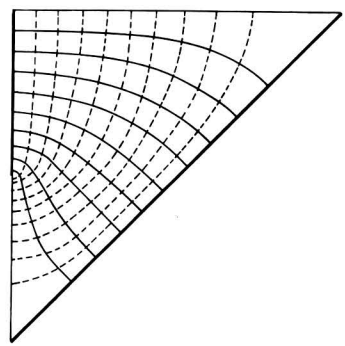

Fig. 11. Equipotentials (broken lines) and the current flow lines (full lines) of a cell shown in Fig. 1d when the cathode is along EA only.

The curves were obtained by the relaxation methods, since analytic computation is made difficult by the lack of appropriate mathematical tables.

Acknowledgments

The authors wish to thank L. E. Q. Walker and D. W. G. Ballentyne for proposing the problem and for many helpful discussions, Miss M. A. Millidge for computing some of the curves, also Miss E. Kowszynis for supplying experimental data for Fig. 5, and the Chief of Research of the Marconi's Wireless Telegraph Company for the permission to publish.

Manuscript received April 22, 1957.

Any discussion of this paper will appear in a Discussion Section to be published in the June 1958 JOURNAL.

REFERENCES

1. C. Kasper, *Trans. Am. Electrochem. Soc.*, **77**, 353 (1940).
2. R. O. Hull, "Control of Plating Baths by Plating Cells," "Metal Finishing" Guidebook-Directory, 18th annual ed., p. 367 (1949).
3. R. Gilmont and R. F. Walton, *This Journal*, **103**, 549 (1956).
4. W. R. Smythe, "Static and Dynamic Electricity," McGraw-Hill Book Co., Inc., p. 233 (1950).
5. A. Cayley, "Elliptic Functions," G. Bell & Sons, London or Deighton, Bell & Co., Cambridge, p. 360 (1895).
6. F. Bowman, *Proc. London Math. Soc.*, **39**, 211 (1939).
7. E. Jahnke and F. Emde, "Tables of Functions with Formulae and Curves," Dover Publications, New York (1945).
8. P. F. Byrd and M. D. Friedman, "Handbook of Elliptic Integrals for Engineers and Physicists," Springer Verlag-Berlin, New York (1954).
9. A. E. H. Love, *Am. J. Math.*, **2**, 158 (1889).

Transistor-Grade Silicon

I. The Preparation of Ultrapure Silicon Tetraiodide

Bernard Rubin, Guy H. Moates, and Joseph R. Weiner

Radiochemistry Section, Components and Techniques Laboratory, Electronics Research Directorate, Air Force Cambridge Research Center, Air Research and Development Command, Bedford, Massachusetts

ABSTRACT

A stepwise method of preparing and purifying SiI_4 has been found involving the direct combination of the elements, recrystallization of the product, followed by sublimation and zone purification steps. The values of the segregation coefficients of several impurity elements have been determined, and it is shown that under ideal conditions some of these elements can be removed to concentrations of less than one part impurity per billion parts of SiI_4 in sixty passes for a 50 cm length charge.

The requirements for transistors and other semiconductor devices that operate at temperatures higher than those at which Ge is effective have stimulated considerable research in the preparation of "transistor-grade silicon." This term refers to a Si matrix in which the impurity levels are at concentrations of one part in one hundred million and preferably as low as one part per one hundred billion of Si. Because the sources of this material in the United States are few, the Air Force has initiated a research program in Si chemistry in order to provide alternate methods of refinement.

Most Si in this country is made according to the reaction

$$2C + SiO_2 \rightarrow 2CO + Si$$

in electric arc furnaces. A typical product[1] has the following spectrographic analysis shown in Table I (1). Semiconductor devices made of Si with levels of impurities as shown in Table I would be of little practicality and transistor devices with acceptors, donors, and lifetime-killers at such high concentrations would not function. Two approaches are available for removing these impurities, a metallurgical and a physicochemical. The former involves the zone refining technique originated by Pfann (2). By this

[1] Obtained from Coleman and Bell Company, Norwood, Ohio.

Table I. Spectrographic analysis of reagent Si

Impurity element	Conc. in parts of impurity per million parts of Si
Al	6900
As	150
B	60
Ca	7100
Co	7
Cr	250
Cu	300
Fe	6700
Ga	<10
In	3
K	<10
Li	2.5
Mg	120
Mn	350
Na	18
Ni	80
P	80
Ta	140
Ti	1300
Tl	5
V	60
Zr	250

method, some elements, e.g., Al, may be removed effectively from Si. However, B, with a segregation coefficient of about 0.9 (3) cannot be separated efficiently from the matrix. In addition, because of the high melting point of Si (1420°C), contamination by leaching from the container material presents problems. For these reasons, the physicochemical approach which involves the synthesis of a convenient compound of Si, its purification to the desired levels of purity that are required ultimately for transistor-grade silicon and its decomposition into elemental Si, has been chosen by this laboratory. In order that this approach be effective, there were certain prerequisites. The compound had to be either easily synthesized or available, it had to be capable of being purified to the extent required by the final Si specification, and it had to be capable of being decomposed relatively easily into elemental Si which would not be contaminated in the decomposition process. Of the variety of Si compounds that suggested themselves, i.e., the silanes, siloxanes, silicates, and halides, the latter seemed to be best suited to fulfill the above requirements. They are stable substances, relatively easy to synthesize and handle, and are potentially decomposable or reducible to polycrystalline or single-crystal Si and the halogen or hydrogen halide. Of the four unmixed tetrahalides, SiF_4 is the most stable and decomposes only under extremes of temperature and pressure. Furthermore, it is a gas under normal conditions and, as such, is difficult to handle and purify. $SiBr_4$ and $SiCl_4$ are both liquids possessing the advantages of this state with respect to purification, but both are more difficult to decompose than the tetraiodide. Thermodynamic data indicate that the latter decomposes at about 1500°C at one atmosphere and can be reduced with hydrogen at about 600°C under these conditions. At 1000°C, the dissociation equilibrium constant (Kp) was calculated to be 1.86×10^{-12} from the free energy data. Assuming a partial pressure of 3 mm of SiI_4 in the reaction chamber, then the limiting partial pressure of I_2 is 0.236 mm. By lowering the partial pressure of I_2 below this value, decomposition of the SiI_4 occurs. Since it is a solid under normal conditions with a relatively low boiling point (290°C), it can be purified not only by the usual techniques of recrystallization and distillation, but it lends itself to zone purification. Since SiI_4 offers a different matrix than Si to impurities, it need not be expected that the segregation coefficients of these impurities be the same in both matrices. If the impurities that are not removed in the current technique of zone purification of Si can be removed in SiI_4, then a combination of the two zone purifications could lead to transistor-grade Si. It seemed for most intents and purposes that SiI_4 offered the greatest potentiality as an intermediate in the synthesis of transistor-grade Si.

A literature survey indicated that high purity Si has been prepared by methods utilizing the tetrachloride, the tetrabromide, and the tetraiodide of Si. The tetrachloride is reduced in a quartz apparatus at about 1000°C with Zn vapor as the reductant (4).

Sangster (5) has reduced the purified tetrabromide with H_2. Litton (6) investigated the thermal decomposition of fractionally distilled tetraiodide. More recently, Theuerer (7) reduced $SiCl_4$ with H_2.

Experimental

Preparation of silicon tetraiodide.—SiI_4 was prepared by the direct reaction of I_2 with Si in a horizontal reaction chamber (8). The iodine boiler, heated by a mantle to about 115°C, was a 500 ml round-bottomed Pyrex flask sealed at the top and equipped with a 28/15 ball joint at right angles to the neck. A side arm was present to permit the entry of the dried flushing gas, argon. The reagent was Baker and Adamson resublimed iodine. The reaction chamber was a 30-mm inner diameter Vycor furnace tube, 70 cm long, with 28/15 socket joints at each end. The connection of Pyrex to Vycor permitted easy removal of one joint from the other owing to the difference in coefficients of expansion. The furnace tube was heated by two electric multiple unit furnaces made by Hevi-Duty Electric Company, Milwaukee, Wisconsin, and the temperature monitored by using a chromel-alumel thermocouple adjacent to the furnace tube. The SiI_4 receiver was a 500-ml round-bottomed Pyrex flask similar to the iodine boiler.

In a typical run, reagent Si was ground into particles and then collected between No. 4 and No. 10 sieves to permit as close packing of the particles as was practicable in the furnace tube without channeling or back pressures of I_2. The charged I_2 flask, reaction chamber, and receiver were connected using a minimum of Dow Corning Silicone grease at the joints and a mercury pressure release valve was inserted in parallel with the system. The argon was flushed through the system at a flow rate of about 524 ml/min and the temperature of the Si was raised to 810°C. All exposed connecting sections between boiler, chamber, and receiver were maintained at suitable temperatures by means of heating tapes. When temperature equilibrium was attained, the I_2 was heated to 115°C and carried into contact with the Si. The product as it entered the receiver was a white mist and, after condensation, a pinkish white to red solid. The coloration was probably due to unreacted I_2 or some Si_2I_4 from the reaction:

$$Si + SiI_4 \rightleftarrows Si_2I_4$$

Gravimetric analysis. Calculated for SiI_4: Si, 5.2%; I, 94.8%. Found: Si, 5.6%; I, 91.0%. Emission spectrographic analysis of the crude SiI_4 gave the impurities as listed in Table II.

A comparison with Table I indicates that three elements have increased in concentration: Na, B, and V. An analysis of Pyrex glass showed that Na was present to the extent of about 8.5% and B about 10.8%. It was evident that leaching of these two impurities from the glass took place under the conditions of the SiI_4 synthesis. There was also the possibility of leaching from the Vycor. For this reason, an all-quartz apparatus will be substituted for Pyrex in the synthesis step. The daily production rate is about 450 g of SiI_4 and the apparatus may be scaled up for larger yields if necessary. There is about a 95% conversion to SiI_4 based on I_2.

Table II. Emission spectrographic analyses

Impurity element	Crude SiI_4	Conc. of impurity in parts of impurity per million parts SiI_4 Recrystallized SiI_4	Sublimed SiI_4
Ag	1.0	0.1	N.D.
Al	28.0	6.5	0.2
As	<1	N.D.	N.D.
Au	N.D.*	N.D.	N.D.
B	16.0	N.D.	N.D.
Be	N.D.	N.D.	N.D.
Bi	N.D.	N.D.	N.D.
Ca	N.D.	N.D.	N.D.
Cd	<1	N.D.	N.D.
Co	N.D.	N.D.	N.D.
Cr	1.5	N.D.	N.D.
Cu	12.0	0.3	2.7
Fe	55.0	0.5	0.6
Ga	<0.1	N.D.	N.D.
Hg	<1	N.D.	N.D.
In	<0.1	0.5	N.D.
K	N.D.	N.D.	N.D.
Li	N.D.	N.D.	N.D.
Mg	1.6	0.4	0.1
Mn	4.5	2.0	0.1
Mo	N.D.	N.D.	N.D.
Na	2.0	N.D.	N.D.
Ni	1.0	N.D.	N.D.
P	<5	N.D.	N.D.
Pb	<0.5	N.D.	N.D.
Sb	<1	N.D.	N.D.
Sn	<0.5	N.D.	N.D.
Ti	21.0	16.5	1.3
V	12	N.D.	N.D.
Zn	N.D.	N.D.	N.D.
Zr	1.2	5.0	N.D.

* Not detected.

Analysis of silicon tetraiodide.—Analyses of SiI_4 were carried out[2] after hydrolyzing a sample with conductivity water in Pt crucibles and heating to 500°C until the reaction was complete. Commercially available mixed internal standards were then added to the silica. Thin-walled graphite electrodes were filled with adequate silica and ignited in a He atmosphere for 10 sec at 5 amp. Another silica sample was ignited in air for 50 sec at 10 amp and burned to completion. Those elements whose lines were masked by SiO, SiO_2, and CN bands in the atmospheric run were read from the spectrum obtained in the He run. The sensitivities of some of the impurity elements in SiO_2 are given in Table III.

Crystallization.—Of the various purification techniques that are available for solids, zone purification has the potentiality, if the segregation coefficients are favorable, of yielding a matrix in which the desired concentrations of impurities can be attained practicably. Although successful zone purification is not dependent on attaining low concentrations of impurity initially, the ultimate concentration can be minimized if the initial concentrations are low. For this reason, other methods of preliminary purification have been invoked. The first of these was crystallization of the crude SiI_4 from toluene. The solubility of SiI_4 in toluene was found to be 10.3% by weight at 110°C and 3.2% at 20°C indicating about an 82% recovery of SiI_4 in a single step crystallization.

[2] To be published by the Metal Hydrides Co., *Journal of Analytical Chemistry.*

Table III. Sensitivities of impurities by emission spectrographic analysis

Impurity elements	Sensitivity in parts of impurity per million parts SiO_2
Ag	0.25
Al	0.65
As	15
B	0.50
Be	0.25
Ca	0.50
Cd	1.0
Cr	2.5
Cu	0.25
Fe	0.65
Hg	5.0
Mg	0.25
Mn	0.75
P	25
Sb	3.0
Ti	1.0
Zn	10
Zr	5

In practice, the crude SiI_4 was transferred in the sealed receiver to a dry box, and sufficient fractionally distilled toluene, dried over Na, was added to make a 10% solution. The solution was heated to the boiling point, and the resulting solution was cooled slowly to 0°C. The liquor was decanted, and the remainder removed under vacuum at about 70°C. A spectrographic analysis of the crystallized product is given in Table II.

A comparison of the crystallized and crude product indicates that there is a considerable decrease in the over-all impurity concentrations of most of the elements. It can be postulated that the impurity elements are in a molecular form that is toluene-soluble, and, in all probability, this form is the iodide. It is possible that the efficiency of the crystallization step is the result, in part, of small amounts of silica introduced by the unavoidable hydrolysis of the SiI_4 during handling. Furthermore, since the extraction is a relatively low temperature step, there is little or no occasion for leaching as is indicated by the low concentrations of such constituents of glass as B and Fe. Gravimetric analytical methods on the crystallized SiI_4 yielded the following analysis: Si, 5.4%; I, 91.9%. These values are closer to theoretical than the crude SiI_4, and indicate that some of the I_2 or higher homologues have been removed by the crystallization step. The appearance of the more lightly colored material supports this assumption.

Sublimation.—Fractional distillation of the recrystallized SiI_4 was next considered as a possible purification technique. It was observed that sublimation occurred with use of a vacuum fractional distillation system. Sublimation had also been used as a transfer procedure (6) for SiI_4 and it was decided to utilize it as the second step in the purification. The sublimation apparatus consisted of a 30-cm long Pyrex cylinder 10 cm in diameter with 10-mm ground flanges on each end. Around the cylinder were wrapped two heating tapes individually controlled by Powerstats. A dome with a 4-mm stopcock was connected to one end of the cylinder, and, on the other end, a second dome

equipped with a 32-cm long cold finger. The latter dome was charged in a dry box with enough crystallized SiI_4 to fill it. The apparatus was assembled with the ends held temporarily in position by clamps; a partial vacuum was applied to complete the seals. The charged assembly was then removed from the dry box, connected to a vacuum system, and the charged end was heated by a mantle to about 100°C. When the sublimate appeared as large white crystals on the area adjacent to the heated charge, the sublimation was repeated by heating the first tape, then the second until ultimately the crystals appeared on the dome. The apparatus was disassembled and the product scraped off with Lucite rods. An emission spectrographic analysis of the sublimed product is given in Table II. It is obvious from comparison of the results in Table II that considerable purification is effected by sublimation of the crystallized product, particularly in the cases of Al, Mn, Ti, and Mg. The Cu concentration is seen to increase from 0.3 to 2.7 ppm and this is due to Cu impurities found in the Pt crucibles used in the hydrolysis of the SiI_4 prior to spectrographic analysis. The source of contamination has been eliminated by substituting quartz for Pt. Concentrations of all the impurities detected are now in or below the part per million range. Further purification may be effected by the zone-melting process in the case of impurities with favorable segregation coefficients.

Zone purification.—Determination of effective segregation coefficients, K_{eff}, under a given set of experimental conditions was undertaken. It is emphasized that the values reported are those of effective coefficients, and not equilibrium values. Because more subtle variables such as crystal orientation, convection, effective boundary layer, silica formation, and supercooling were not controlled, there exists some discrepancy in the values reported.

Silicon tetraiodide recrystallized from toluene was encapsulated in sealed Pyrex ampoules, densified, and leveled by repeated vertical reverse passage of a single zone (2). A single molten zone 2-cm long was passed through the 20-cm length of leveled charge. The zone-melted charge was then segmented into ten equal sections, each section hydrolyzed to silica in conductivity water, and finally each section was analyzed spectrographically as described above.

Profiles constructed from the results of these analyses depicted concentrations, C_s, of impurities retained in the solid after passage of one molten zone. The initial concentration, C_o, was taken as the average concentration of the ten segments. This average value is valid because the charge was leveled to assure an invariance of impurity concentrations along the longitudinal axis. By definition

$$C_s = KC_l \qquad \text{(I)}$$

where C_l is the concentration of an impurity in the liquid. At the point of the first freezing (i.e., at $X = 0$, if X is the distance along the charge), $C_l = C_o$. Therefore,

$$K = C_s/C_o \text{ at } X = 0 \qquad \text{(II)}$$

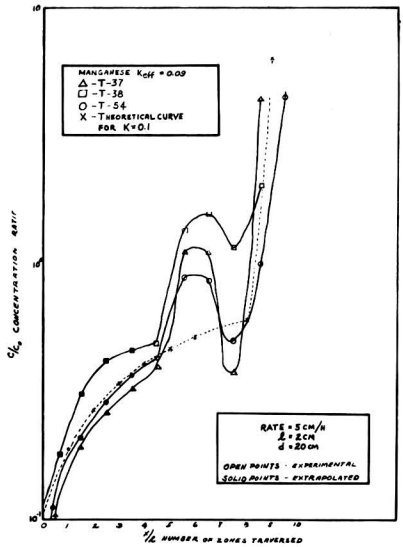

Fig. 1. Concentration profiles of Mn impurity species in a SiI_4 matrix.

By plotting the ratio C_s/C_o vs. X/l (l is the zone length) it was possible to determine K_{eff} from the intersection of the profile with the y-axis. Fig. 1 is a series of experimental profiles for the Mn species in the silicon tetraiodide matrix. Also depicted is the calculated curve for a solute having a K equal to 0.1.

These profiles are typical of those species which display segregation in accordance with K_{eff} of approximately 0.1. The preponderance of impurity solute in the end of the charge toward which the zones traveled is evidence that the segregation coefficient is less than unity. The sharp drops in concentration at the minima observed in the next to last zone are due to the growth of the last zone at the conclusion of the pass. It was necessary to stop the travel of the zone before it proceeded into an unleveled portion of the charge; at this time the final zone grew back into a large part of the preceding zone, and then solidified by normal freezing from both ends.

Although only a single molten zone was passed through the charge, the concentrations in the first half of the charge to be melted were below the limits of spectrographic detectability for about half of the impurities studied. Therefore, it was necessary to resort to a method of mathematical extrapolation in order to extend the profile to the y-axis. The expression

$$C_z = K_{eff}\left[C_o + \frac{C_{z-1}}{K_{eff}} - C_{z-1}\right] \qquad \text{(III)}$$

was employed. Here C_z is the solute concentration frozen out in any given zone (except the last), C_{z-1} is the solute concentration frozen out in the prior zone, and C_o is the initial invariant concentration. The equation is an expression of approximation and becomes less valid as the l/d ratio (zone length: charge length) increases. Values of K_{eff} are substituted until C_{z-1} at $X = 0$ is equal to $K_{eff}\,C_o$. Valid-

ity of these extrapolations is based on the reasonable degree of agreement between computed and experimental curves for impurities detectable in all segments.

Zones have been passed downward through the charge with similar results, thereby eliminating the possibility of any separation by flotation. Therefore, regardless of the anomalies in the profile, it may be assumed that a K of a certain value exists in order to relocate the impurities as depicted. This is so if one assumes that segregation is caused only by the differences in solubility in the solid and liquid phases.

Table IV summarizes the effective segregation coefficients of various impurity species in a SiI_4 matrix. Inasmuch as all values reported in Table IV are less than unity, purification can be effected by moving each of the solute impurities to the end of the charge toward which the molten zones travel.

Applying the value of K_{eff} as determined for boron triiodide (i.e., 0.4) to the family of equations given by Pfann (2), it can be shown that an ultimate concentration ratio of 1×10^{-12} can be attained for a charge having a d/l ratio of 20:1. Furthermore, 70% of this charge will have a concentration which has been reduced to one part in a billion or less if the initial concentration was one part in a million.

The number of passes required to attain this concentration is approximated by

$$K^n = C_{x=0} \qquad \text{(IV)}$$

where n is the number of passes. An efficiency factor (9) of 53% must be applied for a K equal to 0.4. With use of this factor in conjunction with Eq. (IV), 60 passes are required to attain this concentration profile.

Table IV. Effective segregation coefficients of various impurity species in a SiI_4 matrix

(Charge length, d = 20 cm; zone length, l = 2 cm; zone temperature = 135° ±4°C; rate of crystallization = 5 cm/hr)

Impurity species	K_{eff}
B*	0.16 ± 0.07‡
Al	0.70 ± 0.35
Na	0.10 (single run)
Mg*	0.16 ± 0.01
Cu	0.64 ± 0.17
Fe*	0.15 ± 0.08
Ti	0.91 ± 0.08
Mn*	0.09 ± 0.04
Boron triiodide†	0.42 ± 0.22

* Values obtained by extrapolation.
† Doped samples.
‡ Maximum variability of results.

The concentrations computed above indicate that SiI_4 can be purified to less than one part of impurity per billion parts of SiI_4 provided equilibrium conditions prevail to the extent demonstrated in these experiments. Furthermore, it must be assumed that impurities are not leached from container walls. Finally, it should be mentioned that the purity of a sample can be improved by: (*a*) decreasing the value of the effective segregation coefficient (for $K < 1$) by controlling conditions in order to more closely approximate equilibrium, (*b*) controlling the l/d ratio in order to make the ultimate concentration profile more favorable, and (*c*) choosing a smaller fraction of the zone-refined charge.

A more detailed treatment of the zone purification of SiI_4 is forthcoming in the second paper of this series.

Acknowledgments

The authors thank B. Manning of Technical Operations, Inc., Arlington, Massachusetts, for his advice on the design of the zone purification furnace; W. Jackson and R. Morrison of the Engineering Division, Air Force Cambridge Research Center, for the modifications and construction of this apparatus. Acknowledgment is also expressed to A. Kant, Watertown Arsenal, Watertown, Mass., for his helpful suggestions.

Manuscript received July 16, 1956. This paper was prepared for delivery before the Washington Meeting, May 12-16, 1957.

Any discussion of this paper will appear in a Discussion Section to be published in the June 1958 JOURNAL.

REFERENCES

1. Spectrographic Analyses by Metal Hydrides, Inc., Beverly, Mass.
2. W. G. Pfann, *J. Metals*, **194**, 747 (1952).
3. J. A. Burton, *Physica*, **20**, 845 (1954).
4. D. W. Lyon, C. M. Olson, and E. D. Lewis, *J. (and Trans.) Electrochem. Soc.*, **96**, 359 (1949).
5. Hughes Aircraft Co., Quarterly Technical Rpts., Signal Corps Contract No. DA-36-039-SC-42574 (1952-1953).
6. Foote Mineral Co., Quarterly Technical Rpts., Signal Corps Contract No. Da-36-039-SC-5550 and DA-36-039-SC-56993 (1951-1954).
7. H. C. Theuerer, *Bell Labs. Record*, **33**, No. 9, 327 (1955).
8. R. Schwarz and A. Pflugmacher, *Berichte*, **75B**, 1062 (1942).
9. R. J. Dunworth, "Some Theoretical Factors in the Zone Melting Process," ANL-5360, Metallurgy Division, Argonne National Laboratory, Lemont, Ill., (February 1956).

The Systems CaF_2-LiF and CaF_2-LiF-MgF_2

W. E. Roake

Ceramic Fuels Development Operation, Hanford Laboratories Operation,

General Electric Company, Richland, Washington

ABSTRACT

Temperature-composition relationships have been measured in the CaF_2-LiF and the CaF_2-LiF-MgF_2 systems in the areas of liquidus temperatures below 1000°C. A binary eutectic composition of 80.5 mole % LiF and 19.5 mole % CaF_2 was observed to melt at 769°C. A ternary eutectic composition of 59.0 mole % LiF, 2.9 mole % MgF_2, and 13.1 mole % CaF_2 was observed to melt at 672°C.

Current interest in fused salts as metallurgical process media has led to the examination of relatively low melting fluoride mixtures. Of primary interest are those fluorides of metals whose oxides and fluorides are thermodynamically compatible with metallic uranium. Ruff and Busch (1) published phase diagrams for both systems reported here. However, their diagram for the system CaF_2-LiF is somewhat incorrect and their diagram for the system CaF_2-LiF-MgF_2 was constructed from few known points and based on the erroneous assumption that the system MgF_2-LiF contains no solid solutions. More recently Bergman and Dergunov (2) and Counts, Roy, and Osborn (3) reported solid solutions in the system MgF_2-LiF. The third binary combination, CaF_2-MgF_2, was published by Beck (4). The work reported here has defined more accurately the subject systems in the areas of such mixtures melting at temperatures below 1000°C.

Experimental

Mixtures of reagent grade CaF_2 and LiF and Baker and Adamson "purified" MgF_2 were prepared by accurate weighing of components, mixing, and melting in Pt vessels. Spectrographic analysis of the MgF_2 showed only Ca as a major contaminant of the order of 0.1%. The mixtures of fused salts were subjected to continual mechanical agitation while in the molten state, and were so mixed for 30 min before measuring cooling curves from the melt. For each mixture a rough cooling curve was observed to locate the temperature points of interest. These temperatures then were located accurately by cooling from 100°C above each point. This was done by adjusting the power supply of the electric crucible furnace to that voltage which would maintain the furnace at an equilibrium temperature 100°C below the point of interest. At least two reproducible cooling curves were charted at each point of interest. Temperature measurements within the cooling mixtures were obtained by means of a chromel-alumel thermocouple situated in a thin submerged Pt thimble. A calibrated automatic recording potentiometer was used to chart the time-temperature relationships. The chart is easily readable with an accuracy of 1°C. Cooling curve breaks and thermal arrests are generally sharp and reproducible. In those cases in which a well-defined break or arrest was not easily obtained a best estimate of the true value was chosen from smoothed curve plots of temperature points vs. CaF_2 mole %, holding the mole ratio of LiF:MgF_2 constant. Intersections with the boundaries were determined in the same manner. During the time of each experiment no variation of fixed temperature points and no salt discoloration was observed to be caused by salt oxidation, volatilization, or by slight fluoride attack on Pt.

Results

System CaF_2-LiF.—Temperature-composition relationships were measured in the CaF_2-LiF system at compositions containing greater than 60 mole % LiF. An eutectic composition of 80.5 mole % LiF was observed melting at 769°C. No evidence of intermediate compounds or of solid solutions was observed. The experimental data are recorded in Table I and are plotted in Fig. 1.

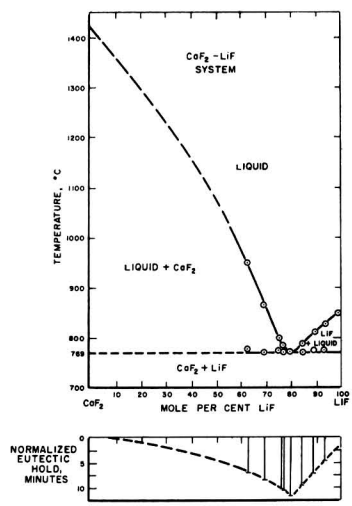

Fig. 1. Phase equilibrium diagram for the system CaF_2-LiF

Table I. Liquidus and eutectic temperatures of mixtures of calcium fluoride and lithium fluoride

CaF_2 g	LiF g	Mole % LiF	Temp of first solidification, °C	Temp of eutectic halt, °C	Time of eutectic halt, min
0	20	100	847	—	—
2.5411	13.3907	93.98	827	773	5.85
4.6596	13.3907	89.63	810	773	9.75
7.5376	13.3907	85.33	785	769	15.75
10.0830	13.3907	80.00	774	769	20.4
12.5098	13.3907	76.32	797	770	20.2
17.4064	13.3907	69.84	865	769	19.5
23.6571	13.3907	63.01	948	770	20.4
10.0800	13.3900	77.99	777	770	19.4

System CaF_2-LiF-MgF_2.—Temperature-composition relationships of the CaF_2-LiF-MgF_2 system were explored in the region of liquidus temperatures below 1000°C. A ternary eutectic composition was observed at 59.0 mole % LiF, 27.9 mole % MgF_2, and 13.1 mole % CaF_2. The melting point of the ternary eutectic is 672°C. Ternary solid solutions are formed except in the CaF_2 primary phase area (cf. Fig. 2). The melting points of CaF_2 and MgF_2 are from Rossini (5).The melting point of LiF is from Kelley (6) and was verified by measurement. Experimental data are recorded in Table II. The phase diagram showing liquidus isotherms, binary and ternary eutectic points, and the boundary curves is plotted in Fig. 2. The solid isotherms are based on experimental data, the dotted line isotherms are extrapolated. Due to the nature of the work and the time involved no attempts were made to determine the extent of binary and ternary solid solutions in the system or to locate three phase boundaries. Examination of Counts, Roy, and Osborne's MgF_2-LiF diagram coupled with the observation of the failure of some of the ternary compositions (cf. Table II) to reach the ternary eutectic discloses the expected complexity of the progress of equilibrium crystallization in the system.

Manuscript received May 18, 1956.

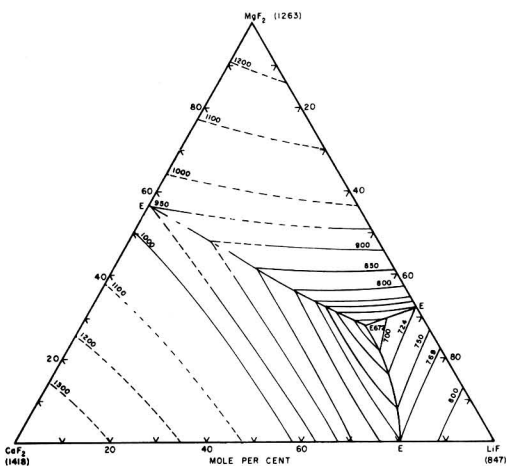

Fig. 2. The system CaF_2-LiF-MgF_2. Primary phase fields and liquidus isotherms. (Solid solutions are not shown.)

Table II. Temperature-composition data for system CaF_2-MgF_2-LiF

Composition, mole %			Fixed points on cooling curves		
			Liquidus,	Boundary,	
CaF_2	MgF_2	LiF	°C	°C	Eutectic, °C
22.9	35.0	42.1	790	—	675
9.1	30.9	60.0	728	686*	672
10.0	30.6	59.4	723	684	672
11.7	30.0	58.3	714	685	672
16.0	28.5	55.5	693*	685	672
17.8	28.0	54.2	715	685	672
20.0	27.2	52.8	740*	687	672
22.0	26.5	51.5	765*	687	672
24.5	25.7	49.8	796*	687	672
28.8	24.2	47.0	847	690	672
0	40	60	837	—	724 (binary)
7.0	37.2	55.8	812*	690	675
10	36	54	801	684	672
13	34.8	52.2	786	684	672
18.1	32.8	49.1	758	742	672
21.7	31.3	47.0	782*	755	—
26.0	29.6	44.4	825	755±3	672
28.5	28.6	42.9	849	755*	672
31.8	27.3	40.9	889	757	Not measured
0	50	50	940	—	724 (binary)
9.1	45.45	45.45	900	715	669
13.8	43.1	43.1	879	719	672
16.8	41.6	41.6	862	747	672
18.9	40.55	40.55	851	764	672
21.1	39.45	39.45	834	782	672
23.0	38.5	38.5	824	800	672
24.9	37.45	37.45	815	814	672
29.9	35.05	35.05	862	814	670
35.4	32.3	32.3	921	812	672
0	15	85	796	—	Not reached
3	14.5	82.5	788	675	Not reached
6.4	14.0	79.6	773	691	Not reached
8.7	13.7	77.6	766	701	Not reached
13.0	13.0	74.0	748	718	Not reached
17.8	12.3	69.9	748	736	Not reached
23.3	11.5	65.2	807*	735	Not reached
28.5	10.7	60.8	860*	735*	Not reached
32.5	10.1	57.4	900	727	Not reached
16.6	27.4	56.0	717	690	680
16.0	27.8	56.2	710	689	680
14.9	28.6	56.5	709	694	676
13.90	29.25	56.85	717	693	679
12.00	27.47	60.53	679	675	672
13.03	27.15	59.82	674	—	670
14.82	26.59	58.59	698	677	672
17.64	25.71	56.65	726	676	671
23.50	23.88	52.62	800	673	671
13.5	27.5	59.0	678	673	672
13.43	27.47	59.10	683	674	672
13.7	27.7	58.6	678	—	673
14.63	27.40	57.97	689	—	672
16.48	26.81	56.71	710	—	672

* Best estimate, *see* text.

Any discussion of this paper will appear in a Discussion Section to be published in the June 1958 JOURNAL.

REFERENCES

1. O. Ruff and W. Busch, *Z. Anorg. Chem.*, **144**, 87 (1925).
2. A. G. Bergman and E. P. Dergunov, *Compt. Rend. Acad. Sci. URSS*, **31**, 755 (1941).
3. W. E. Counts, R. Roy, and E. F. Osborn, *J. Am. Ceram. Soc.*, **36**, 12 (1953).
4. E. Beck, *Metallurgie*, **5**, 504 (1908).
5. F. D. Rossini, *et al.*, "Selected Values of Chemical Thermodynamic Properties," U. S. Department of Commerce, National Bureau of Standards (1952).
6. K. K. Kelley, "Contributions to the Data on Theoretical Metallurgy," U. S. Bureau of Mines Bulletin 393 (1936).

Preparation of Pure Silicon by the Hydrogen Reduction of Silicon Tetraiodide

Gustav Szekely

Chemistry Laboratory, Sylvania Electric Products Inc., Flushing, New York

ABSTRACT

The reduction of silicon tetraiodide by hydrogen to form pure silicon and hydrogen iodide has been investigated. The reaction is heterogeneous, taking place on a hot surface. Dense silicon layers as well as crystals can be deposited. The reaction gives a chemical yield as high as 96%, but the over-all best conditions found resulted in a rate of deposition of 4.4 g Si/dm²/hr at a chemical yield of 55%. Data on the purity of the silicon obtained are presented.

The reaction of silicon and iodine to form silicon tetraiodide and the fractional distillation of this compound are discussed. An apparatus is described which permits good control over the composition of a mixture consisting of two gaseous reactants, one of which is generated from the liquid state by vaporization at a uniform rate of flow.

At the inception of this work two processes for preparing pure Si were prominent. In one, Si crystals are deposited in a quartz tube, kept at 950°C, by passing Zn and $SiCl_4$ vapors through it at atmospheric pressure (1). This process is currently used to fill almost the entire demand for Si needed for semiconductor devices in this country. The second (2) permits deposition of solid Si layers on a hot Ta wire (980°C) by thermally decomposing SiI_4 vapor at a greatly reduced pressure.

The aim of this work was to find a means of combining the attractive features of both of these processes, namely convenient deposition of Si in a furnace tube at atmospheric pressure and high volatility of reactants and by-products to insure highest obtainable purity. For this purpose, the hitherto unreported reaction $2H_2(g) + SiI_4(g) = Si(s) + 4HI(g)$ was investigated.

Small-Scale Experiments

In a preliminary set of experiments H_2, purified with respect to O_2, was passed over liquid SiI_4 (mp about 120°C, bp about 300°C) and the vapor mixture then passed through graphite tubes maintained at temperatures between 900° and 1000°C. Small needles as well as more compact crystals were deposited, which by means of x-ray diffraction were unambiguously identified as elemental Si.[1] In these preliminary experiments a relatively low H_2 flow rate was used resulting in a correspondingly low deposition rate, but in one experiment the chemical yield was found to be 96%. This approaches the theoretical yield based on a calculated equilibrium constant. The SiI_4 was prepared by passing vapors of reagent grade I_2 over an inexpensive grade of Si at about 800°C.

[1] Tammann (3) showed that Si and graphite do not react until temperatures several hundred degrees above the temperatures of these experiments are reached. The absence of SiC formation at these temperatures has been confirmed by means of a chemical test, by means of x-ray diffraction, and by means of metallographic examinations.

Apparatus

Apparatus was built to study the reaction further and, incidentally, increase the rate of Si deposition. During operation, H_2 was passed through a catalytic oxygen removal unit, through a drying tower containing silica gel, through a flowmeter, and through a vessel containing liquid SiI_4. The relative amount of SiI_4 entrained in the H_2 stream depended on the vapor pressure of the liquid and thus on the temperature of this vessel. The gas mixture was passed into a graphite cylinder located inside of a quartz tube and maintained at the reaction temperature by means of high frequency induction heating. Silicon deposited in the hottest part of the graphite tube, while unreacted SiI_4 and the by-product HI could be collected in traps. In one experiment HI was frozen out and identified by its boiling point.

Results

Temperature dependence of reaction.—To study the dependence of the rate of deposition of Si on the reaction temperature a set of three runs was made. The apparatus described above was used but, in addition, a preheater was inserted which heated the gas mixture prior to entry into the reaction zone. The reaction temperature was measured with a calibrated thermocouple located at the center of the

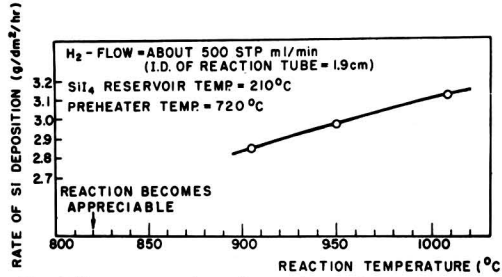

Fig. 1. Temperature dependence of rate of deposition of Si

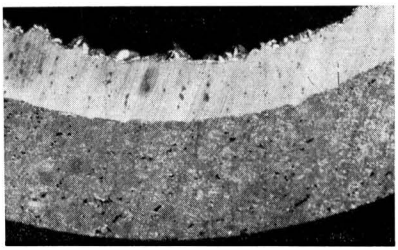

Fig. 2. Sawed through layer of Si on graphite (X8)

inner wall of the reaction tube and indicated the peak of the prevailing temperature distribution. Experimental conditions as well as the results are summarized in Fig. 1. A fourth run indicated qualitatively at which temperature the reaction begins to proceed at an appreciable rate. The low temperature coefficient of the deposition rate in the region studied together with the fact that Si deposited apparently exclusively on the hot wall of the reaction tube seemed to indicate the reaction to be a heterogeneous or surface reaction.

Packed reaction zone experiment.—To further bear on this point, the surface to volume ratio of the reaction zone was increased considerably by packing a graphite tube with small graphite cylinders. The experimental conditions were otherwise comparable to those of the above runs. By this means, it proved possible almost to double the deposition rate (in grams per hour), thus showing that the surface is involved to a considerable extent in this reaction. Presumably, the reactants are adsorbed at the surface, reaction proceeds resulting in the formation of crystalline Si and HI, the latter then being desorbed from the surface.

Deposition rate and chemical yield as functions of reactant gas composition and flow rate.—In order to obtain a further check on the reaction rates obtained so far and to observe whether these rates can be maintained over a longer period of time, a run lasting over 7 hr and at experimental conditions equivalent to those of Fig. 1 was undertaken. The resultant deposition rate turned out to be 2.8 g Si/dm²/hr, in good agreement with the previous shorter runs.

Fig. 2 shows a cross section of the Si thus obtained on its graphite substrate. On several spots of this sample, formation of crystals set in (Fig. 3). Under certain experimental conditions, it proved possible to grow crystals almost exclusively. Needles

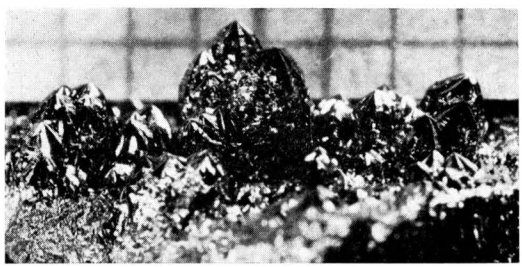

Fig. 3. Crystal growth on Si layer (x 10½)

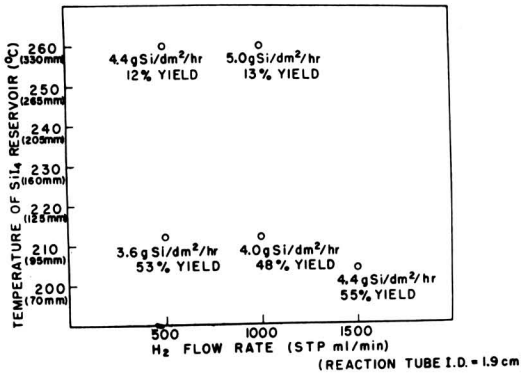

Fig. 4. Rate of deposition and chemical yield obtained in 5 runs at a reaction zone temperature of about 950°C.

as well as more compact types of crystals could be grown. Needles of regular hexagonal cross section were found, while the compact crystals frequently exhibited equilateral triangular faces, apparently (111) faces.

It was now of interest to study at least qualitatively the dependence of the rate of deposition and the chemical yield on the gas composition and velocity. The apparatus used was that described above, the preheater having been eliminated. The results of these experiments are listed in Fig. 4. Underneath

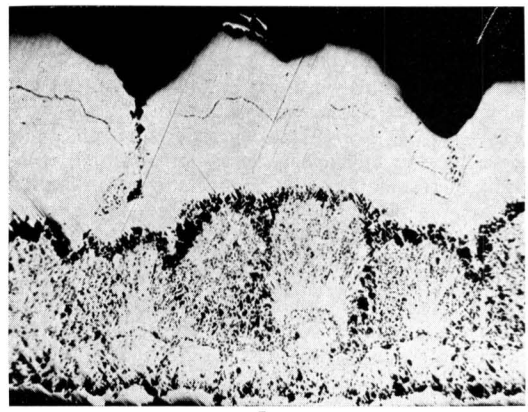

5a

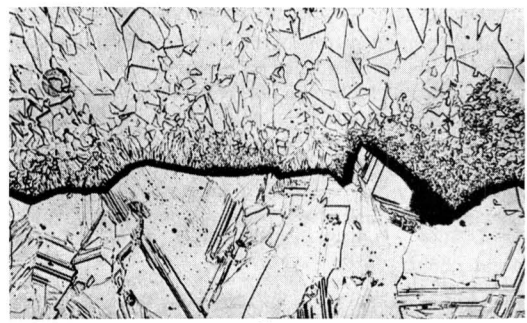

5b

Fig. 5. Series of Si layers on graphite. a. (top) polished (75X before reduction for publication); b. (bottom) detail of outermost two layers; polished and etched (300X before reduction for publication).

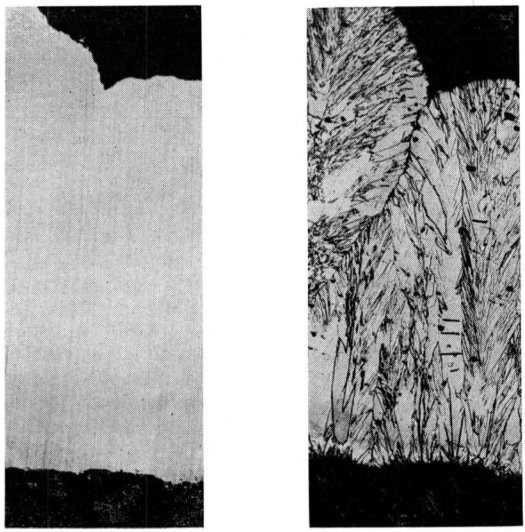

6a 6b

Fig. 6. Metallographic section of Si on graphite deposited by "best" conditions. a. left) polished (75X before reduction for publication); b. (right) polished and etched (75X before reduction for publication).

the iodide reservoir temperatures the corresponding vapor pressures of SiI_4 (4) are written in parentheses to serve as a qualitative guide to the gas composition. Deposition rates throughout this work were determined by weighing the reaction tube before and after the run. The weight thus obtained checked well with that of the Si after removal of the substrate. Chemical yields were determined by using the weight of Si deposited and the weight of the iodide vessel before and after each run.

A cross section of a successive series of Si layers deposited on graphite is seen in Fig. 5a. The outermost dense Si layer is due to the decomposition conditions on the lower right in Fig. 4. The structure of the dense layers is seen in Fig. 5b.

To substantiate these findings, another run was made at an iodide reservoir temperature of 204°C and a H_2 flow rate of about 1500 STP ml/min, but lasting more than 6 hr. The deposition rate found

Table I. Purity of starting Si (97%) and refined product (part Pyrex, part quartz apparatus)

	97% Si starting material	H_2 reduction product	
	Spectrographic analysis	Spectrographic analysis	Activation analysis
Al	$10^4 - 10^5$ ppm	$10 - 10^2$ ppm	
B	$10 - 10^2$ ppm	—	
Ba	$10 - 10^2$ ppm	—	—
Ca	$10^3 - 10^4$ ppm	—	
Cr	$10^2 - 10^3$ ppm	—	—
Cu	$10 - 10^2$ ppm	< 1 ppm	3 ppm
Fe	$10^3 - 10^4$ ppm	—	a trace
Mg	$10 - 10^2$ ppm	< 1 ppm	
Mn	$10^3 - 10^4$ ppm	—	—
Ni	$10 - 10^2$ ppm	—	—
Ti	$10^2 - 10^3$ ppm	—	
As	—	—	0.9 ppm
Na			0.03 ppm
K			0.3 ppm

Table II. Purity of starting Si (99.9%) and refined product (part Pyrex, part quartz apparatus)

	99.9% Si starting material	H_2 reduction product	
	Spectrographic analysis	Spectrographic analysis	Activation analysis
Al	$10^2 - 10^3$ ppm	—	
B	$10 - 10^2$ ppm	—	
Ba	—	—	—
Ca	$10^2 - 10^3$ ppm	—	—
Cr	$10 - 10^2$ ppm	—	—
Cu	$1 - 10$ ppm	< 1 ppm	—
Fe	$10 - 10^2$ ppm	—	—
Mg	$1 - 10$ ppm	—	
Mn	$10 - 10^2$ ppm	—	—
Ni	—	—	—
Ti	$10 - 10^2$ ppm	—	
As	—	—	—
Na			—
K			—
La			a trace

was 4.1g/dm²/hr, in fair agreement with the corresponding short run. Due to an experimental difficulty, the yield could not be confirmed. Fig. 6 shows a metallographic cross section of the deposit, again exhibiting the highly dense structure.

Analytical results.—In the preparation of SiI_4, which was used without further purification for H_2 reduction, two grades of starting material Si were used: a very inexpensive grade analyzing to be about 97% Si and a more expensive grade analyzed to be about 99.9% Si.[2] Typical analyses of these materials and the refined Si obtained from them are given in Table I and II. The spectrographic analyses are general qualitative ones. The activation analyses are described in more detail elsewhere (5). In brief, Si samples are activated by neutron bombardment. Some of the impurity atoms form radioisotopes emitting γ-radiation, the energy of which is measured and the impurity atoms are thereby identified. The γ-scintillation spectrometer permits measurement of these energies on the bombarded Si sample without carrying out any separations. It is seen that the two refining steps, formation of the iodide and reduction of this compound with H_2, resulted in considerable purification.

Substrate study.—As a substrate material for Si deposition, graphite has the advantage of being obtainable in a form of considerably higher purity than, for example, quartz. The porosity of graphite, however, causes the Si deposit to lock into the pores which makes separation of the two materials difficult. A study designed to find a substrate on which Si can be deposited, and subsequently removed readily, showed Ta to be such a material.[3] The reaction tube can be lined by a thin foil of this metal and at completion of a run, Si slides freely off the foil. The foil may require periodic replacement because of H_2 embrittlement. A sample of Si deposited in this way was analyzed by the scintillation spectrometer technique and found to contain 3.8 ppm Ta. After removing 2.8% of the sample weight by etching, the Ta content dropped below the limit of detection of the method, 2.7 ppm Ta. This, borne

[2] Both these materials are obtained from the Electro Metallurgical Company, Union Carbide and Carbon Corporation.

[3] Litton and Andersen (2) have used Ta as a substrate metal in their work with somewhat different chemical species present.

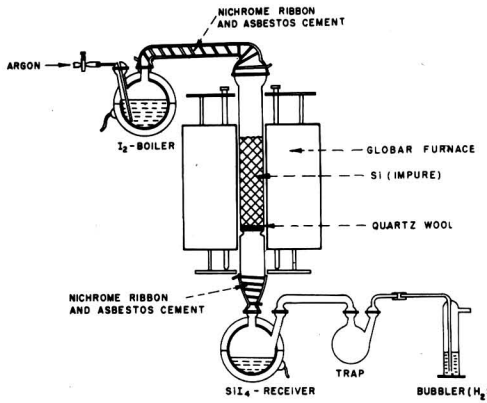

Fig. 7. Large iodination apparatus (fused quartz)

out by other similar experiments, shows the Ta contamination to be located mainly at the surface of the Si sample.

Large-Scale Experiments

It was of interest to experiment with larger equipment. All Pyrex parts in contact with SiI_4 or at elevated temperatures were eliminated and replaced by fused quartz. A fractional distillation apparatus was built to further purify the SiI_4 before its use in the H_2-reduction. The reduction apparatus was built according to a new design.

Iodination

The apparatus to carry out the reaction $Si(s) + 2I_2(g) = SiI_4(g)$ is shown in Fig. 7. Prior to operation, it is flushed with dry argon gas. The temperature of the iodine boiler is then brought up to the boiling point of I_2 (183°C) and the halogen is distilled onto a bed of raw material Si maintained at 750°-850°C (furnace tube ID = 6.2 cm). SiI_4 is collected as liquid at a rate of 1.3 kg/hr. The reaction yield is practically 100%. Frequently after about 7-9 kg of SiI_4 are collected, larger channels begin to form in the Si bed through which unreacted I_2 commences to flow. The apparatus is then opened up and a new charge of Si is placed into it. A particle size of 30-80 mesh is suitable. It has been found desirable, but not always necessary, to etch the Si raw material with HF (aq), rinse, and dry (methanol, ether) prior to insertion into the iodination apparatus.

At the end of a set of iodination runs, a wool-like residue remains in the reaction tube. Qualitative spectrographic analysis showed this Si-rich material to have a total detectable impurity content about six times that of the 99.9% Si starting material. Particularly noticeable is the enrichment of the residue in Al, B, Cr, Fe, and Mg but to a lesser extent also in other elements. These results are further confirmed by a spectrographic analysis of the oxide obtained by hydrolysis of the SiI_4. This material showed a reduction of detectable impurity content by about a factor of 30 below that in the starting Si.

Fractional Distillation

To purify the SiI_4 further, an all-quartz fractionation apparatus was built. The column (1.5 m long, 4 cm ID) was packed with small lengths of quartz tubing (about 5 x 5 mm) and kept adiabatic by the usual means of a compensating heat jacket. The still head was of the swinging funnel type and the fraction splitter also contained a pivoting funnel controlled by a magnet. The apparatus was operated at a throughput of 0.7 kg/hr, a reflux ratio of 9:1, and at atmospheric pressure. (A sample of SiI_4 was refluxed for 10 hr at atmospheric pressure without any decomposition occurring. Subsequently, most of the sample distilled between 300°-302°C.) The size of the fractions in these runs was approximately: 1st fraction = 1.8 kg, main fraction = 4.3 kg, residue in still pot = 1.8 kg.

Table III. Analytical results on fractional distillation of SiI_4 (fused quartz apparatus)

	Distillation residue	First fraction	Main fraction	
Al	10 – 10^2 ppm	1 – 10 ppm	1 – 10 ppm	Qualitative spectrographic analysis on hydrolyzed SiI_4 samples.
Cu	<1 ppm	——	——	
Mg	1 – 10 ppm	1 – 10 ppm	1 – 10 ppm	
B	>5 ppm	<0.1 ppm	<0.1 ppm	Spectrographic analysis on hydrolyzed SiI_4 samples (arced in inert atmosphere to suppress SiO bands).
As	15 ppm	11 ppm	1.6 ppm	Activation analysis on SiI_4 samples.
Na	1.4 ppm	1.3 ppm	0.16 ppm	
Fe	10 ppm	<10 ppm	<10 ppm	

An indication of the effectiveness of the fractional distillation apparatus in separating impurities from SiI_4 is obtained from Table III. On the basis of qualitative spectrographic analysis of hydrolyzates the impurity content of the distilled SiI_4 (main fraction) was reduced by a factor of about 6 below that of the iodide collected in the iodination procedure.

Hydrogen Reduction

In building a larger all-quartz H_2-reduction apparatus, it was desired to obtain improved control over the composition of the gas mixture entering the reaction chamber. Fig. 8 shows how this was accomplished. During operation of this equipment, H_2 is passed through a catalytic unit converting traces of O_2 to H_2O, through a silica gel drying tower, through a mechanical filter, into a flow meter, through a preheater maintained at about 720°C, and into a Venturi. Liquid SiI_4 is maintained in a reservoir from which at intervals it is transferred to a U-tube by the application of argon pressure. This U-tube is of special design. In one arm of the U, a cylindrical quartz felt wick is partly immersed in the liquid SiI_4. A heater surrounds the portion of the U-tube containing the unimmersed part of the wick. By capillary action SiI_4 is drawn up into the

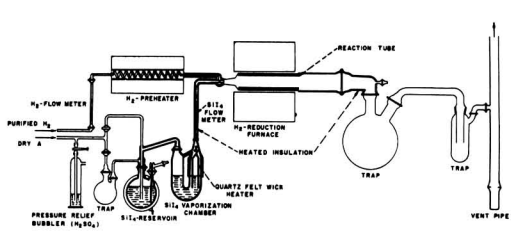

Fig. 8. Large H_2-reduction apparatus

wick and is smoothly vaporized off its surface. The rate of vaporization is controlled by the temperature of the heater. In this way a large range of uniform flow rates can be obtained through the SiI_4 flow meter and into the Venturi, where the two gaseous constituents are thoroughly mixed and passed into the reduction zone. The train is completed by a trap in which unreacted SiI_4 is collected, a second trap where HI can be frozen out, and finally a vent tube through which excess H_2 leaves the system.

At the present time a study is under way with this apparatus to determine the dependence of deposition rate and chemical yield upon the gas composition and velocity. It can be stated that deposition rates closely approaching those obtained with the small apparatus already have been obtained.

Acknowledgments

The contributions of the following are greatly appreciated: C. O. Creter, apparatus construction and experimental runs; K. D. Earley and V. C. DeMaria, glass and quartz apparatus construction; J. F. Cosgrove, scintillation spectrometric analyses; T. J. Veleker, spectrographic analyses; R. L. Rupp, boron determinations; H. Woods, metallographic examinations of Si samples; J. Pacher, x-ray diffraction work.

Much valued discussion is acknowledged with G. H. Morrison, D. J. Bracco, and D. H. Baird.

Manuscript received April 25, 1957. Part of this paper was presented before the Cincinnati Meeting, May 1-5, 1955.

Any discussion of this paper will appear in a Discussion Section to be published in the June 1958 JOURNAL.

REFERENCES

1. D. W. Lyon, C. M. Olson, and E. D. Lewis, *J. (and Trans.) Electrochem. Soc.*, **96**, 359 (1949).
2. F. B. Litton and H. C. Andersen, *This Journal*, **101**, 287 (1954.)
3. G. Tammann, *Z. anorg. u. allgem. Chem.*, **115**, 141 (1921).
4. H. C. Andersen and L. H. Belz, *J. Am. Chem. Soc.*, **75**, 4828 (1953).
5. G. H. Morrison and J. F. Cosgrove, *Anal. Chem.*, **27**, 810 (1955).

Electrolytic Reduction of 2-Amino-4-chloropyrimidine, 2-Amino-4-chloro-6-methylpyrimidine, and 2-Aminopyrimidine

Kiichiro Sugino, Kozo Shirai, Taro Sekine, and Keijiro Odo

Laboratory of Organic Electrochemistry, Department of Chemical Engineering, Tokyo Institute of Technology, Tokyo, Japan

ABSTRACT

2-Amino-4-chloropyrimidine and its 6-methyl derivative give two polarographic waves in the *p*H region of 7.4-8.9; 2-aminopyrimidine and 2-amino-6-methylpyrimidine yield but a single wave in this region. Macroscale electrolysis at lead or mercury cathodes in ammoniacal medium shows that the first wave of the chlorocompounds arises from reductive dehalogenation. The second wave of the chlorocompounds coincides with the single wave of their parent compounds, the 2-aminopyrimidines, and is ascribed to reduction of the pyrimidine nucleus in both cases. The macroreduction of 2-aminopyrimidine takes place easily at lead or mercury cathodes in ammoniacal medium to yield 2-aminodihydropyrimidine. The mechanism of reduction is tentatively identified as pure electrolytic reduction.

The reduction of 2-amino-4-chloropyrimidine to 2-aminopyrimidine at cathodes of lead and mercury in aqueous methanolic ammonium sulfate was found to be impractical on a preparative scale. On the other hand at spongy cadmium the reduction takes place in 90% yield. At spongy zinc the yield is poorer due to further reduction of the pyrimidine nucleus. However, for the reduction of 2-amino-4-chloro-6-methylpyrimidine zinc is superior to cadmium as a cathode.

2-Amino-4-chloropyrimidine and its 6-methyl derivative suspended in dilute aqueous ethanolic alkali are reduced at a lead cathode to 2-aminopyrimidine and 2-amino-6-methylpyrimidine, respectively, in 60% yield together with further reduced product (1). Further investigation resulted in a method for nearly quantitative production of 2-amino-6-methylpyrimidine (2). 2-Amino-4-chloro-6-methylpyrimidine suspended in an aqueous-methanolic solution of ammonia and ammonium sulfate is reduced at a spongy zinc cathode with greater than 90% yield and about 80% current efficiency. However, when the same procedure was applied to 2-amino-4-chloropyrimidine, 2-aminopyrimidine could not be obtained in greater than 60% yield due to further reduction of the pyrimidine nucleus. If cadmium is substituted for zinc, the yield approaches 90% with a current efficiency of 65% (3).

The anomalous behavior of these compounds prompted polarographic and macroelectrolytic studies which would throw some light on the mechanism

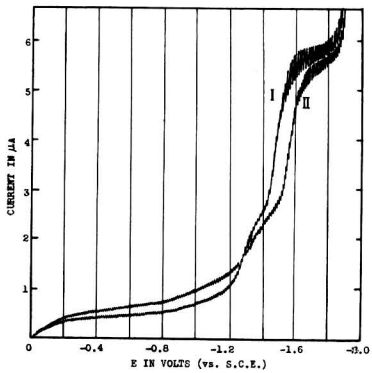

Fig. 1. Polarograms for 2-amino-4-chloropyrimidine and 2-amino-4-chloro-6-methylpyrimidine at pH 7.4. Curve I, 2-amino-4-chloropyrimidine, $E^{1/2}$: —1.35 v (1st wave) and —1.48 v (2nd wave); curve II, 2-amino-4-chloro-6-methylpyrimidine, $E^{1/2}$: —1.36 v (1st wave) and —1.56 v (2nd wave).

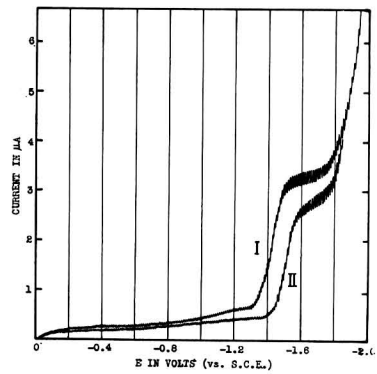

Fig. 2. Polarograms for 2-aminopyrimidine and 2-amino-6-methylpyrimidine at pH 7.4. Curve I, 2-aminopyrimidine, $E^{1/2}$: —1.45v; Curve II, 2-amino-6-methylpyrimidine, $E^{1/2}$: —1.53 v.

of the reductions. The present paper reports the results of these studies and is also a summary of work on chloropyrimidines carried out in this laboratory.

No literature was found on the electrolytic reduction of these compounds.

Polarographic studies were carried out in the *p*H range of 4.7-10.3. In this paper, only the polarograms at *p*H 7.4 of each compound are shown for purposes of comparison. The polarograms at *p*H 8.9 are included, because this is the approximate *p*H of the macroscale electrolyses.

Experimental

An improved Heyrovsky-Shikata polarograph, Model 52-Type PS, made by Yanagimoto Company, Kyoto, Japan, was used with a galvanometer having an intrinsic sensitivity of 3.29×10^{-9} μa/mm. The sensitivity used at all times was 3.29×10^{-8}. A cell of conventional design having a saturated calomel electrode (S.C.E.) as reference electrode was used. The dropping mercury electrode had a drop time of 3.5 sec at 45 cm mercury height; the capillary constant, $m^{2/3} t^{1/6}$, was 1.37 $mg^{2/3}$ $sec^{-1/2}$. A TOA DEMPAS type HM-3 *p*H meter and glass electrode was used for *p*H measurements. Stock solutions of the compounds were prepared by dissolving 1 millimole in 50 cc ethanol. 2-Amino-4-chloropyrimidine (mp 164°-165°C dec.[1]), 2-amino-4-chloro-6-methylpyrimidine (mp 182°-183°C), and 2-amino-6-methylpyrimidine (mp 158°-159°C) were prepared and purified according to previously published procedures (2,4). 2-Aminopyrimidine, obtained from Calco Chemical Division, American Cyanamid Company, Bound Brook, New Jersey, was recrystallized from hot benzene (mp 127°-128°C). The buffer solutions used were:

(*a*) CH_3COOH-CH_3COONa, *p*H 4.7-5.6
(*b*) Na_2HPO_4-KH_2PO_4, *p*H 6.8-7.4
(*c*) $Na_2B_4O_7$-H_3BO_3, *p*H 8.0
(*d*) $Na_2B_4O_7$-NaOH, *p*H 8.9-10.3

Test solutions were prepared from the proper volumes of stock and buffer solutions to produce a concentration of the pyrimidine of 6×10^{-4}M/l in all cases. The solutions were deoxygenated with hydrogen for 15 min before use.

[1] All melting points are uncorrected.

Polarographic Studies

Polarographic behavior at pH 7.4.—Polarograms obtained from solutions of the four pyrimidines buffered at *p*H 7.4 are shown in Fig. 1 and 2. Table I lists the values of the diffusion current, i_d, and the diffusion current constant, *I*, for each compound.

The half-wave potentials of the first waves are nearly identical, but the second wave for the 6-methyl compound occurs at a potential approximately 80 mv more negative than that of the parent 2-amino-4-chloropyrimidine.

2-Aminopyrimidine and 2-amino-6-methylpyrimidine each give a single well-defined wave at —1.45 and —1.53 v vs. S.C.E., respectively. Again the half-wave potential for the 6-methyl derivative is 80 mv more negative than that of its parent compound.

Comparison of the polarograms of Fig. 1 and 2 demonstrates the probability that the second waves of the chlorinated compounds correspond to the single waves of the parent compounds. The reduction wave of 2-aminopyrimidine was found to be due to the reduction of pyrimidine nucleus based on the result of macroelectrolysis to be described later. If the second waves of 2-amino-4-chloropyrimidine (and its 6-methyl derivative) are regarded as the reduction wave of the pyrimidine nucleus, the first waves may be due to reductive dehalogenation.

Table I.

	i_d (μa)		I (i_d/C $m^{2/3} t^{1/6}$)	
	Wave I	Wave II	Wave I	Wave II
2-amino-4-chloropyrimidine	1.02	2.04	1.23	2.48
2-amino-4-chloro-6-methylpyrimidine	0.86	2.17	1.04	2.64
2-aminopyrimidine	—	2.03	—	2.47
2-amino-6-methylpyrimidine	—	1.48	—	1.80

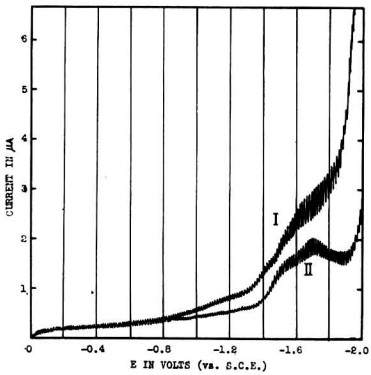

Fig. 3. Polarograms for 2-amino-4-chloropyrimidine and 2-amino-4-chloro-6-methylpyrimidine at pH 8.9. Curve I, 2-amino-4-chloropyrimidine, $E^{1/2}$: —1.40 v (1st wave) and —1.57 v (2nd wave); Curve II. 2-amino-4-chloro-6-methylpyrimidine, $E^{1/2}$: —1.46 v (1st wave) and —1.63 v (2nd wave).

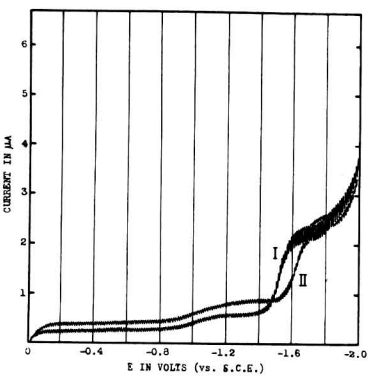

Fig. 4. Polarograms for 2-aminopyrimidine and 2-amino-6-methylpyrimidine at pH 8.9. Curve I, 2-aminopyrimidine, $E^{1/2}$: —1.52 v; Curve II, 2-amino-6-methylpyrimidine, $E^{1/2}$: —1.62 v.

Polarographic behavior at pH 8.9.—Polarograms of solutions of the four compounds buffered at pH 8.9 are shown in Fig. 3 and 4. The values of i_d and I are also given in Table II.

These polarograms are of similar shape to those at pH 7.4, but the wave heights are considerably lower. The half-wave potentials also shift to more negative values.

Polarographic behavior of hydrogenated pyrimidines.—Polarograms of buffered solutions of the hydrogenated pyrimidines in the pH region 4.7-8.9 showed no wave prior to the final current rise of hydrogen ion discharge.

Table II.

	i_d (μa) Wave I	i_d (μa) Wave II	I ($i_d/C\ m^{2/3}\ t^{1/6}$) Wave I	I ($i_d/C\ m^{2/3}\ t^{1/6}$) Wave II
2-amino-4-chloropyrimidine	0.66	0.59	0.80	0.72
2-amino-4-chloro-6-methylpyrimidine	0.92	0.33	1.12	0.40
2-aminopyrimidine	—	1.08	—	1.32
2-amino-6-methylpyrimidine	—	1.19	—	1.45

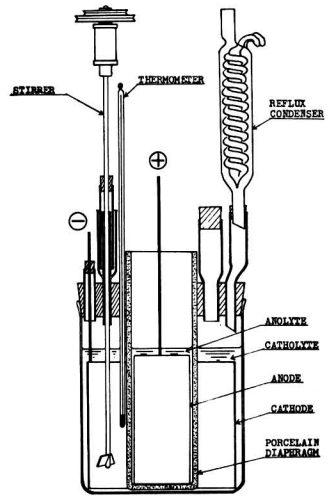

Fig. 5. Electrolytic cell

Macroelectrolysis

Apparatus.—The apparatus used is similar to that described in the preceding paper (5), but is of somewhat different design; details are shown in Fig. 5.

The catholyte (suspensions except for 2-aminopyrimidine) was thoroughly stirred by a glass stirrer rotated at 800 rpm. Anodes were chiefly of platinum in the small-scale electrolyses. In the anolyte containing both sulfate and chloride ions, the pure lead dioxide electrode previously reported by one of the authors could be used.[2]

Results and Conclusions

1. *Preliminary investigation of 2-amino-4-chloropyrimidine.*—Macroreduction of 2-amino-4-chloropyrimidine suspended in an aqueous methanolic solution of ammonium sulfate[3] was carried out at lead or mercury as cathode in order to confirm the postulated polarographic behavior. The electrolysis conditions were:

Anode: Pt, anolyte: 50 cc 0.2*N* H_2SO_4, catholyte: (*a*) 1.30 g, (*b*) 6.50 g 2-amino-4-chloropyrimidine, 6.6 g $(NH_4)_2SO_4$, 45 cc methanol, 45 cc water, a few cc of ammonia added to adjust the pH at 7.6, cathode area: Hg, 0.33 dm^2, Pb, 0.65 dm^2, cathodic current density: 1.5 amp/dm^2, temp: (*a*) 12°-18°C, (*b*) 60°-65°C.

It was found that even a small current density of 0.32 amp/dm^2 seemed to exceed the limit, due to the extremely low solubility of the compound in the catholyte. In case (*a*), therefore, 10-11 hr were needed to complete the reduction. At the higher temperature this rate was not increased. In case (*b*), after reduction for 4 hr, 4.8-4.9 g of starting material was recovered unchanged.

[2] This electrode is a thick sheet of pure lead dioxide of rectangular shape described in Method I in Ref. (6) and now being manufactured at Sanwa Pure Chemical Co., Dodobashi-cho, Ohta-ku, Tokyo, Japan.

[3] The reduction of 2-amino-4-chloropyrimidine cannot be carried out in acidic medium due to its instability. In alkaline medium at a lead cathode, some difficulty was experienced performing the reduction described above; at inefficient cathodes such as copper, 2-amino-4-alkoxypyrimidine is formed in the presence of alcohols.

After reduction a large amount of chloride ion was detected in the catholyte, indicating dechlorination by reduction. Then the catholyte was treated according to the procedure described later to isolate 2-aminopyrimidine. However, this did not succeed, suggesting the further reduction of 2-aminopyrimidine. In this procedure, upon evaporation of the ether extract, no material was recovered. The residue was again extracted with ethanol. The evaporation of this extract left a glutinous substance which would not crystallize.

In a separate run, 1.30 g 2-amino-4-chloropyrimidine suspended in the same catholyte was reduced at a lead cathode at a current density of 3 amp/dm^2 at 12°-18°C for 11 hr. After 5 hr of electrolysis an additional 6.6 g ammonium sulfate was added to decrease the cell resistance. After the reduction a saturated solution of ammonium picrate was added to the electrolyte without any prior treatment. A picrate melting at 192°C (recrystallized from ethanol) which differed from that of 2-aminopyrimidine was obtained. This was later identified as the derivative of 2-aminodihydropyrimidine.

From these results it was concluded that the polarographic reduction of 2-amino-4-chloropyrimidine on a macroscale was impractical due to its slowness. Moreover, the reduction yielded the further reduced 2-amino-dihydropyrimidine rather than the desired 2-aminopyrimidine. Therefore different solution compositions and cathode materials were investigated in an attempt to improve the yield of 2-aminopyrimidine.

When the reductions of 2-amino-4-chloropyrimidine and also its 6-methyl derivative in very dilute aqueous ethanolic sodium hydroxide were carried out at a lead cathode, 2-aminopyrimidine and its 6-methyl analog were obtained in 60% yield. If methanol is substituted for ethanol the corresponding 4-methoxy derivatives were obtained due to alkaline methanolysis being more rapid than the reductive dehalogenation.[4] The results are shown in Table III.

The reduction may take place through chemical dehalogenation by the lead cathode followed by reelectrodeposition of lead from the alkaline catholyte.[5] This observation led to the following improved method for the preparation of 2-aminopyrimidine and its 6-methyl derivative.

2. *Preparation of 2-aminopyrimidine and its 6-methyl derivative by the electrolytic reduction of 2-amino-4-chloropyrimidine and 2-amino-4-chloro-6-methylpyrimidine.*—A suspension of 2-amino-4-chloropyrimidine and also 2-amino-4-chloro-6-methylpyrimidine in an aqueous methanolic solution of ammonia and ammonium sulfate was reduced at a higher temperature using a spongy cadmium or zinc cathode respectively to give 2-aminopyrimidine and its 6-methyl derivative in nearly quantitative yields. The completeness of the reduction could be estimated by the disappearance of the crystals of the chloropyrimidines and the appearance of those of the corresponding 2-aminopyrimidines as shown by microscopic examination of the cooled catholyte. These crystals are easily differentiated by their characteristic form.

After reduction, the catholyte was neutralized with acid and the insoluble matter filtered off. The solution was then evaporated to dryness under reduced pressure. The residue was treated with sodium bicarbonate to regenerate free 2-aminopyrimidine (or its 6-methyl compound) which was then extracted with hot benzene or ether. The extract was evaporated to dryness to give crystals of 2-aminopyrimidine (or its 6-methyl compound).

The results of the reduction of 2-amino-4-chloropyrimidine at a cadmium cathode are shown in Table IV; the yields are the optimum obtainable.

The results of the reduction of 2-amino-4-chloro-6-methylpyrimidine at zinc (2) are shown in Table V.

It was observed that the reduction at zinc and at cadmium began to occur when the temperature was raised sufficiently even though current was not passed. This observation suggested that the reaction might again be a purely chemical one of 2-amino-

Table III.

Anode: Platinum; anolyte: 0.5% sodium hydroxide solution; catholyte: (1) 6.45 g 2-amino-4-chloropyrimidine, 75 cc 80% ethanol, 0.4 g NaOH, (2) 7.18 g 2-amino-4-chloro-6-methylpyrimidine, 85 cc 80% ethanol, 0.4 g NaOH; cathodic current density: 2.5-5.0 amp/dm^2; temp: 40-55°C; amount of current: 3.0-3.5 times the theoretical.

Run No.	2-amino (6-Me) pyrimidine* g	%	Others %
1	2.81	60	about 40
2	3.75	60	40

* mp 2-aminopyrimidine 118°C, 2-amino-6-methylpyrimidine 156-157°C.

Table IV. Reduction of 2-amino-4-chloropyrimidine at Cadmium

Anolyte: 40 cc 0.2*N* H_2SO_4; cathode: spongy cadmium deposited on iron from a catholyte containing 7.32 g $Cd(OH)_2$; catholyte: 6.50 g 2-amino-4-chloropyrimidine, 6.6 g $(NH_4)_2SO_4$, 3.3 cc 28% NH_4OH, 100 cc 1:1 methanol water, *p*H 7.2-7.4; current: 1 amp; current density: 2.0 amp/dm^2; temperature: 72°-73°C; current consumed: 3.38 amp-hr.; yield: 4.30 g (91%) 2-aminopyrimidine, mp 124°-125°C.

Table V. Reduction of 2-amino-4-chloro-6-methylpyrimidine at zinc

Anolyte: 50 cc 0.2*N* H_2SO_4; cathode: spongy zinc deposited on zinc from catholyte containing $ZnSO_4 \cdot 7H_2O$; starting catholyte: 14.36 g 2-amino-4-chloro-6-methylpyrimidine, 2.5 g $(NH_4)_2SO_4$, 90 cc 1:1 methanol water, a little NH_4OH added to adjust the *p*H to 7-9; catholyte of runs 2-4: the catholyte of the previous run after removal of the 2-amino-6-methylpyrimidine which crystallized out on cooling to −10°C addition of 14.36 g of starting material and readjustment of *p*H; current density: 2.5 amp/dm^2; temp. 60°-65°C.

Run	Current passed (amp-hr)	Yield (g)	%	Current efficiency %
1	6.50	10.02 (8.63) *	91	75
2	5.57	(9.62)	88	85
3	5.83	(10.10)	93	85
4	6.80	(10.21)	94	74

* Figures in parentheses are yields of product obtained on cooling the catholyte to −10°C.

[4] When an inefficient electrode, such as copper, was used, the product consisted of 2-amino-4-ethoxypyrimidine in the concentrated ethanolic solution.

[5] Sodium hydroxide was useful to dissolve lead chloride formed on the electrode surface by chemical reaction. Ammoniacal catholyte was inefficient for the same purpose, because it could not dissolve lead chloride.

chloropyrimidines with the cathode metal and that the current was being used simply to reduce the metal ion thus formed back to metal. However, little noticeable change occurred at the electrode surface.

3. *Electrolytic reduction of 2-aminopyrimidine at a lead cathode in ammoniacal medium.*—In an attempt to duplicate the reduction corresponding to the polarographic wave and to identify the product resulting from the reduction of the pyrimidine nucleus a run was made with 2-aminopyrimidine as starting material at a lead cathode.

Anode: platinum; anolyte: 60 cc 2*N* H_2SO_4; catholyte: 19.0 g of 2-aminopyrimidine, 6.6 g $(NH_4)_2SO_4$, 200 cc water, *p*H of 6.0-8.0 maintained by adding sulfuric acid during the electrolysis; amp: 3; cathodic current density: 3.0 amp/dm^2; temp: 10°-12°C. The theoretical amount of current for 4H was passed.

It was found that hydrogen began to be evolved vigorously at the cathode after an amount of electricity equivalent to 2H[6] had been passed. It was also found that the reduction product was stable only at low temperatures in aqueous medium so that cooling in an ice-bath was necessary to obtain reasonable yields.

The reduction product was obtained as the picrate only, by adding a saturated solution of ammonium picrate to the ice-cooled catholyte after reduction. (The yield was 54.1 g or 83% of theoretical for the dihydro compound.) The picrate melted at 192°C and decomposed on crystallization from hot water; it can be recrystallized from ethanol without change in melting point, indicating a single compound.

Anal. calcd for $C_{10}H_{10}O_7N_6$: C, 36.8; H, 3.09; N, 25.8
Found: C, 36.6; H, 3.08; N, 25.7

In order to convert this compound to a stable product for identification a catalytic hydrogenation of the catholyte was carried out by the following procedure.

Fifty cc of the catholyte was reduced by hydrogen at atmospheric pressure in the presence of 2 g Pd-$CaCO_3$ catalyst (Pd: 1.3%) at 15°C. After absorbing about 1 mole of hydrogen based on moles of picrate obtained (749 cc at 0°C and 760 mm) 10.9 g of a picrate was obtained. The picrate melted at 179°-180°C after recrystallization from ethanol. The monohydrochloride and carbonate derived from the picrate melted at 145°-146°C and 237°C (dec.), respectively.

Anal. Picrate:
calcd for $C_{10}H_{12}O_7N_6$: C, 36.6; H, 3.69; N, 25.6
Found: C, 36.5; H, 3.44; N, 25.4
Hydrochloride:
calcd for $C_4H_{10}N_2Cl$: C, 35.4; H, 7.43; Cl, 26.2
Found: C, 35.4; H, 7.17; Cl, 26.0

The picrate may be that of 2-amino-tetrahydropyrimidine[7] based on the quantity of hydrogen absorbed and the elemental analysis. Decomposition by alkali (a mixture of 2.5 g of the hydrochloride, 10 g NaOH in 150 cc water was heated) resulted in the formation of 1,3-diaminopropane (dihydrochloride; mp 243°C, calcd for $C_3H_{12}N_2Cl_2$; N, 19.05; found: N, 18.80), ammonia, and carbon dioxide. The absence of formic acid among these products eliminated the possibility that the compound was 2-aminohexahydropyrimidine or contained any of the latter as contaminant.[8] The decompositions in alkali are formulated as:

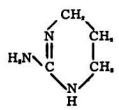

$$+2\,H_2O = H_2N(CH_2)_3NH_2 + CO_2 + NH_3$$

and:

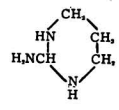

$$+ 2H_2O \rightarrow NH_2(CH_2)_3NH_2 + HCOOH + NH_3$$

Catalytic hydrogenation did not occur after the catholyte had been heated to decomposition.

From these results, the product of the electrolytic reduction of 2-aminopyrimidine was shown to be an unstable 2-amino-dihydropyrimidine.

The reduction of 2-aminopyrimidine at a mercury cathode was found to proceed in the same manner as that at a lead cathode and to the same product. The reduction of 2-amino-6-methylpyrimidine, will be reported later.

Nature of the reduction process.—By combining the results of the polarographic study and the macroelectrolysis, the nature of each reduction process is considered to be as follows:

1. It has been indicated by polarography that 2-amino-4-chloropyrimidine and its 6-methyl compound are reduced electrolytically not only to the dechlorination product, but also to a hydrogenation product of the pyrimidine nucleus. Results of preliminary macroelectrolysis at a lead or mercury cathode in ammoniacal solution substantiated these observations.

2. The reduction of 2-amino-4-chloropyrimidine and its 6-methyl compound at cadmium and zinc, respectively, in ammoniacal solution seems to be of a different nature from the polarographic reduction. This may be the chemical reaction of the starting material with the cathode surface in the presence of ammonia which dissolves the resulting metal chloride, the current being used mainly to redeposit metal on the cathode. In this case, the reduction may be carried out at the potential at which the deposition of metal occurs if the current density is less than the limiting one for the reduction of metal ion to metal. However, if a current greater than the limiting one is applied or the electrolysis is continued after all 2-amino-4-chloropyrimidine or its 6-methyl compound disappears, a hydrogenation product of the pyrimidine nucleus will be formed.

[6] The value of "n" obtained by the analysis of polarogram at *p*H 7.4 was about 1.3.

[7] Recently, Smith and Christensen (8) obtained 2-amino-dihydropyrimidine (?) and 2-amino-tetrahydropyrimidine by the catalytic hydrogenation of 2-aminopyrimidine and 2-amino-4,6-dichloropyrimidine, respectively. They reported that the dihydrochlorides melted at 231°C (2-amino-dihydro-) and 208°C (2-aminotetrahydro-). The reference to the patent of Sugino in their paper is incorrect.

[8] Kitani and Sodeoka (7) carried out the hydrogenation of 2-amino-4,6-dichloropyrimidine with a Pd catalyst. They reported 2-aminohexahydropyrimidine as the final product, the picrate and carbonate of which melt at 179°-180° and 237°C, respectively. They did not carry out the decomposition of this compound by alkali.

The reason for obtaining 2-aminopyrimidine and its 6-methyl compound quantitatively by a suitable combination of chloropyrimidine with the metal appears to depend entirely on the nature of the chemical reaction. 2-Aminopyrimidine and 2-amino-6-methylpyrimidine were not obtained quantitatively at both metals. Of the two metals, zinc is more active than cadmium. The parent 2-amino-4-chloropyrimidine was more reactive than its 6-methyl compound.

3. The reduction of 2-aminopyrimidine at lead cathode in ammoniacal solution seems to be essentially a pure electrochemical reduction corresponding to the polarographic wave. This gives a hydrogenation product of pyrimidine nucleus, the unstable 2-aminodihydropyrimidine.

Summary

1. 2-Amino-4-chloropyrimidine or its 6-methyl compound is reduced polarographically first to 2-aminopyrimidine or its 6-methyl compound and then to the hydrogenated pyrimidine. At cathodes of lead or mercury in an ammoniacal catholyte macroreduction proceeds in two successive rapid steps to a hydrogenation product of the pyrimidine nucleus. However, it is of dubious practical preparative value due to slowness necessitated by low solubility of the starting material. On the other hand, the macroreduction of 2-aminopyrimidine itself on account of its solubility proceeds very easily even at low temperature to the unstable 2-aminodihydropyrimidine in a pure state. This is the reaction corresponding to the polarographic wave.

2. At cathodes of cadmium or zinc at a higher temperature another reaction can occur. 2-Amino-4-chloropyrimidine or its 6-methyl compound is reduced to the corresponding 2-aminopyrimidine. Almost quantitative yields may be obtained by the selection of cathode metal suitable to each compound.

Manuscript received Nov. 3, 1955. This paper was prepared for delivery before the Pittsburgh Meeting, Oct. 9-13, 1955.

Any discussion of this paper will appear in a Discussion Section to be published in the June 1958 JOURNAL.

REFERENCES

1. K. Sugino and K. Shirai, *J. Chem. Soc. Japan, Pure Chemistry Section*, **70**, 111 (1949).
2. K. Sugino, K. Odo, and K. Shirai, *ibid.*, **71**, 396 (1950); K. Shirai, Y. Usui, and K. Odo, *J. Electrochem. Soc. Japan*, **20**, 28 (1952).
3. K. Shirai, *ibid.*, **21**, 387 (1953).
4. K. Sugino, K. Odo, K. Shirai, and Y. Sugito, *J. Chem. Soc. Japan, Industrial Chemistry Section*, **53**, 219 (1950).
5. M. Yamashita and K. Sugino, *This Journal*, **104**, 100 (1957).
6. K. Sugino, *Bull. Chem. Soc. Japan*, **23**, 115 (1950).
7. K. Kitani and H. Sodeoka, *J. Chem. Soc. Japan, Pure Chemistry Section*, **74**, 624 (1953).
8. V. H. Smith and B. D. Christensen, *J. Org. Chem.*, **20**, 829 (1955).

Preparation of Feed Materials for Electrolytic Production of Thorium Metal

Charles E. Fisher and James L. Wyatt

Horizons Incorporated, Cleveland, Ohio

ABSTRACT

A potentially economical method for production of thorium metal is the electrolysis of fused thorium tetrachloride in sodium chloride. Preparation of suitable feed constituents for the electrolyte is described. Thorium nitrate was converted to thorium tetrachloride by aqueous chemical and thermal decomposition techniques; intermediate steps include the formation of an ammonium complex which may be dehydrated.

During the past decade much emphasis has been placed on the development of processes for the production of fissionable materials, thorium as well as uranium. Because of the greater availability of Th, and probable lower cost, it seems almost a certainty that the civilian atomic energy program will utilize its potentialities to the fullest extent in the not too distant future.

Dunworth (1) has outlined the possible role of Th in nuclear energy and emphasized its potentiality. Carlson, *et al.* (2) discussed all phases of Th production from ore processing to finished metallurgical products, following techniques developed at Ames. This is the only method for producing Th that has been operated on a large scale. A brief description of the more promising methods of preparing Th is given by Hampel (3).

Driggs and Lilliendahl (4) produced Th electrolytically, and Kaplan (5) describes the preparation of Th by electrolysis of fused salt systems.

This paper describes the pilot and development programs which were carried out in order to produce Th-bearing cell feed materials suitable for conversion to metal. A companion paper (6) describes in part the metal production phase.

An exhaustive laboratory evaluation here (7) of the various methods for preparation of Th led to the conclusion that electrolysis of the fused chloride is

by far the most feasible method for metal production. Accordingly, this system has been established, and has been operated on a small tonnage basis to produce quantities of high quality metal.

Feed materials processing is not too dissimilar from the Ames procedures (8). Thorium nitrate is reacted with sodium carbonate to produce thorium oxycarbonate, which is dissolved in HCl, the chloride complexed with NH_4Cl, dried, and separated by thermal decomposition. The anhydrous thorium tetrachloride is utilized as cell feed for preparation of Th metal.

Deposits of metal produced by electrolysis, consisting of coarse, granular metal interspersed with salt, are removed from the cells periodically, crushed, and recovered by aqueous techniques. The process lends itself well to remote operation, is relatively economical to operate, and utilizes inexpensive reagents and standard chemical engineering equipment for all processing steps except electrolysis. Recognized engineering organizations have estimated that production costs of a different order of magnitude may be realized as compared with reported costs for the Ames process (7).

Feed Materials Preparation

Any metal production operation dealing with fuel materials for atomic power must of necessity encompass techniques which provide for utilization of materials from which fission products have been extracted. While many changes undoubtedly will occur during the coming years, at the present time a nitric acid solution step is contemplated; it therefore is a requirement of the process that the feed materials preparation end be able to process nitrates.

The development operations herein reported have been established with this requirement in mind, the starting raw material being crystalline form of hydrated thorium nitrate. The process is equally suitable for carbonates, oxalates, oxides, and other compounds.

Conversion Chemistry

The electrolytic process requires anhydrous chloride feed. Early experiments demonstrated that aqueous Th solutions evaporated to dryness decomposed to produce first a thorium oxychloride, then a thorium oxide, giving off hydrogen chloride gas. Even under conditions during which hydrogen chloride atmospheres under pressure were maintained, dewatering of thorium chloride without oxide formation proved to be a major problem.

Thorium tetrachloride forms a complex with NH_4Cl which can be dehydrated under atmospheric pressure with either an inert atmosphere or a partial HCl atmosphere to produce an anhydrous thorium complex. The complex may then be broken up by heating to an elevated temperature, driving off NH_4Cl, and leaving anhydrous thorium chloride.

Pilot Preparation of Feed Materials

Process

Figure 1 is a flow diagram of the procedure which was established for the aqueous preparation of anhydrous cell feed. The operation involves the following steps: preparation of thorium nitrate and sodium carbonate solutions; precipitation of thorium oxycarbonate; dissolution of thorium oxycarbonate in HCl; complexing with NH_4Cl; dehydration; sublimation; and fusion.

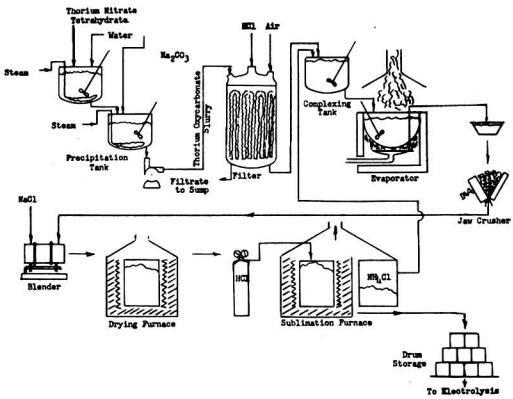

Fig. 1. Flow diagram for preparation of cell feed

Thorium nitrate was supplied by the Atomic Energy Commission in crystalline, hydrated form. It was dissolved in hot water and added directly into a solution of sodium carbonate, where the following reaction occurred:

$$Th(NO_3)_4 \cdot xH_2O + 2Na_2CO_3 \xrightarrow{H_2O} ThOCO_3 + 4NaNO_3 + CO_2 + xH_2O$$

The thorium oxycarbonate precipitation is quantitative.

Subsequent steps included settling the precipitate, decanting the nitrate solution, repulping in fresh water, repeating the decant step, and finally filtering on a vertical pressure-type Oliver filter. Filtrates were found to be completely free of radioactivity and hence could be directed to waste disposal without any unusual safeguards.

Then 37% HCl was pumped directly into the pressure filter, where it reacted with the thorium oxycarbonate to produce an aqueous thorium chloride solution. The enclosed pressure filter was ideally suited to the dissolution operation, since it confined all radioactive vapors.

The thorium chloride solution was pumped into a mixer vessel to which were added 2 moles of solid NH_4Cl per mole of contained Th. A slight excess over this amount was generally desirable. The aqueous chlorides were boiled down to a syrupy consistency, to a maximum temperature of approximately 126°C, and cast into a chill mold for solidification. The solidified cake was then crushed, mixed with NaCl, and fed into a dryer where the temperature was raised to 260°C. Dehydration of the solid complex was thus effected without going through a fused state again.

The dry chloride complex was placed into a denitrating vessel where NH_4Cl was sublimed off, at temperatures ranging from 600° to 800°C. In this manner a completely fused product, precisely the composition required for electrolysis, was obtained from the over-all processing. The fused product was

handled in a number of ways, including: solidification in the crucible, followed by mechanical removal; tapping into a cold wall receiver; removal in the molten state by siphon techniques.

In an integrated plant, in which cell feed would be manufactured adjacent to the electrolytic plant, the most logical procedure would be to pump or tap the molten salt directly into the electrolytic cells without going through intermediate stages of solidification, crushing, and feeding to the cells as a solid constituent.

Equipment

Specifications on the metal product limited contaminants to parts per million or less and corrosion of equipment had to be held to a minimum. Materials of construction and equipment designs were therefore governed to a large extent by the purity criteria. Wherever possible, rubber-lined equipment was used. This included dissolving tanks, filter, and pumps.

For dissolving thorium nitrate, sodium carbonate, and precipitating thorium oxycarbonate, two 1200-gal rubber-lined tanks were used. These vessels were provided with openings at the top for introduction of solids and for removal of gases such as CO_2 during the precipitation. Tanks were equipped with rubber-covered agitators and Monel immersion heaters. Outlets at the bottom of each tank provided for transfer either of liquid solution or of slurry to respective receivers. In some operations rubber diaphragm pumps were used for liquid transfer; in others an all-plastic pump was provided for this service. All piping was polyvinyl chloride.

Filtration of the thorium oxycarbonate solution was carried out in a vertical Oliver filter containing seven leaves of varying sizes. The shell of the filter was rubber coated, and filter leaves were constructed of polystyrene. The filter cloth was Vinyon. Pressure was applied by means of compressed air which was prefiltered.

On completion of a filtration cycle HCl was pumped into the filter, and liquor was drawn off into a rubber-lined holding vessel which fed a specially designed evaporator. Originally, glass-lined steel pots were selected for the evaporation cycle; but excessive breakage of the lining, contamination of the product by glass particles, and pickup of boron necessitated elimination of any form of glass in contact with the boiling liquor.

As an alternative, a semicylindrical vessel was constructed from stainless steel and lined with a graphite lining approximately ¾ in. thick. A thin layer, approximately ½ in. thick, of densely packed lampblack was placed between the graphite pot liner and the stainless steel shell itself. The entire unit was supported in a brick furnace and was underfired with gas burners. The evaporator was equipped with an agitator constructed of graphite and an exhaust system for ducting away vapors emanating from the evaporation process. The evaporator was operated on a batch basis, fresh liquor being added incrementally until the concentrated solution nearly filled the evaporating pot. This material was then cast into a stainless steel chill mold, where it solidified into pigs. The pigs were crushed to −¼ in., mixed with NaCl, and placed in a graphite furnace for dehydration.

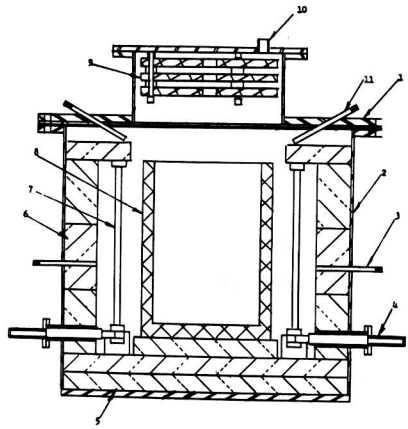

Fig. 2. Denitration furnace used to decompose ammonium-thorium complex.

The dehydrating apparatus consisted of a Glo-bar resistor heated furnace, insulated with firebrick and equipped with a graphite crucible concentrically positioned. Dimensions of the crucibles were approximately 18 in. in diameter and 26-30 in. high, with a capacity of between 200 and 300 lb of total feed material. Approximately 8 hr were required to bring the mass to a temperature of 260°C, and an additional 8 hr to complete the processing of each batch. The temperature was maintained at 260°C until all the water had been driven off, as indicated by a Carl Fischer analysis for moisture.

The graphite vessel containing the dehydrated salt was then placed in a totally enclosed sublimation unit heated by graphite resistors and capable of much higher temperatures. The graphite crucibles were interchangeable between the two types of furnaces, allowing for direct transfer from one to the other. The sublimation furnace was equipped with a side-arm condenser, a sparging system for maintaining HCl atmospheres, and a gas off-take to a scrubber system. The furnace shell was constructed of nickel, and all internal components other than insulation were made of graphite. Fig. 2 is a cross section of a typical furnace used for sublimation.

Operations

Operations were scaled on the basis of accommodating a precipitate batch containing 165 kg of Th. Thorium nitrate in crystalline form, the starting raw material, generally averaged between 41 and 43% Th by weight.

City water heated to 80°C was run into the oxycarbonate precipitation tank to a level of approximately 44 in. (equivalent to 510 gal). The tank agitator was started and an immersion heater used in order to maintain uniform temperature. While thermal equilibrium was being established at 80°C, 179.5 kg of light soda ash were weighed up and 157 kg dissolved in hot water. A hold-out of approximately 22½ kg was found desirable in practice,

since the free acidity of thorium nitrate was somewhat variable. The hold-out material was used to complete the chemical precipitation reaction when near-equilibrium was approached.

The soda ash solution was formulated for approximately 7.5% caustic by weight, a concentration which proved to be one of the determining factors for achieving the desired physical properties in the precipitated thorium oxycarbonate.

Simultaneously with preparation of the sodium carbonate solution, hot water was run into the thorium nitrate dissolver tank to a level of 50 in. (equivalent to 420 gal), and the immersion heater and agitator turned on. When thermal equilibrium was reached, 410 kg of thorium nitrate were added and completely dissolved. This represents a solution of approximately 10% Th by weight.

On completion of the dissolving steps, the thorium nitrate solution was pumped into the sodium carbonate tank at an initial rate of approximately 20 gal/min. Continuous agitation was maintained during the mixing step.

No noticeable reaction occurs until chemical equilibrium is approached. At this point a white precipitate begins to form, followed shortly thereafter by severe foaming. Careful regulation of the rate of introduction of thorium nitrate solution was required at that point; it generally was necessary to stop the thorium nitrate addition several times in order to permit the foam to subside, a factor attributable to limited tank volume.

Upon reaching equilibrium, the foaming subsided entirely; however, equilibrium was seldom reached until some or all of the additional 22.5 kg of soda ash was added incrementally. Completion of the reaction was determined by *p*H measurement, the final *p*H being adjusted to 7.6-8.0 with soda ash.

Thorium oxycarbonate when precipitated cold tends to be somewhat slimy and difficult to filter. Careful control of concentration, temperature of precipitation, and *p*H, however, results in a product which is granular and is relatively easy to filter.

The precipitated slurry, containing approximately 15% solids, was agitated for 5-10 min, allowed to settle for 6 hr, and the supernatant liquor decanted. Additional quantities of water were added, the slurry agitated, allowed to settle and again decanted. The decantation-wash cycle was repeated twice, followed by further additions of water in order to provide a suitable slurry for feed to the pressure filter.

The thorium oxycarbonate slurry served as a reserve for several filtration and hydrochlorination batches. The filter was limited in capacity to approximately 36 kg of contained Th per batch, this representing a buildup on the leaves of approximately 1¼ in. in thickness. Some three hours were required for each filtration cycle, followed by a washing cycle of from 1½ to 3 hr, using water heated to 120°F. Washing generally was continued until the wash water showed negative results when tested for nitrate ion, and specific gravity measurements indicated 1.0000 ±0.0001. The cake was then blown with filtered air, using pressures of approximately 25 psi, for a period of 2 hr in order to remove most of the contained moisture.

On completion of the partial dehydrating step, HCl (37%) was sprayed into the top of the filter through a pressure opening, a vigorous reaction occurring between the acid and the thorium oxycarbonate. Introduction of acid was intermittent, by-product gases being vented through a port in the lid into a scrubber system. Approximately 1 hr was required to complete the dissolution step, converting all of the Th values to $ThCl_4$ in aqueous solution. Sampling of the liquor provided analytical data from which the quantity of excess free HCl was determined. This was adjusted to a minimum of 5% HCl by volume.

The hydrochlorinated Th solution was then pumped into a rubber-lined storage tank, it serving as a reservoir for intermittent feed to the graphite-lined evaporator. Ammonium chloride in proportions of approximately 2.1 moles of NH_4Cl per mole of Th contained was added in the rubber-lined holding vessel prior to transfer of the complexed liquor into the evaporator.

Evaporation of the chloride complex was carried out semicontinuously, with additions of further solution as the volume increased. When the evaporator was nearly filled with concentrated liquor, the consistency being similar to syrup, the entire batch was cast into stainless steel molds and allowed to solidify in air. The casting operation took place generally between 135° and 145°C, this being partially dependent on the excess amount of HCl in the bath, the mole fraction of NH_4Cl, and certain other minor factors. Agitation was maintained throughout the evaporation cycle until increased viscosity discouraged the use of agitators.

Cast pigs of the NH_4Cl-Th complex were crushed and placed in a storage bin for feed to the next step in the operation. The cast and crushed materials contained 3-10% moisture.

To the crushed chloride complex was added enough NaCl to produce a product $ThCl_4$-NaCl analyzing approximately 35% Th by weight. After thorough blending, the mix was placed in graphite crucibles with a capacity of approximately 17 kg of contained Th, and loaded into Glo-bar heated furnaces for the dehydration step. Three furnaces of this type were required in order to process materials at the rate supplied by the evaporation cycle, each dehydration stage requiring approximately 8 hr after reaching a temperature of 260°C. The entire dehydration cycle required nearly 24 hr, including the heat-up, holding, and cooling stages. Throughout this operation a continuous bleed of HCl gas was maintained through the furnace, moisture and excess HCl being ducted to a scrubber system.

Thermocouples centered in the charge two-thirds of the way down from the uppermost layer were utilized in the determination of temperatures in the charge. Actual temperatures achieved near the perimeter of the crucible were somewhat higher than 260°, this being not too critical as long as the entire mass reached that temperature. It was found by experiment that the moisture content remaining

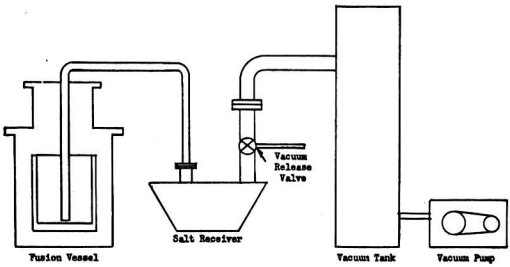

Fig. 3. System used to siphon molten salt from fusion vessel

after such treatment was always less than 1%, and generally less than 0.5%, as determined by the Carl Fischer method.

On completion of dehydration the charge was transferred to a graphite resistor-heated furnace, completely enclosed from the atmosphere. The unit was evacuated, flushed with argon, and heated under inert atmosphere to a temperature of 600°-860°C, during a cycle time of approximately 36 hr. Some 18 hr were required to reach the desired temperature; the vessel was held at temperature for 3 hr, and the remainder of the time was consumed in cooling. On completion of the cycle the graphite crucible was removed, the charge chipped out, jaw crushed, and stored as feed material for the electrolytic operation.

Alternatives to the sublimation process included the use of HCl as an atmosphere in preference to argon. Comparable results were obtained, it being a matter of economics to determine which system to use.

As a modification to the chipping operation, later aspects of the program incorporated heating the NaCl-$ThCl_4$ mix to a temperature somewhat above the fusion point, i. e., to 750°C, in order to achieve thorough homogenization of the charge and provide an easier method of removal from the crucible. The design of the equipment precluded tapping directly, but a system was devised wherein siphoning techniques were utilized to transfer the molten salt from the graphite crucible to a water-cooled nickel salt receiver. Figure 3 shows the siphoning system.

In operation a vacuum surge tank was pre-evacuated to a level of 100-500μ pressure. A quick-opening valve, positioned between the surge vessel and the tapping receiver, was then opened, causing the duplex system to equalize at a level of 4-6 psi of negative pressure. This pressure differential immediately effected a flow of molten salt through a connecting tube between the receiver and the graphite vessel containing the molten salts. Once established, flow continued until all molten salt had been transferred. In a typical salt-transfer operation of this type, some 250-300 lb could be transferred in less than 5 min through a ½ in. diameter nickel tube. By this technique the entire system could be maintained under a partial vacuum or inert atmosphere until the entire salt mass had been solidified without fear of moisture contamination. The Th salt cake resulting from the siphon operation was then chipped from the receiving vessel, crushed, and stored for use as cell feed to the electrolytic operations.

Table I. Typical analysis of thorium-sodium chloride cell feed

Constituent	Analysis, wt %
Thorium	33.2
Sodium	18.2
Chlorine	48.4
Insolubles*	0.06
Moisture	0.04
Total	99.9

* Insolubles determined by dissolving salt sample in water, treating residue with HCl. Insolubles represent ThO_2.

Cell feed materials were analyzed prior to acceptance for electrolysis and to provide a basis for Th accountability. Table I shows a typical analysis of the product.

Operational Efficiencies

The process as described was operated on a continuous basis for several months and supplied a small tonnage of cell feed for electrolytic operations which were carried out concurrently. Feed material preparation was operated on a 3-shift, 5-day week basis with a crew of two men per shift, operations being controlled and supervised by a single crew leader.

During full-scale production operations the normal yield was 100 kg of contained metal per week. The over-all metal recovery for the life of the campaign averaged 92.8% on the basis of total Th charged. During the last three months this average was increased to 95%, and probably could be improved upon with certain minor additions and modifications to equipment. The percentages indicated are recovered quantities, and do not include Th absorbed into crucible linings in the furnacing equipment.

Summary and Conclusions

This paper has presented a method for the production of Th cell feed which has been found suitable in quantity and quality for moderate-scale experimental electrolytic production of Th metal. In general, the equipment and materials of construction described have proven adequate.

Several hundred pounds of adequate quality Th metal for Atomic Energy Commission applications were produced from cell feed manufactured by the method described above. It is therefore concluded that the procedures are feasible and might be considered for commercial production operations should the need arise.

Acknowledgments

The pilot operation for preparation of Th cell feed was carried out under Atomic Energy Commission Contract AT(30-1)-1335. Permission to publish this paper is gratefully acknowledged.

The work was carried out under the general direction of Eugene Wainer, Director of Research of the laboratory, by personnel in the Department of Process Engineering. The efforts of these men led to a successful pilot operation in a minimum of time, and their commendable efforts are hereby acknowledged.

Manuscript received Jan. 23, 1957.

Any discussion of this paper will appear in a Discussion Section to be published in the June 1958 JOURNAL.

REFERENCES

1. "Proceedings of the International Conference on the Peaceful Uses of Atomic Energy," 16 vol., United Nations Press, New York (1956).
2. *Ibid.*, Vol. 1, pp. 335-336.
3. Hampel, "Rare Metals Handbook," Chap. 23, pp. 429-454, Reinhold Publishing Co., New York, (1954).
4. F. H. Driggs and W. C. Lilliendahl, *Ind. Eng. Chem.*, **22**, 1302 (1930).
5. Ref. 1, **9**, pp. 74-106.
6. E. L. Thellmann and J. L. Wyatt, *This Journal*, To be published.
7. B. C. Raynes, J. C. Bleweiss, M. E. Sibert, and M. A. Steinberg, "Electrolyte Preparation of Thorium Metal," To be published in *Journal of Metals*.
8. Ref. 1, **8**, pp. 184-187.

Stoichiometric Numbers and Hydrogen Overpotential

A. C. Makrides

Department of Chemistry, The University of Texas, Austin, Texas

ABSTRACT

An extended definition of the stoichiometric number of a mechanism is given and its use is demonstrated with a number of proposed hydrogen evolution reaction mechanisms.

Stoichiometric numbers were introduced in electrochemical kinetics in 1939 by Horiuti and Ikusima (1). A generalized treatment was recently given by Parsons (2).

Stoichiometric numbers provide an additional criterion for differentiating between possible reaction mechanisms. The expected stoichiometric number for a mechanism, commonly defined as the number of times the postulated rate-determining step is repeated when the over-all reaction occurs once, may be compared with a number computed from measured quantities. While the usefulness of this procedure is obvious, its employment is limited by difficulties in measuring overpotentials at current densities close to the exchange current. However, it is probable that, with recent techniques, stoichiometric numbers can be determined for an increasingly wider variety of systems.

The Parsons Derivation

In the theory of electrode processes given by Parsons (2), stoichiometric numbers are formally introduced by assuming that the completion of one over-all process, as represented by the stoichiometric equation, requires the formation and decomposition of ν activated complexes. The stoichiometric number, ν, is defined as some integer, equal to or greater than unity, with which the rate-determining equation must be multiplied to yield the stoichiometric equation.[1] Expressions for ν in terms of observable quantities are then derived by employing transition state theory to calculate specific reaction rate constants. Among other parameters, the Galvani potential difference, $\Delta\phi$, between metal and solution is used. Quantities p (and q), defined as the electrical part of the work of transferring the reactants (or products) from the original (or final) state to a state immediately preceding the energy barrier for the reaction, are also introduced.

[1] However, as shown below, even with this definition, ν can be less than unity.

Of the two expressions for ν derived by Parsons (2), one is applicable to states slightly removed from equilibrium and gives ν in terms of $(\partial\eta/\partial i)_{\eta\to 0}$, where η is the overpotential and i the current density. The other involves quantities $\left(\frac{\partial \ln i}{\partial \eta}\right)$ evaluated at large values of η for both the anodic and cathodic parts of the η vs. i curve. This paper deals with the former case.

Although Parsons' treatment is satisfactory on the whole, it is restricted to a certain extent by the assumptions involved in his derivation. The use of quantities $\Delta\phi$, p, and q, for example, implies a separation of the total work of transfer across an interface into electrical and chemical parts,[2] an operation which is not generally feasible (3). A more serious limitation of Parsons' derivation lies in his definition of stoichiometric numbers (2). As noted above, it rests essentially on the statement: let the rate determining reaction occur ν times when the over-all reaction occurs once. This definition apparently precludes their use in cases where two competing reaction mechanisms, both yielding the same over-all reaction but having different stoichiometric numbers, operate at comparable rates. An example of such a case is hydrogen evolution on a cathode where both discharge of hydrogen ions and electrochemical removal of adsorbed hydrogen atoms are slow.

An objection of a different nature may be raised on the following grounds. Parsons' treatment is based on absolute reaction rate theory and refers to the general case of an electrochemical reaction. Accordingly, the equilibrium postulate of absolute re-

[2] While for any given composition of the reaction system "the final expressions involve changes in the Galvani potential difference which can be measured" (2), difficulties still arise from the use of Galvani potentials. For example, to compare results obtained with a given electrode in solutions of different composition, a constant $\Delta\phi$ is specified. If the solutions are so concentrated that single ion activities cannot be calculated, the specification is of no practical value since it cannot be carried out. Similar difficulties are encountered in separating the dependence of p and q on $\Delta\phi$ and solution composition.

action rate theory is assumed for states far removed from thermoydnamic equilibrium. Although this assumption is probably satisfied for reactions slow enough to be measurable, proof of its validity is lacking (4-6). The postulate is rigorously applicable only to reversible reactions proceeding at dynamic equilibrium. Parsons' procedure, for the cases of interest here, is complicated thus unnecessarily: expressions are derived first for states far removed from equilibrium, and are then extrapolated to the equilibrium state for which the postulate is exact. The alternative procedure, i.e., extrapolation from the equilibrium state, is preferable.

It is shown below that an extended definition of the stoichiometric number of a mechanism can be formulated from the kinetic behavior of systems neighboring equilibrium without recourse to any particular model of reaction rate theory. While the extended definition coincides with that of Parsons for single reactions, it can also be used in the case of two or more competing reaction mechanisms.

Reaction Rates Close to Equilibrium

The conditions satisfied by rate laws at states close to equilibrium have been examined by Prigogine and co-workers (7,8), and by Manes, Hofer, and Weller (9), among others. Prigogine, Outer, and Herbo (8) have shown that for sufficiently small values of the affinity, A, the net reaction rate, v, is proportional to the affinity:

$$v = L\,(A/T) \qquad (I)$$

Here

$$A = -\sum_i a_i \mu_i$$

with a_i the coefficients in the corresponding stoichiometric equation, μ_i the chemical potentials, and T the temperature. Equation (I) follows from the fact that v and A vanish together at equilibrium. It assumes that there are no discontinuities in the region of equilibrium and that the forward and reverse reactions proceed at finite rates. Subject to these conditions, Eq. (I) has extreme generality, being independent of all hypotheses as to the reaction mechanism. The coefficient of proportionality, L, is however a function of both thermodynamic and nonthermodynamic variables, and its magnitude depends on the actual mechanism of the reaction.

A more detailed examination shows that for simple reactions L is equal to v^e/R, where v^e is the rate at equilibrium (in either direction), and R the gas constant. A demonstration is given by Prigogine (7). Consider the reaction

$$A + B \rightarrow C$$

with a net rate in the direction indicated

$$v = \vec{v} - \overleftarrow{v} = \vec{k} c_A c_B - \overleftarrow{k} c_C = \vec{k} c_A c_B \left(1 - \frac{\overleftarrow{k}}{\vec{k}} \frac{c_C}{c_A c_B}\right)$$

where $\vec{k}/\overleftarrow{k} = K(T)$, the equilibrium constant. The chemical potentials, assuming an ideal system, are

$$\mu_i = \mu_i^\circ(T) + RT \ln c_i$$

and the affinity

$$A = -\sum_i a_i \mu_i^\circ(T) - RT \sum_i a_i \ln c_i = RT \ln \frac{K(T)}{c_A^{-1} c_B^{-1} c_C}$$

Substituting in the expression for the net rate

$$v = \vec{v}\,[1 - \exp(-A/RT)] \qquad (II)$$

For small values of A, i.e., $A/RT << 1$,

$$v = \frac{v^e}{R}\,(A/T) \qquad (III)$$

where v^e ($\vec{v}^e = \overleftarrow{v}^e$) is the value of $\vec{v}$ at equilibrium ($A = 0$).

Only rarely, however, does the stoichiometric equation coincide with the rate laws for the reaction. Generally, the over-all reaction is the sum of a series of simple reactions which frequently involve species not appearing in the stoichiometric equation. To treat this case, an analysis given by Manes, Hofer, and Weller (9) is used.

Let

$$aA + bB + \ldots \rightarrow mM + nN + \ldots$$

be the stoichiometric equation for the over-all reaction, written, for convenience, with the smallest possible integral coefficients $a, b, \ldots m, n, \ldots$. If v_f is the rate of the forward reaction and v_r that of the reverse,

$$v_f = V_f[(A), (B), \ldots (M), (N), \ldots (X), \ldots]$$
$$v_r = V_r[(A), (B), \ldots (M), (N), \ldots (X), \ldots]$$

where V_f and V_r are, in general, complex algebraic functions of the concentrations of reactants and products and are assumed to be the actual rate laws, independent of the arbitrary coefficients of the stoichiometric equation. Species not appearing in the over-all reaction, for example, catalysts, are denoted by (X). The dependence of V_f and V_r on (X) must be such that, at equilibrium, (X) does not appear in the ratio V_f/V_r.

The only restrictions imposed by classical thermodynamics on the rate laws are

$$\frac{v_f}{v_r} = 1 \text{ for } A = 0; \frac{v_f}{v_r} > 1 \text{ for } A > 0 \qquad (IV)$$

To fulfill conditions (IV) it is sufficient to assume

$$\frac{v_f}{v_r} = \frac{k_f}{k_r}\left[\frac{(A)^a (B)^b \ldots}{(M)^m (N)^n \ldots}\right]^z \text{ with } \frac{k_f}{k_r} = K^z \qquad (V)$$

where z is any constant, positive number, and K the equilibrium constant. An example of such functions V_f and V_r which includes the case of simultaneous reactions, is given by Manes, Hofer, and Weller (9).

From (V)

$$\ln \frac{v_f}{v_r} = z\left[\ln K - \ln \frac{(M)^m (N)^n \ldots}{(A)^a (B)^b \ldots}\right] = z \frac{A}{RT}$$

Expanding around $A = 0$ and neglecting higher order terms [$A << RT$]

$$v = v_f - v_r = z \frac{v^e}{R}\,(A/T) \qquad (VI)$$

where $v^e = v_f^e = v_r^e$, the rate in either direction at equilibrium. Equation (VI) is of the form (I) with $L = zv^e/R$.

Stoichiometric Numbers

The constant of proportionality appearing in Eq. (I) can be decomposed, as shown by Eq. (VI), into the rate at equilibrium and a constant z. The origin of this last factor can be demonstrated best by an example.

Consider the reaction

$$2A + 2B \rightarrow C_2$$

and assume for the mechanism

$$A + B \rightarrow C \quad \text{(slow)} \qquad \text{(i)}$$

$$C + C \rightleftarrows C_2 \quad \text{(fast)} \qquad \text{(ii)}$$

Provided we are sufficiently close to equilibrium, the net rate of (i) is

$$v_i = \frac{v_i^e}{R}(A_i/T)$$

where

$$A_i = \mu_A + \mu_B - \mu_C$$

Since the mechanism assumes step (i) to be rate determining, $v_i/v_i^e = v/v^e$. Substituting

$$v = \frac{v^e}{R}(A_i/T)$$

The affinity of the over-all reaction is[3]

$$A = 2A_i + A_{ii}$$

According to the assumed mechanism, $A_{ii} \cong 0$, and $A_i = (\frac{1}{2})A$.[4] Substituting

$$v = \frac{1}{2}\frac{v^e}{R}(A/T)$$

The factor z gives therefore the relation between the affinity for the over-all reaction and the affinity for the rate-determining step or steps. This relation is determined by the mechanism of the reaction. The value of z for any assumed mechanism may be obtained by an analysis similar to the above, or by comparing Eq. (V) with the expression for the ratio, at equilibrium, of the forward to the reverse reaction rates as given by the mechanism. Examination of the usual kinetic expressions for reactions with a single rate-determining step, including cases involving equilibria between reactants and/or products and intermediate species, and of mechanisms where a steady state is postulated (e. g., collision theory), shows that z gives the number of times the over-all reaction occurs when the rate-determining step occurs once. In these cases therefore one may identify z with the reciprocal of the stoichiometric number as defined by Parsons (2). In cases of reactions proceeding through more than one path, a value of z can again be calculated using the same procedure. This case is examined below.

Conditions (IV) allow z to take any constant, positive value. In view of the above, z is usually equal to the ratio of two small integers and is smaller than one in most cases. There are however reactions for which z is larger than one [the corresponding value of ν, as defined by Parsons (2), being less than one]. Thus for chain mechanisms (10), the slow step is often followed by a series of fast reactions involving additional molecules of the reactants so that the stoichiometric equation may be repeated several times for each occurrence of the slow step. This is also true for the mechanisms of certain photochemical reactions (10).

Competing reaction mechanisms.—A reaction proceeding through only two competing reaction mechanisms is considered. The argument can be extended easily to any number of competing reaction mechanisms.

Let the reaction

$$A_2 + B_2 \rightarrow 2C$$

proceed through the independent mechanisms

[1]
$$A_2 \rightleftarrows A + A \qquad \text{(i)}$$

$$B_2 \rightleftarrows B + B \qquad \text{(ii)}$$

$$A + B \rightarrow C \quad \text{(slow)} \qquad \text{(iii)}$$

and

[2] $$A_2 + B_2 \rightarrow 2C \quad \text{(slow)}$$

The net rate of the reaction is $v = v_1 + v_2$ and similarly $v^e = v_1^e + v_2^e$, where the subscripts (1) and (2) refer to reaction mechanisms [1] and [2] respectively. If $A << RT$,

$$v_1 = \frac{v_1^e}{R}(A_{iii}/T) = \frac{1}{2}\frac{v_1^e}{R}(A/T)$$

$$v_2 = \frac{v_2^e}{R}(A/T)$$

Therefore

$$v = \frac{(\frac{1}{2}v_1^e + v_2^e)}{R}(A/T)$$

If $v_1^e >> v_2^e$, $v = (\frac{1}{2})\frac{v^e}{R}(A/T)$ and $z = \frac{1}{2}$, while for $v_2^e >> v_1^e$, $v = \frac{v^e}{R}(A/T)$ and $z = 1$. If $v_1^e = v_2^e$ then $v^e = 2v_1^e$ and

$$v = \frac{3}{4}\frac{v^e}{R}(A/T)$$

form which $z = \frac{3}{4}$. In general, $\frac{1}{2} \leqq z \leqq 1$, the value of z within this interval being determined by the relative rates of mechanisms [1] and [2].

Electrochemical Systems

Electrochemical systems involve phases which may be at different electrical potentials. With charged species the μ's used above depend on the electrical state of the phase as well as on its chemical composition. It is therefore convenient in these cases to speak of electrochemical potentials, $\tilde{\mu}_i$, and electrochemical affinities, $\tilde{A} = -\sum_i a_i \tilde{\mu}_i$ (11). With this change in notation, Eq. (VI) reads

$$v = z\frac{v^e}{R}(\tilde{A}/T)$$

[3] In general, $A = \sum_\rho \alpha_\rho A_\rho$, where A is the affinity for the over-all reaction, A_ρ the affinities of individual steps, and the α_ρ constants. Prigogine (7) writes $A = \sum_\rho A_\rho$ and similarly omits the factor z in the expression for L. It is clear, however, that in the cases examined by Prigogine the stoichiometric and rate equations coincide.

[4] To be exact, $A_{ii} = \frac{2v_i^e}{v_{ii}^e}A_i$. Since the mechanism postulates $v_{ii}^e >> v_i^e$, A_{ii} may be neglected in comparison to A_i and, therefore, $2A_i + A_{ii} \cong 2A_i \cong A$.

To express this relation in terms more familiar in electrochemical kinetics, consider a half-cell reaction occurring at an electrode immersed in a solution of constant composition. A current i is impressed on the electrode and the electrode potential is determined as a function of i. The affinity of the reaction taking place is

$$\tilde{A} = -\sum_i a_i \tilde{\mu}_i = -\sum_i a_i (\tilde{\mu}_i - \tilde{\mu}_{i_0})$$

where $\tilde{\mu}_{i_0}$ are the electrochemical potentials at equilibrium ($\sum_i a_i \tilde{\mu}_{i_0} = 0$). If η is the difference between the potentials with current i flowing and at equilibrium

$$\tilde{A} = -\sum_i a_i (\tilde{\mu}_i - \tilde{\mu}_{i_0}) = nF\eta$$

where n is the number of electrons involved in the half-reaction and F is Faraday's constant.[5] Here η is equal to the difference between the electrode-solution electric potential difference when current i is flowing and that at equilibrium, i.e., η is the overpotential [*see* Parsons (2)].

Noting that

$$v/v^\circ = i/i_o$$

where i is the net current and i_o the exchange current, Eq. (VI) may be written in the form

$$i = z\frac{nFi_o}{R}(\eta/T) \quad |\eta| << \frac{RT}{r}$$

or

$$\frac{1}{z} = \frac{nFi_o}{RT}\left(\frac{\partial\eta}{\partial i}\right)_{\eta\to 0} \qquad \text{(VII)}$$

which is the relation derived by Parsons (2) with $z = 1/\nu$.[6] Equation (VII) can be used to calculate z for any reaction for which the overpotential curve for $\eta \to 0$ and i_o are known. The exchange current can be measured with systems which are essentially at equilibrium (say, by use of tracers). Commonly however i_o is found by extrapolation from the region of large values of η, where the reverse reaction may be neglected, to $\eta = 0$. This procedure assumes that the reaction mechanism remains the same over the range of η values considered.

It should be noted that the actual numerical values of z, or ν, are trivial in the sense that they depend on the arbitrary formulation of the stoichiometric equation. This is reflected in Eq. (VII) which shows that z depends on n, the number of electrons involved in the half-reaction as written. However, relative values of z for different reaction mechanisms, which may be used as an additional criterion for the reaction mechanism, are independent of n.

Application to Hydrogen Overpotential

In this section expected stoichiometric numbers for various possible reaction mechanisms for the hydrogen evolution reaction, $2H^+ + 2e \to H_2$, are derived by using the procedure given above. Slow combination, slow discharge, slow electrochemical, and the case where both the rates of discharge and of electrochemical removal of adsorbed hydrogen atoms are slow, are considered. The first three cases demonstrate the procedure used here, the results being identical with counting the number of times the rate determining step occurs when the over-all reaction occurs once. The last case is an example of a mechanism involving two simultaneous reaction paths of comparable rates.

1. *Slow combination.*—The mechanism postulates (12),

$$H^+ + e \overset{\text{fast}}{\rightleftharpoons} H_{ads} \qquad \text{(i)}$$

$$H_{ads} + H_{ads} \overset{\text{slow}}{\to} H_{2(g)} \qquad \text{(ii)}$$

If $A << RT$

$$v = \frac{v^\circ}{R}(A_{11}/T)$$

but

$$A = 2A_1 + A_{11} \cong A_{11} \qquad \text{(VIII)}$$

from which

$$v = \frac{v^\circ}{R}(A/T)$$

Comparing to (VI), $z = 1$ (or $\nu = 1$).

Alternatively, the rates of the forward and reverse reactions are

$$i_o = k_f x^2$$
$$i_o = k_r P_{H_2}(1-x)^2$$

where x is the fraction of the surface covered by adsorbed hydrogen atoms. From (i) and at equilibrium

$$\frac{x}{1-x} = (\text{Const.})\, a_{H^+}$$

Therefore at equilibrium

$$\frac{v_f}{v_r} = 1 = \frac{k_f}{k_r}\frac{x^2}{P_{H_2}(1-x)^2} = \frac{k_f}{(\text{Const.})k_r}\left[\frac{a_{H^+}^2}{P_{H_2}}\right]$$

and by comparing to (V), $z = 1$.

2. *Slow discharge* (13).—(*a*) Slow discharge followed by fast combination: The mechanism postulates

$$H^+ + e \overset{\text{slow}}{\to} H_{ads} \qquad \text{(i)}$$

$$H_{ads} + H_{ads} \overset{\text{fast}}{\rightleftharpoons} H_2(g) \qquad \text{(ii)}$$

Sufficiently close to equilibrium,

$$v = \frac{v^\circ}{R}(A_i/T) \qquad \text{(IX)}$$

and from (VIII) with $A_{11} \cong 0$, $A = \frac{1}{2}A$. Therefore

$$v = \frac{1}{2}\frac{v^\circ}{R}(A/T)$$

and $z = \frac{1}{2}$.

(*b*) Slow discharge followed by fast electrochemical: In this case (i) is followed by

$$H_{ads} + H^+ + e \overset{\text{fast}}{\rightleftharpoons} H_2(g) \qquad \text{(iii)}$$

The rate is again given by (VIII). Here, however,

[5] It is assumed that the chemical reaction is the only cause of irreversibility present in the system. In other words, the contribution of concentration and ohmic overvoltages to the measured potential difference is assumed to be negligible.

[6] Since the rate of entropy production, $nF\eta i$, is positive, η and i must have the same sign. On cathodic polarization η is negative and therefore i must be given a negative sign.

$$A = A_{\text{I}} + A_{\text{III}}$$

and for $A_{\text{III}} \cong 0$,

$$v = \frac{v^e}{R}(A/T)$$

from which $z = 1$.

3. *Slow electrochemical.*—The mechanism postulates (14)

$$H^+ + e \overset{\text{fast}}{\rightleftharpoons} H_{ads} \qquad \text{(i)}$$

$$H_{ads} + H^+ + e \overset{\text{slow}}{\rightarrow} H_2(g) \qquad \text{(iii)}$$

The rate is

$$v = \frac{v^e}{R}(A_{\text{III}}/T)$$

and from (IX) with $A_{\text{I}} \cong 0$,

$$v = \frac{v^e}{R}(A/T)$$

so that $z = 1$.

4. *Slow discharge and slow electrochemical.*—There are two possible reaction schemes here

(*a*)

$$H^+ + e \overset{\text{slow}}{\rightarrow} H_{ads} \qquad \text{(i)}$$

$$H_{ads} + H_{ads} \overset{\text{fast}}{\rightleftharpoons} H_2(g) \qquad \text{(ii)}$$

$$H_{ads} + H^+ + e \overset{\text{slow}}{\rightarrow} H_2(g) \qquad \text{(iii)}$$

(*b*)

$$H^+ + e \overset{\text{slow}}{\rightarrow} H_{ads} \qquad \text{(i)}$$

$$H_{ads} + H^+ + e \overset{\text{slow}}{\rightarrow} H_2(g) \qquad \text{(iii)}$$

with the rate of (ii) negligible. This may be the case if there is strong localized adsorption of hydrogen with a negligible rate of surface migration, or, less likely, appreciable surface migration but a high energy of activation for surface combination of two adsorbed atoms.

For mechanism (*a*)

$$2A_{\text{I}} + A_{\text{II}} = A$$

and

$$A_{\text{I}} + A_{\text{III}} = A$$

so that with $A_{\text{II}} \cong 0$ and $v^e = v_{\text{I}}{}^e + v^e{}_{\text{III}}$,

$$v = \frac{1}{2}\frac{v^e}{R}(A/T)$$

from which $z = \frac{1}{2}$. Therefore, if (i) is slow and (ii) much faster than (iii), the occurrence of reaction (iii) does not change the value of the stoichiometric number (compare mechanism 2*a*).

For mechansism (*b*)

$$v_{\text{I}} = \frac{v_{\text{I}}{}^e}{R}(A_{\text{I}}/T)$$

$$v_{\text{III}} = \frac{v^e{}_{\text{III}}}{R}(A_{\text{III}}/T)$$

with

$$A_{\text{I}} + A_{\text{III}} = A$$

The steady-state condition, $d[H_{ads}]/dt = 0$, is $v_{\text{I}} = v_{\text{III}}$. If $v^e{}_{\text{III}} > v^e{}_{\text{I}}$, then the rate of the over-all reaction at equilibrium is $v^e = v^e{}_{\text{I}}$. If, say, $v^e{}_{\text{III}} = 10v^e{}_{\text{I}}$, then

$$v = \frac{v^e}{R}(A_{\text{I}}/T)$$

From the steady-state condition, $v^e{}_{\text{I}}A_{\text{I}} = v^e{}_{\text{III}}A_{\text{III}}$, or $A_{\text{I}} = 10A_{\text{III}}$. Therefore, $A_{\text{I}} = (10/11)A$ and substituting

$$v = \frac{10}{11}\frac{v^e}{R}(A/T)$$

from which $z = 10/11$. Thus, for $v^e{}_{\text{III}} >> v^e{}_{\text{I}}$, $z \rightarrow 1$ (slow discharge followed by fast electrochemical). Similarly, if $v^e{}_{\text{I}} >> v^e{}_{\text{III}}$, $z \rightarrow 1$ (slow electrochemical).

If $v^e{}_{\text{I}} = v^e{}_{\text{III}}$, then $A_{\text{I}} = A_{\text{III}}$, or $A_{\text{I}} = A/2$, and

$$v = \frac{v^e}{R}(A_{\text{I}}/T) = \frac{1}{2}\frac{v^e}{R}(A/T)$$

so that $z = \frac{1}{2}$. In general, z approaches 1 as either step becomes much faster than the other, and $\frac{1}{2}$ when $v^e{}_{\text{I}} \sim v^e{}_{\text{III}}$.

The statement (15) that an experimental value of 0.116 v for the Tafel slope at 25°C coupled with $z = \frac{1}{2}$ ($\nu = 2$) uniquely determines 2*a* above as the mechanism of the hydrogen evolution reaction is incorrect. Mechanisms 4*a* and 4*b* (provided $v^e{}_{\text{I}} \sim v^e{}_{\text{III}}$) yield the same values for these two quantities.

Manuscript received Oct. 11, 1956.

Any discussion of this paper will appear in a Discussion Section to be published in the June 1958 JOURNAL.

REFERENCES

1. J. Horiuti and M. Ikusima, *Proc. Imp. Acad. Tokyo*, **15**, 39 (1939); J. Horiuti, *J. Res. Inst. Catalysis*, **1**, 8, (1948).
2. Roger Parsons, *Trans. Faraday Soc.*, **47**, 1332 (1951).
3. E. A. Guggenheim, "Thermodynamics," Interscience Publishers, Inc., New York (1950).
4. E. A. Guggenheim and J. Weiss, *Trans. Faraday Soc.*, **34**, 57 (1938).
5. B. J. Zwolinski and H. Eyring, *J. Am. Chem. Soc.*, **69**, 2702 (1947).
6. H. M. Hulburt and J. O. Hirschfelder, *J. Chem. Phys.*, **17**, 964 (1949).
7. I. Prigogine, "Thermodynamics of Irreversible Processes," C. C. Thomas Publishers, Springfield, Ill. (1955).
8. I. Prigogine, P. Outer, and Cl. Herbo, *J. Phys. Chem.*, **52**, 321 (1948).
9. M. Manes, L. J. E. Hofer, and Sol Weller, *J. Chem. Phys.*, **18**, 1355 (1950).
10. K. J. Laidler, "Chemical Kinetics," McGraw-Hill Book Co., New York (1950).
11. P. Van Rysselberghe, "Electrochemical Affinity," Hermann and Co., Paris (1955).
12. J. Tafel, *Z. physik. Chem.*, **34**, 187 (1900).
13. *See*, for example, Ref. (2) above.
14. A. Frumkin, *Acta Physicochim.*, **7**, 475 (1937).
15. J. O'M. Bockris, "Modern Aspects of Electrochemistry," Academic Press Inc., New York (1954).

The Composition of Copper Complexes in Cuprocyanide Solutions

H. P. Rothbaum[1]

Department of Physical Chemistry, University of Liverpool, Liverpool, England

ABSTRACT

The static potential of copper in a range of cuprocyanide solutions was measured at 20° and at 80°C. The values agreed well with those calculated on the assumption that $Cu(CN)_4^{=}$, $Cu(Cn)_3^{=}$, and $Cu(CN)_2^{-}$ ions are present, and the association constants of these complexes were calculated. Addition of alkali does not affect any of the quantities measured materially. The ultraviolet absorption spectra of the solutions qualitatively confirmed the presence of $Cu(CN)_4^{=}$ ions.

There appears to have been some doubt in the literature as to the form in which Cu exists in cuprocyanide solutions.

Of early workers, Kunschert (1) concluded on the basis of potentiometric experiments that Cu was present as the $Cu(CN)_4^{=}$ ion in solutions containing excess cyanide. Grossman and Von der Forst (2) supported this conclusion from freezing point data, but Höing (3) claimed that $Cu(CN)_3^{=}$ was the highest complex possible. Glasstone (4) gravely criticized Höing's work, but from the variation of the static potential with the Cu to cyanide ratio he also concluded that $Cu(CN)_2^{-}$ and $Cu(CN)_3^{=}$ were the principal ions present. Britton and Dodd (5) partly repeated Glasstone's work and arrived at the same conclusion. But Brintzinger and Osswald (6) showed by dialysis that Cu ions in excess cyanide solutions had a molecular weight of 166 which corresponds closely to a formula of $Cu(CN)_4^{=}$. Thompson (7) in a review suggests that in most copper cyanide plating solutions, Cu is present principally as $Cu(CN)_3^{=}$ with minor amounts of $Cu(CN)_2^{-}$ and $Cu(CN)_4^{=}$, but stresses that some authors have used titration methods for estimating free cyanide in solutions and that these do not furnish evidence for any complexes present, as the equilibrium is disturbed during titration. Yet Gabrielson (8) in an extensive study solely by a titration method for free cyanide concluded that under all conditions $Cu(CN)_3^{=}$ is the main ion, with only a little $Cu(CN)_4^{=}$ present at high cyanide to Cu ratios. Calmar and Costa (9) recently claimed, on the basis of conductometric experiments, that $KCu(CN)_2$ and $K_2Cu(CN)_3$ are the only two compounds present in potassium cuprocyanide solutions.

Since the work for this paper was completed, Penneman and Jones (10), by using infrared ab-absorption spectroscopy, have proved conclusively that $Cu(CN)_4^{=}$ is the principal ion present at high cyanide to Cu ratios and have, for the first time, evaluated the dissociation constants for all cuprocyanide complexes.

In this paper the problem has been re-examined by measurement of the static potential of Cu in stronger cyanide solutions than have so far been used and by u.v. spectrophotometry. It was possible to calculate the static potentials; they are in very good agreement with experimental values for a wide range of conditions. The association constants for the cuprocyanide complexes have also been deduced; they are in good agreement with the values of Penneman and Jones (10) derived by an entirely different method.

It is concluded that substantially all the Cu is in the form of $Cu(CN)_4^{=}$ as long as sufficient cyanide is present, and only at higher Cu to cyanide ratios are lower complexes formed. Thus in most plating baths, where this ratio is about 0.32, $Cu(CN)_3^{=}$ is the principal ion present and at higher ratios $Cu(CN)_2^{-}$ begins to be formed.

Experimental

Cuprocyanide solutions were made from A. R. KCN (loss in weight after melting 0.5%, volumetric cyanide analysis corresponds to 99.5% KCN) and CuCN made from A. R. chemicals by the method of Barber (11) (loss in weight after melting 0.6%, electrolytic Cu analysis corresponds to 99.3% CuCN).

The absorption spectra of a number of cuprocyanide solutions were obtained on a Unicam spectrophotometer using KCN solutions of corresponding concentrations as blanks. All solutions were 4M in total cyanide, except the one highest in Cu which is saturated above 1M. Results are shown in Fig. 1 as density for a 1 cm cell (multiplied by 4 in the one case mentioned), as molecular extinction coefficients would involve exact knowledge of the complexes present.

The potential of a freshly cleaned Cu wire in a large number of cuprocyanide solutions against a calomel electrode was measured on a Vernier potentiometer. As noted by most previous authors (1, 3, 4, 5, 12, 13) potentials, especially in low Cu

[1] Present address: Dominion Laboratory, Department of Scientific and Industrial Research, Wellington, New Zealand.

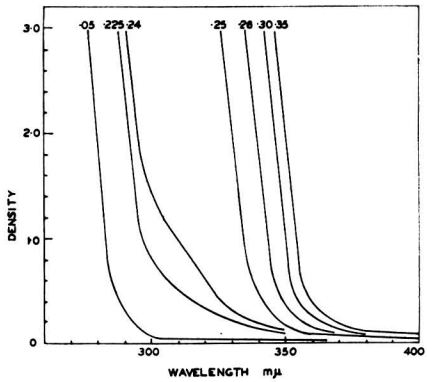

Fig. 1. Ultraviolet absorption spectra of cuprocyanide solutions at Cu:CN ratios indicated. Density is expressed for a 4M cyanide solution in a 1 cm cell.

solutions, fluctuated somewhat erratically initially, but settled to more steady values after some minutes. For each solution a number of readings were taken, covering about 3 hr, and it is estimated that the results quoted are accurate at least to ±0.02 v. Room temperature in all cases was between 18° and 20°C. No thermostating was employed as the accuracy of the results obtained did not warrant it and the temperature coefficient of the potentials was small.

A series of readings at a temperature of 79°-80°C was obtained in a boiling benzene (bp 80.1°C) thermostat.

Theoretical

The absorption spectra (Fig. 1) with a sharp break in character at a Cu:CN ratio of 0.25 suggest very strongly that in low Cu solutions the ion $Cu(CN)_4^{\equiv}$ is present. On the basis of this assumption one has the following equilibria:

$$Cu^+ + 2CN^- \overset{k_1}{\rightleftarrows} Cu(CN)_2^-$$

$$Cu(CN)_2^- + CN^- \overset{k_2}{\rightleftarrows} Cu(CN)_3^{=}$$

$$Cu(CN)_3^{=} + CN^- \overset{k_3}{\rightleftarrows} Cu(CN)_4^{\equiv}$$

All authors agree that k_1 is very large and therefore $[Cu^+]$ may be neglected in comparison with other species present.

Exact treatment of these equilibria gives equations that are too complicated to be easily solved, but on assuming that $1 << k_3 << k_2 << k_1$ (assumptions later verified) great simplifications result. These assumptions imply that the total Cu is always present in the most complex form compatible with the amount of cyanide present.

Let Cu be the total copper concentration and CN the total cyanide concentration in moles/liter. Thus

$$Cu = [Cu(CN)_3^-] + [Cu(CN)_3^{=}] + [Cu(CN)_4^{\equiv}]$$

and

$$CN = [CN^-] + 2[Cu(CN)_2^-] + 3[Cu(CN_3^{=}] + 4[Cu(CN)_4^{\equiv}]$$

On the basis of the above assumptions it can then be shown that

$$[Cu^+] = \frac{k_2^2\,(3Cu - CN)^3}{k_1\,(CN - 2Cu)^2} \quad \left(\text{if } \frac{CN}{2} > Cu > \frac{CN}{3}\right)$$

$$= \frac{k_3^3\,(4Cu - CN)^4}{k_1k_2\,(CN - 3Cu)^3} \quad \left(\text{if } \frac{CN}{3} > Cu > \frac{CN}{4}\right)$$

$$= \frac{Cu}{k_1k_2k_3\,(CN - 4Cu)^4} \quad \left(\text{if } \frac{CN}{4} > Cu\right)$$

If the static potential of Cu in cuprocyanide solutions is dependent only on $[Cu^+]$, it should be possible to calculate it in any solution if total Cu and cyanide are estimated and k_1, k_2, and k_3 are known.

Alternatively, if one potential in each of the three regions has been determined experimentally, the three equilibrium constants can be calculated and from these the potentials at all other Cu:CN ratios and dilutions deduced. This has been done and the results compared with the full range of experimental values.

Results

A series of solutions having total cyanide contents (i.e., CuCN + KCN) of 4M, 2M, 1M, and 0.5M were

Table I. Experimental and calculated static potentials of Cu in cuprocyanide solutions at 20°C on the hydrogen scale

Ratio Cu:CN	Experimental				Calculated			
	4M Cyanide	2M	1M	0.5M	4M Cyanide	2M	1M	0.5M
0.00	−1.37	−1.31	−1.26	−1.17	—	—	—	—
0.025	—	—	—	—	−1.37	−1.32	−1.27	−1.21
0.05	−1.33	−1.26	−1.22	−1.13	−1.34	−1.29	−1.24	−1.18
0.10	−1.31	−1.25	−1.16	−1.12	−1.29	−1.24	−1.19	−1.13
0.15	−1.24	−1.20	−1.14	−1.09	−1.24	−1.19	−1.14	−1.08
0.20	−1.18	−1.14	−1.08	−1.02	−1.17	−1.12	−1.07	−1.01
0.225	−1.09	−1.03	−0.99	−0.93	−1.09	−1.04	−0.99	−0.93
0.24	—	—	—	—	−1.00	−0.95	−0.90	−0.84
0.25	−0.83	−0.86	−0.86	−0.85	—	—	—	—
0.26	—	—	—	—	−0.83	−0.85	−0.86	−0.88
0.275	−0.69	−0.72	−0.75	−0.76	−0.72	−0.74	−0.75	−0.77
0.30	−0.61	−0.64	−0.65	−0.67	−0.61	−0.63	−0.64	−0.66
0.325	−0.55	−0.56	−0.56	−0.54	−0.46	−0.48	−0.49	−0.51
0.35	sat.	sat.	−0.41	−0.39	−0.39	−0.41	−0.42	−0.44
0.375			sat.	−0.35	−0.30	−0.32	−0.33	−0.35
0.40				sat.	−0.24	−0.26	−0.27	−0.29
0.425					−0.21	−0.23	−0.24	−0.26

prepared. The potential was calculated from the formula

$$E = \pi o + \frac{2.30nRT}{F} \log [Cu^+]$$

by using as reference points the following three experimental values on the hydrogen scale:

Cu:CN 0.15 cyanide 4M −1.24 v
Cu:CN 0.30 cyanide 4M −0.61 v
Cu:CN 0.375 cyanide 0.5M −0.35 v

Experimental and calculated values at 20°C are shown in Table I. Saturation of the solutions has been ignored in the calculations, and these values, therefore, extend to higher concentrations than the experimental ones.

Bassett and Corbet (14) made a phase rule study of the system KCN:CuCN:H_2O at 25°C. Their values for the composition of saturated solutions are similar to the ones obtained here. Using the three reference points quoted, the formula derived above, and the most recent value of 0.48 v at 21°C for the standard cuprous potential (15) one has:

$$-1.24 = 0.48 + 0.058 \left[\log \frac{0.6}{(4-2.4)^4} - \log k_1 - \log k_2 - \log k_3 \right]$$

$$-0.61 = 0.48 + 0.058 \left[\log \frac{(4.8-4)^4}{(4-3.6)^3} + 3 \log k_3 - \log k_1 - \log k_2 \right]$$

$$-0.35 = 0.48 + 0.058 \left[\log \frac{(0.5625-0.5)^3}{(0.5-0.375)^2} + 2 \log k_2 - \log k_1 \right]$$

Allowing for the maximum uncertainty of ±0.02 v in the potential readings, at 20°C

$\log k_1 = 21.7 \pm 1.0$ $\quad 5 \times 10^{20} < k_1 < 5 \times 10^{22}$
$\log k_2 = 4.6 \pm 0.30$ $\quad 2 \times 10^4 < k_2 < 8 \times 10^4$
$\log k_3 = 2.3 \pm 0.15$ $\quad k_3 = (2 \pm 0.7) \times 10^2$

If the older, still generally accepted value of 0.52 v for the standard cuprous potential (16) is used, only k_1 is affected and it becomes 3×10^{21} to 3×10^{23}.

Kunschert (1) quotes a value for $K = 2 \times 10^{27}$ (corrected for a cuprous potential of 0.48 v this gives 7×10^{27}). His K corresponds to $k_1 \times k_2 \times k_3$ in this work which comes to 4×10^{28}. Latimer (16) quotes only $k_1 \times 10^{16}$, derived from early work (13) which ignores the existence of complexes higher than $Cu(CN)_2^-$.

Recently (12), k_1 has been redetermined in HCN where it was established that no complexes higher than $Cu(CN)_2^-$ exist in appreciable quantities. However, the square of the not accurately known dissociation constant of HCN enters the calculation. A value for k_1 of the order 5×10^{28} was obtained at 25°C.

k_2 and k_3 have been determined only very recently for the first time by infrared absorption spectroscopy (10). The following values, recalculated as association constants, were obtained:

29°C	25°C
k_2 $(4.1 \pm 0.6) \times 10^4$	approx. 7×10^4
k_3 $(1.4 \pm 0.1) \times 10^2$	approx. 1.8×10^2

The entire work at room temperature was repeated in solutions containing 0.7M KOH; substantially similar results were obtained. The absorption spectra were practically identical with those in Fig. 1 (KOH only absorbs appreciably below 260 mμ) and the values of the association constants were close to those without alkali.

The experiments (without alkali) were performed at 80°C and the potentials calculated as before by using as reference points

Cu:CN 0.15 cyanide 4M −1.23 v
Cu:CN 0.30 cyanide 4M −0.76 v
Cu:CN 0.375 cyanide 0.5M −0.37 v

Experimental and calculated values are shown in Table II.

No experimental value for πo at 80°C is available, but Tourky and Khairy (17) have calculated that the temperature coefficient of the standard cuprous potential is −0.8 mv/°C from 20° to 47°C. Extrapolating this temperature coefficient gives a value for πo at 80°C of 0.44 v. The accuracy of this value affects only the accuracy of k_1.

Using the three reference points quoted,

Table II. Experimental and calculated static potentials of Cu in cuprocyanide solutions at 80°C on the hydrogen scale

Ratio Cu:CN	Experimental 4M Cyanide	Experimental 2M	Experimental 1M	Experimental 0.5M	Calculated 4M Cyanide	Calculated 2M	Calculated 1M	Calculated 0.5M
0.00	−1.38	−1.33	−1.23	−1.21	—	—	—	—
0.025	—	—	—	—	−1.39	−1.33	−1.26	−1.20
0.05	−1.37	−1.28	−1.22	−1.17	−1.35	−1.29	−1.22	−1.16
0.10	−1.30	−1.25	−1.17	−1.13	−1.29	−1.23	−1.16	−1.10
0.15	−1.23	−1.17	−1.10	−1.07	−1.23	−1.17	−1.10	−1.04
0.20	−1.16	−1.11	−1.06	−1.00	−1.14	−1.08	−1.01	−0.95
0.225	−1.12	−1.08	−1.01	−0.99	−1.05	−0.99	−0.92	−0.86
0.24	—	—	—	—	−0.94	−0.88	−0.81	−0.75
0.25	−0.98	−1.00	−0.99	−0.95	—	—	—	—
0.26	—	—	—	—	−1.03	−1.05	−1.07	−1.09
0.275	−0.86	−0.89	−0.92	−0.91	−0.90	−0.92	−0.94	−0.96
0.30	−0.76	−0.80	−0.81	−0.83	−0.76	−0.78	−0.80	−0.82
0.325	−0.63	−0.65	−0.67	−0.64	−0.59	−0.61	−0.63	−0.65
0.35	−0.50	−0.47	−0.43	−0.42	−0.43	−0.45	−0.47	−0.49
0.375	−0.44	−0.40	−0.38	−0.37	−0.31	−0.33	−0.35	−0.37
0.40	−0.41	−0.37	−0.34	−0.33	−0.26	−0.28	−0.30	−0.32
0.425	sat.	sat.	sat.	sat.	−0.21	−0.23	−0.25	−0.27

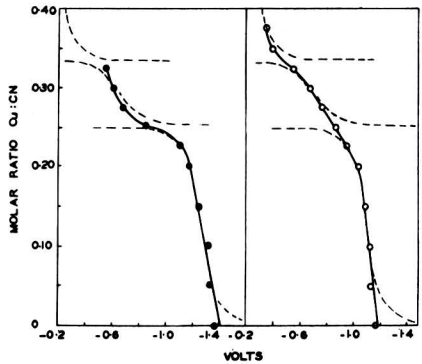

Fig. 2. Static potential of cuprocyanide solutions at 20°C on the hydrogen scale. ● Total cyanide 4M, ○ total cyanide 0.5M. The broken lines show the corresponding calculated values.

$$-1.23 = 0.44 + 0.070\ [-1.0 - \log k_1 - \log k_2 - \log k_3]$$
$$-0.76 = 0.44 + 0.070\ [0.8 + 3 \log k_3 - \log k_1 - \log k_2]$$
$$-0.37 = 0.44 + 0.070\ [-1.8 + 2 \log k_3 - \log k_1]$$

Allowing for the maximum uncertainty of ±0.02 v in the potential readings at 80°C

$$\log k_1 = 17.7 \pm 1.0 \qquad 5 \times 10^{16} < k_1 < 5 \times 10^{18}$$
$$\log k_2 = 3.9 \pm 0.30 \qquad 4 \times 10^{3} < k_2 < 1.5 \times 10^{4}$$
$$\log k_3 = 1.23 \pm 0.14 \qquad k_3 = 17 \pm 5$$

No values for these constants at an elevated temperature were found in the literature.

The work at 80°C was repeated with solutions of total cyanide content of 3.1M, containing 0.7M KOH, because solutions about 2.1M KCN, 1.0M CuCN, 0.7M KOH at about 80°C are commonly employed for high speed and periodic reverse copper cyanide electroplating.

The potentials obtained and the constants calculated were close to those observed without alkali.

Discussion

In general, agreement between the experimental and calculated values for the static potential in cyanide solutions is satisfactory. This is shown in Fig. 2 at 20°C for solutions of total cyanide 4M and 0.5M. Some deviation naturally occurs at the transition stages between the three regions, where the calculated values become infinite.

The calculations predict that, if CN/4 > Cu, a dilution to a half should increase the cuprous ion concentration eight times, while, if Cu > CN/4, a dilution to a half should halve the cuprous ion concentration. The experimental potential values in Table I and II confirm this prediction by the sudden reversal and change in magnitude of the effect of dilution on the potential at a Cu:CN ratio of 0.25.

Table III. Experimental static potentials of Cu in cuprocyanide solutions at 80°C

Ratio Cu:CN	4M Cyanide	2M	1M	0.5M	0.25M	0.125M	0.06M
0.35	−0.50	−0.47	−0.43	−0.42	−0.41	−0.42	−0.44
0.375	−0.44	−0.40	−0.38	−0.37	−0.37	−0.38	−0.39
0.40	−0.41	−0.37	−0.34	−0.33	−0.33	−0.35	−0.36

The calculation of the association constants also verifies the initial assumptions that $1 << k_3 << k_2 << k_1$. Agreement with other published values is satisfactory. At 80°C k_3 has dropped to 17 and, although still comparatively large, some small deviations from the calculated values might be expected.

The most serious deviations from the calculations occur at 80°C at a Cu:CN ratio of 0.35 and above, where dilution changes the potential in the opposite direction to that calculated. However, at lower concentrations it is again in the calculated direction as shown in Table III.

Because of this effect the reference point for the ratio Cu:CN 0.375 was chosen at a low total cyanide concentration. At this ratio at 20°C a low total cyanide concentration reference point was also employed, on account of the solubility limits shown in Table I.

The absorption spectra at room temperature (Fig. 1) confirm the assumption that k_3 is large, by the abrupt transition at a Cu:CN ratio of 0.25. k_3 could not actually be calculated, because even in very dilute solutions no absorption maximum could be obtained, as the spectra may be due to electron transfer.

The absorption spectra do not differentiate between the $Cu(CN)_3^=$ and $Cu(CN)_2^-$ ions, but good independent evidence that $k_3 << k_2$ is provided by titrating cuprocyanide solutions at room temperature with $AgNO_3$ using KI as indicator. Silver iodide is precipitated when sufficient argentocyanide has been formed to leave the Cu:CN ratio 0.33. While this titration cannot be used to study cuprocyanide equilibria in general, it suggests that at the end point $Cu(CN)_3^=$ is the principal ion, and not just a mixture of $Cu(CN)_2^-$ and $Cu(CN)_4^=$ is present. A modification of this titration is used to estimate "free cyanide" in commercial plating baths.

Glasstone (4) argues that $Cu(CN)_2^-$ and $Cu(CN)_3^=$ are the only ions in cuprocyanide solution. Working in solutions from 0.1 to 0.5M cyanide he gets a clear inflexion on his potential curve at a Cu:CN ratio of 0.32 on which he bases his conclusion. Britton and Dodd (5) in similar work obtain an inflexion at a ratio of 0.28. However, taking all three complexes into account, Fig. 2 shows a very clear inflexion at a ratio of 0.25 at high concentrations, but at lower concentrations (more especially at high temperatures) this almost disappears and a pronounced inflexion at 0.33 becomes apparent.

Acknowledgments

The author wishes to thank Dr. A. Hickling for his encouragement and much helpful advice, and Dr. L. H. Sutcliffe for many useful comments. The work was carried out during the tenure of a New Zealand National Research Fellowship.

Manuscript received June 6, 1956.

Any discussion of this paper will appear in a Discussion Section to be published in the June 1958 JOURNAL.

REFERENCES

1. F. Kunschert, *Z. anorg. Chem.*, **41**, 359 (1904).
2. H. Grossmann and P. Von der Forst, *ibid.*, **43**, 94 (1905).

3. A. Höing, *Z. Elektrochem.*, **22**, 286 (1916).
4. S. Glasstone, *J. Chem. Soc.*, **1929**, 690.
5. H. T. S. Britton and E. N. Dodd, *ibid.*, **1935**, 100.
6. H. Brintzinger and H. Osswald, *Z. anorg. Chem.*, **220**, 177 (1934).
7. M. R. Thompson, *Trans. Electrochem. Soc.*, **79**, 417 (1941).
8. G. Gabrielson, *Metal Finishing*, **52**, 60 (1954).
9. C. Calmar and M. Costa, *Compt. rend.*, **243**, 56 (1956).
10. R. Penneman and L. H. Jones, *J. Chem. Phys.*, **24**, 293 (1956).
11. H. J. Barber, *J. Chem. Soc.*, **1943**, 79.
12. M. G. Vladimirova and I. A. Kakovskii, *J. Appl. Chem. U.S.S.R.*, **23**, 615 (1950). (English translation.)
13. F. Spitzer, *Z. Elektrochem.*, **11**, 345 (1905).
14. H. Bassett and A. S. Corbet, *J. Chem Soc.*, **125**, 1660 (1924).
15. S. E. S. El Wakkad, *ibid.*, **1950**, 3563.
16. W. M. Latimer, "The Oxidation States of the Elements and their Potentials in Aqueous Solutions," 2nd ed., pp. 185-6, Prentice Hall, Inc., New York (1952).
17. A. R. Tourky and E. M. Khairy, *J. Chem. Soc.*, **1952**, 2626.

Hydrogen Overpotential on Electrodeposited Ni in NaOH Solutions

I. A. Ammar and S. A. Awad

Chemistry Department, Faculty of Science, Cairo University, Cairo, Egypt

ABSTRACT

Hydrogen overpotential, η, is measured for electrodeposited Ni in 0.01-1.0*N* NaOH solutions. The effect of temperature on η is studied and the heat of activation, ΔHo^*, at the reversible potential is calculated. The pH effect $(\partial\eta/\partial pH)_i$ is calculated at 25°C and is equal to 26 mv per unit increase of pH. The electron number, λ, calculated from the overpotential results at very low current densities, is very near to unity. The Tafel line slope, b, increases with temperature. Results are compared with those obtained for Ni in the form of a wire.

Hydrogen overpotential on electrodeposited metals has not been studied extensively. A few studies are, however, recorded in the literature (1, 2). The uncertainty concerning the magnitude of the true surface area of an electrodeposited electrode, together with the possibility of contaminating the electrode surface during electrodeposition, hinder the progress in this field. Recent work on electrodeposited Ni in HCl solutions (3) has indicated that the parameters of cathodic hydrogen evolution on electrodeposited Ni are different from those observed for a Ni wire. Consequently the mechanism of hydrogen evolution is different for the two types of electrodes. Bockris and co-workers (4, 5) have formulated several criteria for distinguishing between the possible rate-determining mechanisms. The aim of the present work is to study the hydrogen overpotential on electrodeposited Ni in NaOH solutions, particularly at the very low current density range, with the hope of evaluating the number of electrons, λ, necessary to complete one act of the rate-determining mechanism (5).

Experimental

The experimental technique was essentially the same as that of Bockris, *et al.* (4, 6). The electrolytic cell was constructed of arsenic-free glass. All ground glass joints and taps were of the solution-sealed type. This helped to hinder the diffusion of atmospheric oxygen inside the cell. A platinized Pt electrode, in the same solution and at the same temperature as the test cathode, was used as a reference electrode. Electrical contact between the cathode and the reference electrode was made through a Luggin capillary. To avoid complications due to resistance overpotential, the test cathode was adjusted to touch the tip of the Luggin capillary.

Electrodeposition of Ni was carried out from the following bath: 30 g $NiSO_4$, 10 g $(NH_4)_2SO_4$, 150 cc conductance water, and 100 cc concentrated NH_4OH. "AnalaR" grade reagents were used. Electrodeposition was carried out for 2 hr at a current density of 1 ma/cm^2, on a Ni substrate sealed to glass. The apparent surface area of the electrode was 0.8 cm^2. The electrode was thoroughly washed with conductance water before use.

Pure NaOH solutions were prepared under an atmosphere of pure hydrogen. Conductance water ($K = 2.0 \times 10^{-7}$ ohm^{-1} cm^{-1}) was used for the solution preparation. The solution was then extensively purified by pre-electrolysis (7) at 1×10^{-2} amp/cm^2 for 20 hr. A Ni electrode, prepared in the same manner as the test electrode, was used for pre-electrolysis. Pure hydrogen was passed into the cell during pre-electrolysis. Hydrogen was purified from O_2 by Cu heated to 450°C, from CO_2 by soda lime and from CO by a mixture of MnO_2 and CuO, technically known as "Hopcalite" (8).

The direct method of measurements was used and the current density was calculated using the apparent surface area. The potential was measured with a valve potentiometer and the current with a sensitive micromilliammeter. At low currents the current was checked by measuring the potential drop across a standard resistance. The temperature was kept constant, to ±0.5°C, with the help of an air thermostat.

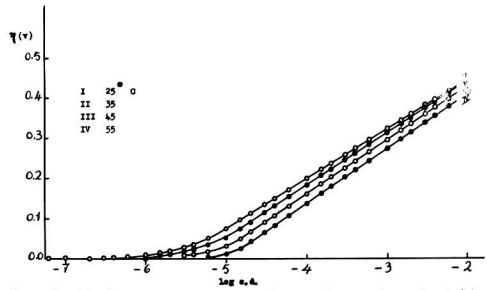

Fig. 1. Hydrogen overpotential on electrodeposited Ni in 0.1N NaOH.

Before each run, all glass parts of the apparatus were cleaned with a mixture of "AnalaR" HNO_3 and H_2SO_4. This was followed by washing with equilibrium water and then with conductance water. Care was also taken to free the previously cleaned cell from oxygen. This was done by filling the cell completely with conductance water (distilled under hydrogen), and then replacing this water by pure hydrogen before the NaOH solution was introduced. With the above precautions, the overpotential results obtained with different test electrodes agreed within ±10 mv at intermediate and high current densities, and ±3 mv at low current densities. For each test electrode, the overpotential results were in agreement within less than ±10 mv. For each concentration and temperature studied, at least six Tafel lines (a new electrode and a new solution for each Tafel line) were measured and the mean line was computed.

Results

The Tafel line slope, b, the transfer coefficient, α, and the exchange current, i_o, for the mean Tafel lines on electrodeposited Ni in 0.01, 0.05, 0.10, 0.50, and 1.0N aq NaOH solutions are given in Table I. Fig. 1 shows four mean Tafel lines on electrodeposited Ni in 0.1N NaOH solution at 25°, 35°, 45°, and 55°C. The transfer coefficient is calculated according to $b = 2.303\ RT/\alpha F$.

The electron number, λ, defined as the number of electrons necessary to complete one act of the rate-determining step (5), is calculated using:

Table I*

Conc. N	Temp, °C	b, mv	α	i_o, amp/cm²	$(\partial\eta/\partial i_c)\,\eta\to 0$‡	λ
0.01	25	122	0.48	1.6×10^{-6}	1.50×10^{4}	1.1
0.05	25	122	0.48	2.0×10^{-6}	1.25×10^{4}	1.0
	35	125	0.49	3.2×10^{-6}	7.50×10^{3}	1.1
	45	128	0.49	5.0×10^{-6}	5.00×10^{3}	1.1
	55	130	0.50	7.9×10^{-6}	2.70×10^{3}	1.3
0.10	25	122	0.48	2.5×10^{-6}	1.06×10^{4}	1.0
	35	130	0.47	4.0×10^{-6}	7.50×10^{3}	0.9
	45	135	0.47	6.6×10^{-6}	4.40×10^{3}	0.9
	55	137	0.47	1.0×10^{-5}	2.65×10^{3}	1.1
0.50	25	122	0.48	3.3×10^{-6}	8.12×10^{3}	1.0
	35	130	0.47	5.0×10^{-6}	5.25×10^{3}	1.0
	45	135	0.47	8.3×10^{-6}	3.50×10^{3}	1.1
	55	138	0.47	1.3×10^{-5}	2.65×10^{3}	0.8
1.00	25	125	0.47	4.5×10^{-6}	6.00×10^{3}	1.0

* Values of α are given to the nearest second decimal figure, and λ to the nearest first decimal figure.
‡ Reproducible within ±3%.

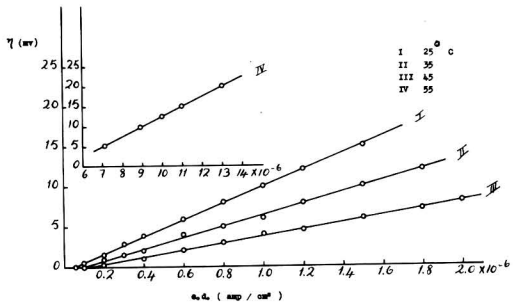

Fig. 2. Relation between overpotential and current density at very low cathodic polarization for electrodeposited Ni in 0.1N NaOH.

$$\lambda = \frac{RT}{i_o F}\,(\partial i_c/\partial\eta)\ \eta \to 0 \qquad \text{(I)}$$

and,

$$\exp\,(\lambda\eta_s F/RT) = 0.05 \qquad \text{(II)}$$

η_s is the overpotential at which the Tafel line departs from linearity owing to the appreciable rate of ionization of adsorbed atomic hydrogen. Eq. II gives approximate values for λ. The values of the electron number calculated according to Eq. (I) are included in Table (I). Values of λ calculated according to Eq. II are in substantial agreement with the values obtained from Eq. (I). The relation between η and the current density for small cathodic polarization (below 20 mv) is shown in Fig. 2 for the mean Tafel lines in 0.1N NaOH.

The effect of pH on hydrogen overpotential is studied at 25°C. The overpotential at three different current densities (10^{-3}, 10^{-4}, and 10^{-5} amp/cm²) is plotted against the pH; the result is shown in Fig. 3. From Fig. 3 it is clear that the value of $(\partial\eta/\partial p\mathrm{H})_i$ at the three different current densities is 26 ± 1 mv/unit increase of pH.

The relation between log i_o and the reciprocal of temperature is shown in Fig. 4 for 0.05, 0.10, and 0.50N aq. NaOH solutions. The heat of activation, ΔHo^*, at the reversible potential is calculated from the slope of log $i_o - 1/T$ relation according to (6,9):

$$i_o = B \exp\,(-\Delta Ho^*/RT) \qquad \text{(III)}$$

where B is the Eyring entropy factor (5, 6, 10). A mean value of 8.8 ± 0.1 kcal/mole is calculated for ΔHo^* from the results in 0.05, 0.10, and 0.50N NaOH according to Eq. (III). Using this mean value of

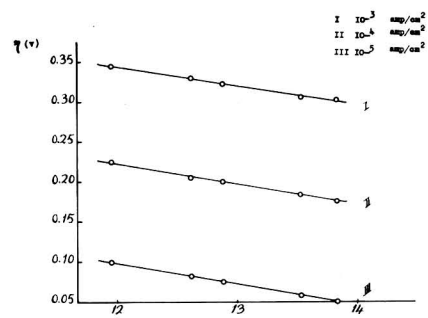

Fig. 3. Effect of pH on overpotential for electrodeposited Ni in NaOH solutions at 25°C.

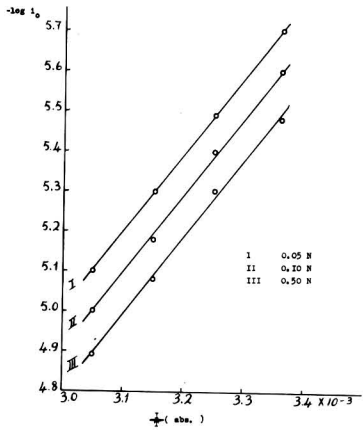

Fig. 4. Relation between the logarithm of the exchange current and the reciprocal of temperature for electrodeposited Ni in NaOH solutions.

ΔHo^* in Eq. (III), log B is calculated, at 25°C, for the various NaOH solutions studied. The relation between log B and log a_{NaOH} is linear with a slope of approximately 0.23. This relation is shown in Fig. 5.

The heat of activation, ΔHo^*, may also be calculated from the rate of change of η with temperature at a constant current density according to (5):

$$(\partial\eta/\partial T)_i = (\Delta Ho^* + \alpha\eta F)/\alpha FT \qquad \text{(IV)}$$

The results obtained by this method are less reproducible than those obtained from the slope of log $i_o - 1/T$ relation (3). ΔHo^* is calculated using the mean values of α, η, and T in the right hand side of Eq. (IV); the results are given in Table (II).

Discussion

The results for electrodeposited Ni are not concordant with the results on Ni in the form of a wire (6, 11, 12). Thus, the overpotential at a constant current density is numerically lower for electrodeposited Ni than that for Ni wire in the same solution and at the same temperature. The exchange currents for electrodeposited Ni are higher than the corresponding values for Ni wire. Thus, the value of i_o for electrodeposited Ni in 0.1N NaOH at 25°C is 2.5×10^{-6} amp/cm² (cf. Table I), whereas for Ni wire i_o in the same solution lies between 4×10^{-7} amp/cm² at 20°C, and 7.9×10^{-7} amp/cm² at 40°C [cf. Ref. (6)]. The difference between the i_o values for electrodeposited and bulk Ni (wire) may be partly attributed to a large true surface area for the former as compared to the latter. The apparent current density corresponds to a lower true current density in the case of electrodeposited Ni and consequently η is numerically smaller than in the case of bulk Ni. The i_o values for electrodeposited Ni are therefore greater than those of bulk Ni. Furthermore, it has been observed (6) that the Tafel line slope b for Ni wire does not vary with temperature, whereas for electrodeposited Ni it is clear from Table (I) that b increases with temperature. This also accounts for the difference between the i_o values obtained in the present investigation and those of Bockris and Potter (6). Since $b = 2.303\ RT/\alpha F$, α may therefore be taken as independent of temperature with a value lying between 0.47 and 0.50. The fact that b increases with temperature is in accordance with the results of others (13, 14). It is also to be noted that no effect of time on the overpotential on electrodeposited Ni is observed in the present investigation. In other words, η reaches a constant value in less than a minute. On the other hand, an appreciable time effect is observed for bulk Ni (11, 15). This is in agreement with the results of Bockris and Parsons (1) who observe that the attainment of the steady-state value of η is quicker for electrodeposited metals probably because of the co-deposition of hydrogen during electrodeposition.

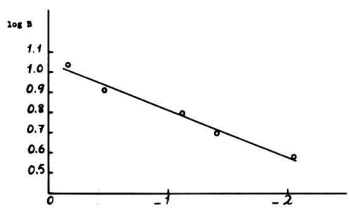

Fig. 5. Relation between the logarithm of the Eyring entropy factor and log a_{NaOH}.

Table II

Conc. N	Temp range, °C	$(\partial\eta/\partial T)_i$ mv/degree	Mean α	Mean η mv, at 10^{-4}amp/cm²	ΔHo^*, kcal	Mean ΔHo^*
0.05	25-35	1.8	0.485	197	8.3	
	35-45	2.1	0.490	178	9.4	9.2
	45-55	2.2	0.495	156	9.9	
0.10	25-35	1.6	0.475	191	7.4	
	35-45	2.3	0.470	172	9.7	9.2
	45-55	2.5	0.470	148	10.4	
0.50	25-35	1.5	0.475	176	6.9	
	35-45	2.1	0.470	158	8.8	8.3
	45-55	2.2	0.470	136	9.2	

The activation overpotential associated with the cathodic evolution of hydrogen may be attributed to a rate-determining slow discharge process, electrochemical desorption, or catalytic combination (5). Other rate-determining mechanisms of less importance are cited in the literature (4). A rate-determining slow discharge is characterized by a Tafel line slope of 0.120 v at 30°C and by $\lambda = 1$. For a rate-determining electrochemical desorption, the Tafel line exhibits two slopes (21) of 0.040 v and 0.120 v at 30°C in the linear logarithmic section, and λ is 2. A rate-determining catalytic combination is distinguished by a Tafel line slope of 0.030 v at 30°C in the range of current densities used in the present investigation. For this mechanism λ is also 2. From this and the data given in Table I it is evident that the rate of hydrogen evolution on electrodeposited Ni in NaOH solutions is controlled by a slow discharge mechanism. This is supported by the fact that the values of the transfer coefficient, α, are very near to 0.5 (cf. Table I), the value usually observed for a slow discharge mechanism (16, 17). Owing to the diminishingly small concentration of H_3O^+ ions in alkaline solutions, it is possible that the discharge takes place from water molecules and not from H_3O^+ ions (18). This is supported by the positive values of $(\partial\eta/\partial pH)_i$ obtained

in the present investigation (cf. Fig. 3). The rate-determining step in the over-all reaction for hydrogen evolution on electrodeposited Ni in NaOH solutions is, therefore, represented by:

$$H_2O + e \rightarrow OH' + MH \qquad (V)$$

where M represents the electrode surface. This is followed either by a fast catalytic combination:

$$MH + MH \rightarrow H_2 \qquad (VI)$$

or by a fast electrochemical desorption:

$$H_2O + MH + e \rightarrow H_2 + OH' \qquad (VII)$$

There is, however, no evidence to favor either the catalytic combination or the electrochemical desorption.

Values theoretically deduced (6) for $(\partial\eta/\partial pH)_i$ in the case of the discharge from water molecules lie between 60 mv and 120 mv per unit increase of pH at 30°C for conditions near and far from the electrocapillary maximum, respectively. The experimentally observed value of $(\partial\eta/\partial pH)_i$ for electrodeposited Ni is 26 mv, thus indicating that the experimental pH effect is much smaller than the theoretical values. Similar observations have been made for Ag in NaOH solutions (20). For Ni wire the pH effect, observed by Bockris and Potter (6), lies between 10 and 25 mv per unit increase of pH whereas the work of Lukovstev and Lewina (12) indicates a pH effect of 40 mv per unit pH. The experimental pH effect cannot be accounted for by Bockris and Watson's mechanism (19), in which the hydrogen originates from Na atoms and water molecules, since this mechanism does not apply to Ni (6). For the discharge from water molecules, Bockris and Potter (6) have taken into consideration the effect of the orientation of water molecules in the double layer. The main postulate of this treatment is that the activity of water in the double layer increases faster than that in the bulk of solution owing to the effect of the high field strength near the electrode. Even with this treatment the theoretical values of $(\partial\eta/\partial pH)_i$ for the discharge from water molecules are still different from the experimental values. Bearing in mind that the discharge for H_2O molecules is rate determining for hydrogen evolution on electrodeposited Ni in NaOH solutions one may proceed to explain the experimental pH effect of 26 mv/unit increase of pH at 30°C.

The expression for the cathodic current density, taking $\alpha = 0.5$, is given by (5):

$$i = i_o \cdot \exp \cdot (-\eta F/2RT) \qquad (VIII)$$

It is clear from Eq. (VIII) and Fig. 3 that:

$$(\partial\eta/\partial pH)_i = 2\left(\frac{2.303\,RT}{F}\right)\left(\frac{\partial \log i_o}{\partial pH}\right) = 0.026 \pm 0.001 \text{ v} \qquad (IX)$$

and from (IX) taking $\partial pH = \partial \log a_{NaOH}$ one gets at 25°C:

$$i_o = K(a_{NaOH})^{0.23} \qquad (X)$$

where K is a constant at constant temperature. Equation (X) is based on the experimental pH effect observed in the present investigation. The dependence of i_o on a_{NaOH} may be attributed to the dependence of the activity of water, in the initial state of the reaction, on a_{NaOH}. Thus, the expression for i_o may be given by (5):

$$i_o = \lambda F X \frac{kT}{h}(a_{H_2O}) \cdot \exp \cdot (\Delta So^*/R) \exp \cdot (-\Delta Ho^*/RT) \qquad (XI)$$

where X is the transmission coefficient, a_{H_2O} is the activity of the reactant (water) in the initial state, ΔSo^* is the standard entropy of activation at the reversible potential, and (kT/h) has its usual significance as given by the theory of absolute reaction rates (10). From (III) and (XI) it follows that:

$$B = \lambda F X \frac{kT}{h}(a_{H_2O}) \cdot \exp \cdot (\Delta So^*/R) \qquad (XII)$$

It has been observed experimentally that ΔHo^*, for hydrogen evolution on electrodeposited Ni in NaOH solutions, is independent of a_{NaOH}. If the assumption is made that ΔSo^* is also independent of a_{NaOH} it follows from (X) and (XI) that :

$$a_{H_2O} \propto (a_{NaOH})^{0.23} \qquad (XIII)$$

and the experimental pH effect observed in the present investigation may, thus, be due to the dependence of the activity of water in the initial state on a_{NaOH} as given by (XIII). The linearity between log B and log a_{NaOH} (Fig. 5) follows, therefore, from Eqs. (XII) and (XIII). Combining (XII) and (XIII) one gets:

$$B = K'(a_{NaOH})^{0.23} \cdot \exp(\Delta So^*/R) \qquad (XIV)$$

ΔSo^* may be calculated according to (XIV) from the value of B corresponding to $a_{NaOH} = 1$ (Fig. 5). If the proportionality constant in (XIII) is assumed to be equal to unity, K' becomes:

$$K' = \lambda F X \frac{kT}{h} \qquad (XV)$$

where X is usually taken as unity (10), and the value of ΔSo^* (standard state $a_{NaOH} = 1$) calculated according to (XIV) and (XV) is —77 cal/degree/mole.

Variation of i_o with a_{NaOH} [Eq. (X)] may also be attributed to the change of the free energy of activation with a_{NaOH}. At present there is, however, no evidence to favor one of the above two possibilities and the solution to this problem will be dealt with in a later publication.

Acknowledgments

The authors wish to express their thanks to A. R. Tourky for his interest in this work, and to J. O'M. Bockris for helpful discussions.

Manuscript received Oct. 22, 1956.

Any discussion of this paper will appear in a Discussion Section to be published in the June 1958 JOURNAL.

REFERENCES

1. J. O'M. Bockris and R. Parsons, *Trans. Faraday Soc.*, **44**, 860 (1948).
2. W. Senett and C. Hiskey, *J. Am. Chem. Soc.*, **74**, 3754 (1952).

3. I. A. Ammar and S. Awad, *J. Phys. Chem.*, **60**, 837 (1956).
4. J. O'M. Bockris, *Chem. Rev.*, **43**, 525 (1948).
5. J. O'M. Bockris and E. C. Potter, *This Journal*, **99**, 169 (1952).
6. J. O'M. Bockris and E. C. Potter, *J. Chem. Phys.*, **20**, 614 (1952).
7. A. Azzam, J. O'M. Bockris, B. Conway, and H. Rosenberg, *Trans. Faraday Soc.*, **46**, 918 (1950).
8. G. Schwab and G. Drikos, *Z. Physik. Chem.*, **185A**, 405 (1940).
9. J. O'M. Bockris, *Ann. Rev. Phys. Chem.*, **5**, 477 (1954).
10. S. Glasstone, H. Eyring, and K. Laidler, *J. Chem. Phys.*, **7**, 1053 (1939); Theory of Rate Processes, p. 588, McGraw-Hill Co. (1941).
11. S. Lewina, P. Lukovstev, and A. Frumkin, *Acta Physicochim.*, **11**, 21 (1939).
12. P. Lukovstev and S. Lewina, *J. Phys. Chem., U.S.S.R.*, **21**, 599 (1947).
13. F. Bowden and J. Agar, *Ann. Report*, **35**, 90 (1938); F. Bowden, *Proc. Roy. Soc.*, **A126**, 107 (1929).
14. B. Post and C. Hiskey, *J. Am. Chem. Soc.*, **72**, 4203 (1950).
15. J. O'M. Bockris and B. Conway, *Trans. Faraday Soc.*, **45**, 989 (1949).
16. A. Frumkin, *Discussion Faraday Soc.*, **1**, 62 (1947).
17. Z. Jofa and A. Frumkin, *Acta Physicochim.*, **18**, 183 (1943).
18. J. O'M. Bockris and R. Parsons, *Trans. Faraday Soc.*, **47**, 914 (1951).
19. J. O'M. Bockris and R. G. Watson, *J. Chim. Phys.*, **49**, c70 (1952).
20. I. A. Ammar and S. Awad, *J. Phys. Chem.*, **60**, 1290 (1956).
21. I. A. Ammar and S. Awad, *This Journal*, **103**, 182 (1956).

Discussion of Papers

December 1957 Discussion Section—A Discussion Section, covering papers published in the January-June 1957 JOURNALS, is scheduled for publication in the December 1957 issue. Any discussion which did not reach the Editor in time for inclusion in the June 1957 Discussion Section will be included in the December 1957 issue.

June 1958 Discussion Section—A Discussion Section, covering papers published in the July-December 1957 JOURNALS, will appear in the June 1958 issue. Those who plan to contribute remarks for this Discussion Section should submit their comments or questions in triplicate to the Managing Editor of the JOURNAL, 1860 Broadway, New York 23, N. Y., *not later than March 1, 1958*. All discussion will be forwarded to the author, or authors, for reply before being printed in the JOURNAL.

Technical Note

The Value of the Electromotive Force of a Voltaic Cell; A Magnitude Without Sign

J. B. Ramsey

Department of Chemistry, University of California, Los Angeles, California

There exists considerable doubt among chemists and other physical scientists regarding the need of giving a sign to the value of the electromotive force of a voltaic cell.

It is the purpose of this paper to present justification for a nonalgebraic definition of the value of the emf of a voltaic cell, that is, for giving the emf of a cell a numerical value (a magnitude without sign) irrespective of the orientation of its two electrodes in its symbolic formulation.

The sign convention quite generally used in assigning an algebraic value to the emf of a voltaic cell is the one originally adopted by Lewis (1). According to this sign convention the value to be given to the electromotive force of a cell *as formulated* "shall represent the tendency of the negative current to pass spontaneously through the cell from right to left." This convention has been reaffirmed in the recommendations made by the Commission on Physico-Chemical Symbols and Terminology and the Commission on Electrochemistry (2), both of the International Union of Pure and Applied Chemistry, at their meeting in Stockholm in 1953. Recently deBethune (3) has given a clarifying discussion of the recommendations of these Commissions.

Proposed nonalgebraic definition of the emf of a voltaic cell.—We propose to define the value of the emf of a voltaic cell as the absolute value of the difference between the electrode potentials of the two electrodes of the cell, which is, therefore, independent of the way in which the cell may be formulated. This definition is expressed by the following relation,

$$\text{emf}_{\text{Cell}} = | V_1 - V_2 | = | \mathcal{E}_1 - \mathcal{E}_2 |$$

where V_i represents the Gibbs-Stockholm (electrostatic) electrode potential of the ith electrode and $\mathcal{E}_i$, the electron chemical potential of the ith electrode as defined by Ramsey (4).

Consequence of this definition.—Consider the occurrence of an isothermal change in state requiring the passage of n faradays of electricity (positive or negative) in the direction required by the change in state considered. The numerical value (magnitude) of the maximum (isothermal) electrical work producible either in the surroundings or in the system (the voltaic cell) during this isothermal change in state is $nE_{\text{Cell}}F$. The sign given to $nE_{\text{Cell}}F$ is dependent on the thermodynamic definition of "work." Most American physical chemists define "work" in such a way that it is given a positive value if produced in the surroundings and a negative value if produced in the system ($Q = \Delta E + W$).

Now if the isothermal change in state being considered occurs spontaneously, then work will be produced in the surroundings during this change and $nE_{\text{Cell}}F$ will have a positive value. If, on the other hand, electrical work must be done on the system (the voltaic cell) in order to bring about the change considered, $nE_{\text{Cell}}F$ must be given a negative value.

The change in free energy, ΔF, accompanying the change in state considered, is then given by the relation.

$$\Delta F = -(nE_{\text{Cell}}F)$$

in which the sign to be given $nE_{\text{Cell}}F$ is determined as described in the preceding paragraph, viz., a positive sign if electrical work is produced in the surroundings (change will occur spontaneously) and a negative sign if electrical work must be done on the system to bring about the change considered (the change would occur spontaneously in the reverse direction to that being considered).

The definition of the electromotive force of a voltaic cell, conceived as a magnitude without sign, in terms of the potentials of its two electrodes depends on the definition of an electrode potential which is used. If the Gibbs-Stockholm electrode potential, V_i, is adopted [*see* Ref. (3)], (where the term "potential" is used in the electrostatic sense) then the emf of a cell is defined as the tendency of positive current to flow through the outer circuit from the electrode having the greater value of V to the one with the smaller value of V. It may be noted the potential, V, applies strictly to the piece of "external circuit" metal connected with each of the electrodes respectively. If, however, the "electron chemical potential," $\mathcal{E}$, of an electrode [*see* Ref. (4)] is adopted (where the term "potential" is used in its thermodynamic sense) then the emf of a cell is defined as the tendency of electrons to flow through the external circuit from the electrode hav-

ing the greater $\mathcal{E}$-value to the one having the smaller $\mathcal{E}$-value. It should be noted that nothing is said in these definitions of the emf regarding the orientation of the two electrodes of the cell *as it may be arbitrarily formulated.*

The justification for considering the value of the emf of a cell to have a magnitude without sign may be summarized as follows: when a sign convention has been adopted for the maximum (isothermal) electrical work, $W_{rev.el.}$, transferred during the isothermal change in state considered, namely (according to many thermodynamicists) that it, $W_{rev.el.}$, have a positive sign if work is produced in the surroundings and a negative sign if produced in the system (the voltaic cell in this case), the adoption of an additional sign convention for the electromotive force of a voltaic cell, as formulated, is redundant and serves no useful purpose.

Manuscript received July 9, 1957.

Any discussion of this paper will appear in a Discussion Section to be published in the June 1958 JOURNAL.

REFERENCES

1. G. N. Lewis and M. Randall, "Thermodynamics and the Free Energy of Chemical Substances," p. 390, McGraw-Hill Book Co., Inc., New York, New York (1923).
2. J. A. Christiansen and M. Pourbaix, Compt. rend. XVII. Conf. Inter. Union Pure and Appl. Chem., held in Stockholm in 1953, Maison de la Chemie, Paris (1954), pp. 82-84.
3. A. M. deBethune, *This Journal*, **102**, 288C (1955).
4. J. B. Ramsey, *ibid.*, **104**, 255 (1957).

FUTURE MEETINGS OF
The Electrochemical Society

New York, N. Y., April 27, 28, 29, 30, and May 1, 1958

Headquarters at the Statler Hotel

Sessions probably will be scheduled on Electric Insulation, Electronics, Electrothermics and Metallurgy, Industrial Electrolytics, and Theoretical Electrochemistry (including a symposium on "Electrokinetic and Membrane Phenomena")

★ ★ ★

Ottawa, Canada, September 28, 29, 30, October 1, and 2, 1958

Headquarters at the Chateau Laurier

★ ★ ★

Philadelphia, Pa., May 3, 4, 5, 6, and 7, 1959

Headquarters at the Sheraton Hotel

★ ★ ★

Columbus, Ohio, October 18, 19, 20, 21, and 22, 1959

Headquarters at the Deshler-Hilton Hotel

★ ★ ★

Chicago, Ill., May 1, 2, 3, 4, and 5, 1960

Headquarters at the Lasalle Hotel

★ ★ ★

Houston, Texas, October 9, 10, 11, 12, and 13, 1960

Headquarters at the Shamrock Hotel

★ ★ ★

Papers are now being solicited for the meeting to be held in New York, N. Y., April 27-May 1, 1958. Triplicate copies of each abstract (*not exceeding 75 words in length*) are due at the Secretary's Office, 1860 Broadway, New York 23, N. Y., *not later than January 2, 1958* in order to be included in the program. *Please indicate on abstract for which Division's symposium the paper is to be scheduled.* Complete manuscripts should be sent in triplicate to the Managing Editor of the JOURNAL at 1860 Broadway, New York 23, N. Y.

Book Reviews

Instrumental Analysis by Paul Delahay. Published by Macmillan Co., New York, 1957. xi + 384 pages, 16 × 24 cm; $7.90.

Physicoanalytical chemistry has become much too vast a field to be treated more than superficially in a single course, especially at the undergraduate level. As Dr. Ralph H. Müller has been saying for years, adequate education in this subject requires a curriculum of several courses based on the recognition that instrumentation has grown to the stature of a distinct scientific discipline, and for which the orthodox courses in chemistry, physics, and mathematics ordinarily required for a bachelor's degree in chemistry would be prerequisite. We can have faith that such a program ultimately will become a part of university curricula. Meanwhile, however, we seem to be faced with the choice of either offering separate courses, according to our individual competence, which delve deeply and critically into only one or two areas of physicochemical analysis, or of presenting a survey-type course under the pseudonym "instrumental analysis," which attempts to give a glimpse of the whole field. This textbook is intended for the latter alternative.

The book is designed for a course of 40 to 60 lectures. The topics treated include potentiometry, polarography, amperometric titrations, electrogravimetry, coulometric analysis, conductimetry at both kilo- and megacycle frequencies, emission spectroscopy, absorption spectrometry, fluorimetry, turbidimetry, nephelometry, Raman spectroscopy, x-ray methods, mass spectrometry, and nuclear radiation methods. The text concludes with a set of about 50 laboratory experiments which illustrate cardinal principles of the various techniques.

Since Professor Delahay's special interest is electroanalytical techniques it is not surprising that these occupy much more space (150 pages) than such subjects as emission spectroscopy (30 pages), absorption spectrometry (30 pages), mass spectrometry (15 pages), or nuclear radiation methods (30 pages), which in terms of volume of applications might be regarded as more important. There is scarcely any mention of either solution or gas chromatography, nor of nuclear magnetic resonance techniques, although these surely can qualify as important instrumental methods of analysis.

In general the treatment is restricted to skeletal principles and the discussions are at about the level of an elementary physical chemistry text. In several places the discussions are too elementary for students who presumably will already have had fundamental courses in analytical and physical chemistry. This is particularly noticeable in the treatment of electrode potentials in Chapter 2 and of titration curves in Chapter 3, which do not go beyond the level of most modern texts of elementary quantitative analysis. However, this oversimplification is alleviated to a considerable degree by suggestions for further study and by sets of problems at the end of each chapter. These problems are perhaps the most valuable feature of the book, and the student who masters them will acquire a sound understanding of many facets of physicoanalytical chemistry.

James J. Lingane

The Chemistry of Organometallic Compounds by Eugene G. Rochow, Dallas T. Hurd, and Richard N. Lewis. Published by John Wiley & Sons, Inc., New York, 1957. 344 pages, $8.50.

This volume begins with a brief chapter which defines the scope of the book and considers in very general terms the physical and chemical properties of organometallic compounds. The second chapter describes the types of carbon-metal bonds to be met with and lays the foundation for an interpretation of the chemistry of organometallic compounds in terms of the carbon-metal bonds they contain. The third chapter describes in general terms the methods of preparing organometallic compounds. These three chapters should be read *after* as well as before the next seven chapters in which organometallic compounds are discussed in groups corresponding to the periodic groups of the metals they contain. A chapter on the use of organometallic compounds in organic synthesis and a chapter on special types of organometallic compounds (e.g., fluorocarbon derivatives, metal carbonyls, metal-olefin complexes, carbides, and hydrides) complete the volume. The final chapter contains a brief section on materials-handling techniques.

It is a major accomplishment to cover the subject of organometallic compounds in the space of a single volume of modest size. The authors have succeeded in doing this by emphasizing the properties that are common to various classes of organometallic compounds, by relating properties to bond types, and by reference to more detailed treatments elsewhere. This volume does not take the place of such detailed treatises as that of Kharasch and Reinmuth on the "Grignard Reactions of Nonmetallic Substances," but it should be read carefully as an excellent general survey which can then be supplemented by reference to the detailed treatises. It is recommended generally to chemists who are interested in the broad outlines of the chemistry of the organometallic compounds and specifically to chemists who plan to do research in this field.

There are a few errors in the book and a few statements that are not clear. In the periodic arrangement of the elements on p. 6 the symbol Ti is given for thallium. On p. 110 the statement that a "methanol suspension of mercuric acetate absorbs one molecule of ethylene in an hour" does not have much meaning in the absence of additional information about the volume of solution and the rate of gas flow. Thiophene as well as furan can be mercurated to a tetraacetoxymercuri derivative (p. 118). The third equation on p. 200 should be balanced by having $MgCl_2$ and $MgBr_2$, not 2 $MgBr_2$, as products. On p. 277 the statement that "Propylene oxide and its homologs condense at the terminal carbon atom to give secondary alcohols" is not consistent with the accompanying equation showing the formation of

primary alcohols. In the discussion of synthetic uses of organometallic compounds on p. 283 it should be made clear that the formation of hydroperoxides from Grignard reagents and oxygen is of much more practical value than the formation of alcohols. The use of the simple hexagon for a phenyl group in the last equation on p. 287 may lead to confusion since the phenyl groups on p. 288 are written in the Kekulé form. Finally, the statement on p. 295 that "the reactivity of the organometallic compound varies inversely with the activity of the compound from which it is made" is not clear since no criterion of activity of the parent compound is given. From the context it would appear that "acidity" not "activity" was intended. These eight items that have just been listed are quite unimportant in terms of the over-all accomplishment of the authors.

A. H. Blatt

Physical Chemistry by N. K. Adam. Published by Clarendon Press, London, 1956. 658 pages, $10.00.

The author of this book has clearly had the intention that it should become a standard work on physical chemistry. It covers the requirements of most courses in undergraduate physical chemistry in U. S. universities. Little knowledge of mathematics is needed to read it.

There may be distinguished two types of approaches in physical chemistry texts. There is the Nernst-Glasstone approach in which most stress is thrown on experimental facts and their thermodynamic treatment, and the Eucken-Moelwhyn-Hughes approach, in which the stress is on the description of material systems in terms of models subject to statistical mechanical treatment. This book has basically the first of these approaches, but something of the second approach has been grafted on.

The writing is easy to understand. The section on nuclear chemistry is outstandingly clear and detailed (although it appears to cover material only up to about 1952). The historical mode of presentation shows up well: for example, it is common to read texts in which the impression is given that the theory of interionic attraction in very dilute solutions was first given by Debye and Hückel in 1923. Adam makes clear that van Laar in 1895 suggested that lack of ideal behavior in electrolytes sprang from interionic forces and the essential calculations were carried out by Milner in 1912. Debye and Hückel's achievement was to provide a simple method of calculation by which van Laar's suggestion could be properly tested.

The book has asides which may appropriately be termed "jolly." Thus, the origin of the unit "barn" for the unit of cross section (10^{-24} cm^2) in atomic collisions is stated to have occurred when Fermi said that the unit was: not small, but "as big as a barn" (p. 52). Three body collisions are described in terms of the "chaperon effect," where a chaperon acts "to prevent too ardent affinity for a person of the opposite sex resulting in a hasty and unstable association" (p. 460).

The order of presentation of the chapters appears illogical. It starts off with atoms instead of thermodynamics or kinetic theory, and goes on to gases, then to quantum theory, then solids. Only after this is thermodynamics revealed, to be followed by the Phase Rule, kinetics, etc. It is clear that there is a degree of arbitrariness in ordering the material of physical chemistry, but Thermodynamics, Statistical Mechanics, Quantum Theory, i.e., the fundamental basis of Chemical Theory, surely need to be treated rather early in a book and not sandwiched in between the development of special topics.

Sometimes the language is slipshod, as when the electrons are stated to be "kicked out of" atoms on p. 147. The section on liquids is poor. It consists of 23 pages in which structure is discussed on 3, whereas 4 are used up in describing how to measure surface tension. Holes in liquids are regarded as existing "partly for mathematical convenience" and "It seems doubtful . . . if such holes have . . . more than a transient existence" (p. 244).

A much more serious matter than the occasional lapses in standard arises from the frequent appearance of out-of-date attitudes or material. Thus, the author appears to be distrustful of the idea of activation energy (cf. p. 246). On p. 373, the mechanism described for proton transport in aqueous solution is one published in 1933 and superseded for the last 15 years. The attitude toward electrode kinetics (most recent reference: 1951) is worthy of 1941: the mechanism of hydrogen evolution is still discussed as if the problem were one of deciding once and for all between a "right" and a "wrong" mechanism and the impression is given that it is not possible to distinguish between different modes of desorption. The most recent reference on the section on Heterogeneous Reactions is of 1940. Text Books of Physical Chemistry become out of date soon enough: for one to *start* many years behind is disastrous.

This book is beautifully produced. It is outstanding in respect of this feature, and for its historical sections.

J. O'M. Bockris

The Science of Engineering Materials, J. E. Goldman, Editor. Published by John Wiley & Sons, Inc., New York, 1957. xv + 528 pages, $12.00.

This volume has grown out of a series of lectures delivered at the Carnegie Conference on the Impact of Solid State Science on Engineering Education held in Pittsburgh, Pa., at the Carnegie Institute of Technology in June 1954. It is written in six parts. Part I, entitled "The Structure of Matter," contains chapters on "Applications of Solid State Science in Engineering: An Introductory Survey" by H. Brooks; on "Structure of Atoms and Atomic Aggregates" by Bardeen, W. Bitter, and J. E. Goldman; on "Accomplishments and Limitations of Solid State Theory" by H. Brooks; and on "Crystal Imperfections" by J. Bardeen. Part II is concerned with "Metals and Alloys" and includes chapters on "The Metallic State: Theory of Some Properties of Metals and Alloys" by R. Smoluchowski; on "Electron Theory of Alloy Formation and Elastic Properties" by H. Jones; on "Dislocations in Solids" by R. Smoluchowski; on "Dislocation Theories of Mechanical Properties" by H. W. Paxton; on "Experimental Evidence for Behaviour of Dislocations" by E. R. Parker; and on "Phase Transformations in Metals and Their Influence on Mechanical Properties" by T. A. Read. An extensive contribution by R. Gomer on "Surface Phenomena" takes up the whole of Part III, while Part IV contains offerings by J. E. Goldman on "The Theoretical Basis of Magnetic Phenomena" and by R. M. Bozorth on "The Physics of Magnetic Materials." The discussions of Part V are by K. Lark-Horowitz and V. A. Johnson on "The Physics of Semi-Conductors" and by E. M. Conwell and W. J. Leivo on "Semiconductor Devices." Part VI, entitled "Non-Crystalline Materials," extends the coverage of the book beyond what is usually considered the domain of solid-state science to include contributions by S. Brunauer on "Some Aspects of the Physics and Chemistry of Cement," by T. Alfrey, Jr., on "Molecular Structure and Mechanical Be-

havior of High Polymers," and by T. H. Davies on "The Physics of Glass."

It was the intention of these well-known authorities to present broad summaries of the states of their special fields, as of about the end of 1953, which might serve as the basis for formal course work in engineering. Bibliographies giving references to specific original investigations and sources for further reading are provided. Despite the variety of viewpoints, the material of the book is well coordinated, so that each subject is developed naturally and there is little overlapping.

This volume is of more than ordinary interest. For the sufficiently competent reader there is a wealth of material on theory and applications clearly presented from a fundamental point of view. To round out the picture, limitations of the theory have been carefully delineated and directions for future investigation pointed out. Experts, of course, should find this compendium useful only for those parts which are not within the field of their specialties. The book is strongly recommended to interested advanced undergraduates and graduate students as well as to physical scientists who wish to become acquainted with the subject of solid-state science.

James N. Sarmousakis

Division News

Theoretical Electrochemistry Division

Spring 1958 Symposium

A symposium on **Electrokinetic and Membrane Phenomena** is being arranged by the Theoretical Electrochemistry Division for the meeting of the Society to be held in New York, N. Y., April 27 to May 1, 1958. The program is to include invited and contributed papers.

The committee arranging this program is: *Chairman,* Dr. Paul Delahay, Louisiana State University, Baton Rouge, La.; Professor J. J. Hermanns, Rijks University, Leiden, Netherlands; Dr. R. M. Hurd, University of Texas, Austin 12, Texas; Dr. T. Shedlovsky, The Rockefeller Institute for Medical Research, New York 21, N. Y.

Abstracts (not exceeding 75 words in length) of contributed and invited papers for this symposium and papers for the general sessions of the Theoretical Division should be submitted to the Secretary's Office, 1860 Broadway, New York 23, N. Y., in triplicate, *not later than January 2, 1958.*

Ralph Roberts, *Secretary-Treasurer*

Section News

Southern California-Nevada Section

Officers were elected and changes in the Bylaws were approved at the June 14 meeting of the Southern California-Nevada Section. Dave Stern gave a report on the meeting held in Washington of the Council of Local Sections, and the proposed Bylaws for the Section were modified to conform with the recommendations of the Council.

The following officers were elected for the coming season:

Chairman—W. M. Hetherington, Jr., 742 29th St., Manhattan Beach, Calif.
Vice-Chairman—Q. H. McKenna, 201 W. Washington Blvd., Whittier, Calif.
Secretary-Treasurer—L. J. Droege, 209 39th St., Manhattan Beach, Calif.
Representative on Council of Local Sections—M. E. Carlisle (2 yr)

Bill Hetherington, as the new Chairman, extended his thanks and those of the Society to Tom Blair for his work as Charter Chairman of the Section. He then introduced the speaker for the evening, Mr. Bruce Birchard, Patent Counsel for Hoffman Electronic Corp., who spoke on the conversion of solar to electric energy. His talk reviewed the development of silicon solar energy convertors and described such devices. A demonstration was presented to exhibit the application of some of these units.

L. J. Droege,
Secretary-Treasurer

New Members

In September 1957 the following were elected to membership in The Electrochemical Society by the Admissions Committee:

Active Members Sponsored by a Sustaining Member

Alex Katona, Hooker Electrochemical Co., Electrochemical Research Group, Niagara Falls, N. Y. (Industrial Electrolytic)
David B. Peck, Sprague Electric Co., North Adams, Mass. (Battery, Industrial Electrolytic)
Gordon K. Teal, Texas Instruments Inc., 6000 Lemmon Ave., Dallas 9, Texas (Electronics)

Battery Division Extended Abstracts Booklet

The Battery Division has prepared an extended abstracts booklet of the 28 papers presented at the fall meeting of the Society in Buffalo, October 6-10, 1957.

This bulletin is available at $2.00 per copy, and can be obtained by sending a check to the Secretary of the Battery Division:

E. J. Ritchie
Eagle-Picher Research Lab.
Joplin, Mo.

Reinstatement and Transfer from Active to Active Sponsored by a Sustaining Member

Charles H. Moore, P. R. Mallory & Co., Inc., 3029 E. Washington St., Indianapolis, Ind. (Electrothermics & Metallurgy)

Active Members

George E. Adam, American Potash & Chemical Corp.; Mail add: Box 1196, Trona, Calif. (Industrial Electrolytic)
Jules Andrus, Bell Telephone Labs., Inc., 2C-337, Murray Hill, N. J. (Electronics)
Gerald M. Bestler, Minneapolis-Honeywell Regulator Co., 2835 Nicollet Ave., Minneapolis 8, Minn. (Electronics)
J. Daniel Bode, J. and L. Steel Corp.; Mail add: 940 Washington Rd., Pittsburgh 28, Pa. (Corrosion, Electrodeposition)
Eugene C. Bosl, Hanson-Van Winkle-Munning Co., 717 E. 61 St., Los Angeles 1, Calif. (Electrodeposition)
T. Gerald Branin, Radio Corp. of America, New Holland Pike, Lancaster, Pa. (Electrodeposition)
Donald B. Burkhardt, E. I. du Pont de Nemours & Co. Inc.; Mail add: 20 Monterry Dr., Brookside, Newark, Del. (Electronics, Industrial Electrolytic)
John A. Ciano, Raytheon Manufacturing Co.; Mail add: 87 Swains Pond Ave., Melrose, Mass. (Electrodeposition, Electronics, Electrothermics & Metallurgy)
H. Irving Crane, Clevite Transistor Products; Mail add: 38 Clark Lane, Waltham 54, Mass. (Electronics)
Georges Destriau, Laboratoire de Physique IV, Faculte des Sciences, 12 rue Cuvier, Paris 5, France (Electronics)
Robert Ellison, Consolidated Mining and Smelting Co. of Canada, Ltd., P. O. Box 1030, Place d'Armes, Montreal 1, Que., Canada (Electronics, Electrothermics & Metallurgy, Industrial Electrolytic)
Paul R. Graham, American Potash & Chemical Corp.; Mail add: 8713½ W. Knoll Dr., Los Angeles 46, Calif. (Electrodeposition, Electrothermics & Metallurgy, Industrial Electrolytic)
Thomas J. Hennigan, Naval Ordnance Lab.; Mail add: 900 Fairoak Ave., Chillum Terrace, Md. (Battery)
Jan J. Hermans, State University, Leiden; Mail add: 31, Hugo de Grootstraat, Leiden, Netherlands (Theoretical Electrochemistry)
Robert L. Hibbard, Pure Carbon Co., St. Marys, Pa. (Electrothermics & Metallurgy, Theoretical Electrochemistry)
Kenneth B. Higbie, Beryllium Corp.; Mail add: Temple Inn, Temple, Pa. (Electrothermics & Metallurgy)
Emanuel C. Hirakis, Horizons Inc.; Mail add: 318 E. 330 St., Willowick, Ohio (Electrodeposition, Electrothermics & Metallurgy)
Andre Hone, Ecole Polytechnique; Mail add: 625 Berwick, Town of Mount Royal, Que., Canada (Theoretical Electrochemistry)
Eugene H. Howard, Aluminum Co. of America; Mail add: 2887 Seventh St. Rd., New Kensington, Pa. (Industrial Electrolytic)
William P. James, Wai Met Alloys Co., 1999 Guoin St., Detroit 7, Mich. (Electrothermics & Metallurgy)
Menutcher F. Kiachif, Carborundum Co.; Mail add: 48 Roycroft Blvd., Snyder 26, N. Y. (Electrothermics & Metallurgy)
Robert L. Koffler, Davison Chemical Co.; Mail add: 3931 Duvall Ave., Baltimore 16, Md. (Industrial Electrolytic)
George R. Krsek, Merck & Co., Inc., Rahway, N. J. (Electronics)
Jerome Kuderna, Automatic Electric Co.; Mail add: 2836 No. Lotus Ave., Chicago 41, Ill. (Electrodeposition)
Walter C. Lamphier, Sprague Electric Co.; Mail add: Willow Lane, Williamstown, Mass. (Electric Insulation)
Charles Z. Leinkram, Tung-Sol Electric; Mail add: 97 Union Ave., Passaic, N. J. (Electronics)
Robert M. Little, Home Plating Co.; Mail add: 6363 Monitor Dr., Indianapolis, Ind. (Electrodeposition)
Lahmer Lynds, American Potash & Chemical Corp.; Mail add: 12518 Martha St., North Hollywood, Calif. (Theoretical Electrochemistry)
Clarence T. Marshall, Pittsburgh Coke & Chemical Co., Grant Bldg., Pittsburgh 19, Pa. (Electrodeposition, Electrothermics & Metallurgy, Industrial Electrolytic)
Shadburn Marshall, Air Reduction Co., Inc., Research Labs., Murray

Notice to Members

By now you have received your official voting ballot from Society Headquarters. If you have not already done so, please return the ballot by *December 15* so that your vote can be included in the final election count.

Hill, N. J. (Electrothermics & Metallurgy)

James W. Newsome, Aluminum Co. of America; Mail add: 7907 W. Washington St., Belleville, Ill. (Electronics)

Raymond C. Petersen, Sprague Electric Co.; Mail add: 32 Hoxsey St., Williamstown, Mass. (Electro-Organic, Theoretical Electrochemistry)

Thomas R. Pezzack, Electro Metallurgical Co.; Mail add: 805 Davenport Rd., Toronto 4, Ont., Canada (Industrial Electrolytic)

Pat R. Pondy, Bell Telephone Labs., Inc.; Mail add: 105 Tuttle Rd., Watchung, N. J. (Corrosion, Electronics, Electrothermics & Metallurgy)

James B. Ramsey, University of California, Dept. of Chemistry, Los Angeles 24, Calif. (Theoretical Electrochemistry)

Frank E. Robbins, Jr., B. E. Shlesinger, 1323 Lincoln-Alliance Bank Bldg., Rochester 4, N. Y. (Electro-Organic, Electrothermics & Metallurgy)

Thomas J. Rollins, Keldon Research Corp., Box 2555, Terminal Annex, Los Angeles 54, Calif. (Theoretical Electrochemistry)

Mario A. Sellani, Philco Corp.; Mail add: 1017 Delaware Ave., Lansdale, Pa. (Electrodeposition, Electronics, Theoretical Electrochemistry)

John W. Shea, National Carbon Co., Div. of Union Carbide, 30 E. 42 St., New York 17, N. Y. (Electrothermics & Metallurgy)

Marshall Sittig, American Lithium Institute, Inc.; Mail add: P. O. Box 549, Princeton, N. J. (Industrial Electrolytic)

Allen L. Solomon, Sylvania Electric Products Inc., 35-22 Linden Place, Flushing 54, N. Y. (Electronics)

Victor R. Spironello, Pittsburgh Metallurgical Co., Inc.; Mail add: Box 292, Calvert City, Ky. (Electrothermics & Metallurgy)

Edgel P. Stambaugh, Battelle Memorial Institute; Mail add: 4923 Solar Dr., Columbus 14, Ohio (Electrothermics & Metallurgy)

Hamburg Tang, Alpha Metals Inc.; Mail add: 135 W. 84 St., New York, N. Y. (Electronics, Electrothermics & Metallurgy)

Hobart Tipton, Radio Corp. of America, Semiconductor Div.; Mail add: 24 Holmes Oval, New Providence, N. J. (Electronics)

Tadao Tomonari, Yokohama National University; Mail add: 1 Gumyoji-cho, Minami-ku, Yokohama, Naka Post Office, Japan (Electrothermics & Metallurgy, Industrial Electrolytic, Theoretical Electrochemistry)

ECS Membership Statistics

The following three tables give breakdown of membership as of October 1, 1957. The Secretary's Office feels that a regular accounting of membership will be very stimulating to membership committee activities. In Table I it should be noted that the totals appearing in the right-hand column are *not* the sums of the figures in that line since members belong to more than one Division and, also, because Sustaining Members are not assigned to Divisions. But the totals listed are the total membership in each Section. In Table I, Sustaining Members have been credited to the various Sections.

Table I. *ECS Membership by Sections and Divisions*

Section	Division: Battery	Corrosion	Electric Insulation	Electro-deposition	Electronics	Electro-Organic	Electrothermics & Met.	Industrial Electrolytic	Theoretical Electrochem.	No Division	Total as of 10/1/57	Total as of 4/1/57	Net Change
Boston	14	30	5	34	44	8	20	14	22	8	126	117	+ 9
Chicago	14	38	4	46	18	5	13	15	20	13	115	113	+ 2
Cleveland	57	38	2	50	41	12	25	32	43	15	204	195	+ 9
Columbus, Ohio	1	13	0	13	4	2	21	2	8	6	44	0	+44
Detroit	8	17	5	43	6	8	5	5	20	20	82	80	+ 2
India	8	6	2	16	5	5	7	13	9	3	33	27	+ 6
Indianapolis	10	6	4	9	9	4	5	2	5	2	37	0	+37
Midland	5	17	0	5	2	2	7	17	10	3	44	41	+ 3
Mohawk-Hudson	5	15	15	9	13	1	7	3	11	6	56	0	+56
New York	75	104	22	138	116	33	68	65	96	45	479	447	+32
Niagara Falls	11	23	0	21	3	6	75	60	23	23	168	156	+12
Ontario-Quebec	10	22	0	14	2	3	33	25	7	15	72	64	+ 8
Pacific Northwest	4	15	0	11	1	1	5	11	8	10	46	47	− 1
Philadelphia	24	30	4	39	55	16	20	18	50	29	171	155	+16
Pittsburgh	4	49	3	31	25	5	35	19	37	10	134	117	+17
San Francisco	5	15	2	17	12	3	13	23	21	4	63	60	+ 3
Southern Calif.-Nevada	16	20	1	24	24	3	13	19	20	10	94	87	+ 7
Washington-Baltimore	32	42	9	39	22	3	10	12	30	7	127	117	+10
U. S. Non-Section	52	92	13	89	62	40	55	76	110	37	396	486	−90
Foreign Non-Section	39	56	6	62	29	27	37	59	68	55	220	212	+ 8
Total as of Oct. 1	394	648	97	710	493	187	474	490	618	321	2711		
Total as of April 1	377	618	86	680	411	183	426	454	578	321		2505	

Table II. *ECS Membership by Grade*

	Total as of 10/1/57	Total as of 4/1/57	Net Change
Active	2413	2142	+271
Delinquent	70	146	− 76
Active Representative Patron Members	8	8	0
Active Representative Sustaining Members	64	60	+ 4
Total Active Members	2555	2356	+199
Life	15	15	0
Emeritus	47	44	+ 3
Associate	34	28	+ 6
Student	55	57	− 2
Honorary	5	5	0
	2711	2505	+206

The figures pertaining to Patron and Sustaining Member Representatives have been added to reflect reclassifications and changes in membership status.

Table III. *ECS Patron and Sustaining Membership*

	Total as of 10/1/57	Total as of 4/1/57	Net Change
Patron Member Companies	4	4	0
Sustaining Member Companies	123	119	+ 4

By action of the Board of Directors of the Society, all prospective members must include first year's dues with their applications for membership.

Also, please note that, if sponsors sign the application form itself, processing can be expedited considerably.

Charles W. Tullock, Du Pont Experimental Station; Mail add: 2202 W. 18 St., Wilmington, Del. (Electro-Organic)

Michael G. Vucich, Weirton Steel Co., Quality Control Bldg., Weirton, W. Va. (Electrodeposition, Industrial Electrolytic, Theoretical Electrochemistry)

Charles F. Wahlig, E. I. du Pont de Nemours & Co., Inc., Experimental Station, Wilmington, Del. (Electronics)

Franklin H. Wells, A. M. P., Inc., Harrisburg, Pa. (Electric Insulation)

Jack M. Wilson, Standard Telecommunication Labs. Ltd., Progress Way, Gt. Cambridge Rd., Enfield, Middlesex, England (Electronics)

William R. Wolfe, Jr., E. I. du Pont de Nemours & Co., Inc., Chemical Dept., Experimental Station, Wilmington, Del. (Industrial Electrolytic, Theoretical Electrochemistry)

Student Associate Members

Jonathan Booker, Western Reserve University; Mail add: 9711 Parkgate Ave., Cleveland 8, Ohio (Electrodeposition)

Wayne J. Subcasky, University of Illinois; Mail add: 606 W. Ohio St., Urbana, Ill. (Battery, Theoretical Electrochemistry)

Associate Members

Richard E. Edgington, Good-All Electric Manufacturing Co.; Mail add: 614 Student Dr., Ogallala, Nebr. (Electrodeposition, Electronics, Industrial Electrolytic)

W. Douglas Goode, Jr., Battelle Memorial Institute, 505 King Ave., Columbus 1, Ohio (Corrosion)

Rebecca Ann Parker, National Bureau of Standards, Washington 25, D. C. (Theoretical Electrochemistry)

Reinstatement to Active Membership

Nicholas Carabitses, Hudson & Carabitses Engineers; Mail add: 31 Compton St., Boston 18, Mass. (Battery, Electric Insulation, Electronics)

Reinstatements and Transfers from Student To Active Membership

Edward Hillner, Westinghouse Electric Corp.; Mail add: 5334 Keeport Dr., Pittsburgh 36, Pa. (Corrosion, Electrothermics & Metallurgy, Theoretical Electrochemistry)

Gerald S. Lozier, Radio Corp. of America Labs.; Mail add: 75 Jefferson Rd., Princeton, N. J. (Battery)

Anand Mohan, Ms. M. L. Alkan Ltd.; Mail add: 17 Hartington Rd., London W. 13, England (Corrosion, Electrodeposition, Theoretical Electrochemistry)

Transfers from Student Associate to Associate Membership

Jerry C. Laplante, Engelhard Industries, Inc.; Mail add: #4 Llewellyn Gates, Hutton Ave., West Orange, N. J. (Electrodeposition, Electrothermics & Metallurgy)

Subbaraya Sathyanarayana, Central Electrochemical Research Institute, Karaikudi, S. Rly, India (Battery, Corrosion, Electrodeposition, Electro-Organic, Electrothermics & Metallurgy, Industrial Electrolytic)

1958 Bound Volume

Members and subscribers who wish to receive bound copies of Vol. 105 (for 1958) can receive the volume for the low, prepublication price of $6.00 if their orders are received at Society Headquarters, 1860 Broadway, New York 23, N. Y., *by December 1.* After that date members will be charged $12.00, and nonmembers, including subscribers, $18.00.

Bound volumes are *not* offered independently of JOURNAL subscription.

Announcements from Publishers

Free Price List of AEC Reports Issued

A new free price list of Atomic Energy Commission unclassified research reports for sale by the Office of Technical Services, U. S. Dept. of Commerce, is now available from OTS on request.

This cumulative listing of the more than 4500 AEC reports in the OTS collection includes new documents acquired since December 31, 1956. To obtain the new list, request AEC Research Reports Price List No. 28 from OTS, U. S. Dept. of Commerce, Washington 25, D. C.

Price lists are issued semiannually, and the next list will be available in February 1958. OTS also publishes **U. S. Government Research Reports,** a monthly publication which lists new research reports as soon as they are released by the AEC. It also describes reports from the Army, Navy, Air Force, and other Government agencies available to the public through OTS. This publication may be obtained on a subscription basis from the Superintendent of Documents, U. S. Government Printing Office, Washington 25, D. C., at $6.00 a year.

Titanium Metallurgy Studies Released for Industry Use

Three reports of research in titanium metallurgy for the Armed Forces have been released to industry through the Office of Technical Services, U. S. Dept. of Commerce, Washington 25, D. C. They are briefly described below.

Research on Intermetallic Containers for Melting Titanium, W. B. Crandall and others, State University of New York College of Ceramics at Alfred University, for Wright Air Development Center, U. S. Air Force, Feb. 1957. 39 pages, $1.00 (Order PB 121948 from OTS).

The Preparation and Properties of Titanium Tetrabromide, J. M. Blocher, Jr., and others, Battelle

Notice to Subscribers

Your subscription to the JOURNAL of The Electrochemical Society will expire on *December 31, 1957.* Avoid missing any issue. Send us your remittance now in the amount of $18.00 for your 1958 subscription. (Subscribers located outside the United States must add $1.00 to the subscription price for postage, and payment must be made by Money Order or New York draft, not local check.) An expiration notice has been mailed to all subscribers.

A bound volume of the 1958 JOURNALS can be obtained at a prepublication price of $6.00 by adding this amount to your remittance. However, no orders will be accepted at this rate after *December 1, 1957,* when the price will be increased to $18.00 subject to prior acceptance. Bound volumes are *not* offered independently of your JOURNAL subscription.

Memorial Institute, for Office of Naval Research, July 1955. 30 pages, $1.00 (Order PB 121542 from OTS). Since the literature on the compounds of titanium is incomplete, progress is hindered by the unavailability of reliable values for some of the physical and thermodynamic properties of the titanium halides which represent potential intermediates in the extractive metallurgy of the metal. The work covered in this report is part of a project to establish such values. High-purity $TiBr_4$ was prepared by direct synthesis with high-purity materials, followed by distillation.

Phase and Free Energy Relationships in the System Titanium-Zirconium-Oxygen, M. Hoch and others, Ohio State University Research Foundation, for Wright Air Development Center, U. S. Air Force, Jan. 1957. 32 pages, $1.00 (Order PB 121981 from OTS). In this research, phase relationships in the system at 1500°C were determined by x-ray. All of the one-, two-, and three-phase regions in the diagram were located, except in the near vicinity of the binary systems Zr-O and TiO_2-ZrO_2. The stabilization of cubic ZrO_2 by TiO was confirmed and the approximate limits of the cubic ZrO_2 phase were located.

Chemical Analysis Technique for Newer Alloying Metals

Improved methods for chemical analysis of the newer alloying metals are described in a report of Air Force research just released for industry use through the Office of Technical Services, U. S. Dept. of Commerce, Washington 25, D. C. Another report on the development of stainless steel compositions with better hot-strength properties also is available.

Tantalum Determination, R. W. Moshier and J. E. Schwarberg, Wright Air Development Center, U. S. Air Force, June 1956. 39 pages, $1.00 (Order PB 121819 from OTS). This report describes methods developed for rapid, accurate, simple chemical analysis of the newer alloying metals. During this research, improved methods of separation of molybdenum plus tungsten from tantalum, niobium, titanium, and zirconium were developed. Another technique enables subsequent separation of tantalum from niobium, titanium, and zirconium and its quantitative determination. The developments grew out of studies on the organic reagents *N*-nitrosophenylhydroxylamine and *N*-benzoylphenylhydroxylamine for precipitation of metals.

Development of Lean-Alloy Chromium-Nickel Stainless Steels for High Temperature Use, Cornell Aeronautical Lab., Inc., for Bureau of Aeronautics, U. S. Navy, Dec. 1954. 86 pages, $2.25 (Order PB 121026 from OTS). This final report reviews development of modified chromium-nickel stainless steel compositions with improved hot-strength properties. Three titanium and titanium-boron stainless steels showed particular improvement in hot strength.

Electroplating Baths for Ultra-High-Strength Steels. Part 1—Use of Aliphatic Amino Acids in Cadmium Baths to Reduce Hydrogen Embrittlement, P. N. Vlannes, S. W. Strauss, and B. F. Brown, Naval Research Lab., March 1957. Order PB 121836 from OTS. 15 pages, 50 cents.

The results of research indicated that electroplating high-strength steel from an ammonical bath containing salts of amino acids results in markedly lower hydrogen embrittlement than plating from the standard cyanide bath.

Bibliography of Research on Deuterium and Tritium Compounds 1953 and 1954, National Bureau of Standards Circular 562, Supplement 1, issued July 15, 1957, 31 pages, 25 cents. (Order from Superintendent of Documents, U. S. Government Printing Office, Washington 25, D. C. NOTE: Foreign remittances must be in U. S. exchange and should include an additional one-fourth of the publication price to cover mailing costs.)

This Circular is a bibliography of 720 published articles on the properties of deuterium and tritium compounds for the years 1953 and 1954. It is divided into three sections; the first contains a bibliography and author index; the second, a subject index; and the third, a compound index.

Advertiser's Index

The Electrochemical Society

INSTRUCTIONS TO AUTHORS OF PAPERS

Address all correspondence to the Editor, JOURNAL OF THE ELECTROCHEMICAL SOCIETY, 1860 BROADWAY, NEW YORK 23, N. Y.

FORM

Manuscripts submitted for publication should be in triplicate to expedite review. They should be typewritten, double-spaced, with 2½-4 cm (1-1½ in.) margins.

Title should be brief, followed by the author's name and his business or university connection.

Abstract of about 100 words should state the scope of the paper and give a brief summary of results.

ILLUSTRATIONS

Drawings will be reduced to column width, 8.3 cm (3¼ in.), after reduction should have lettering at least 0.15 cm (1/16 in.) high. Original drawings in India ink on tracing cloth or white paper are preferred. Curves may be drawn on coordinate paper only if the paper is ruled in blue. All lettering must be of lettering-guide quality. See sample drawing on reverse page.

Photographs must be glossy prints and mounted flat.

Captions for all figures must be included on a separate sheet. Captions and figure numbers should not appear in the body of the figure.

General—Figures should be used only when necessary. Omit drawings or photographs of familiar equipment. Figures from other publications are to be used only when the publication is not readily available, and should always be accompanied with written permission for reprinting.

REFERENCES

Literature and patent references should be listed at the end of the paper on a separate sheet, in the order in which they are cited. They should be given in the style adopted by *Chemical Abstracts*. For example:

R. Freas, *Trans. Electrochem. Soc.*, **40**, 109 (1921).

H. T. S. Britton, "Hydrogen Ions," Vol. **1**, p. 309, D. Van Nostrand Co., New York (1943).

H. F. Weiss (To Wood Conversion Co.), U. S. Pat. 1,695,445, Dec. 18, 1928.

UNITS OF MEASUREMENT

Metric units should be used throughout but, where desirable, English units may be given in parentheses.

Corrosion rates in the metric system should preferably be expressed as milligrams per square decimeter per day (mdd), and in the English system as inches penetration per year (ipy).

As regards algebraic signs of potentials, the standard electrode potential for $Zn \rightarrow Zn^{++} + 2e$ is negative; for $Cu \rightarrow Cu^{++} + 2e$, positive.

ABBREVIATIONS

Abbreviations should conform with the American Standards Association's list of "Abbreviations for Scientific and Engineering Terms."

GENERAL

Authors should be as brief as is consistent with clarity, and must omit all material which can be regarded as familiar to specialists in the particular field.

The use of proprietary names, trade-marks, and trade names should be avoided if possible. If used, these should be capitalized so that the owner's legal rights are not jeopardized.

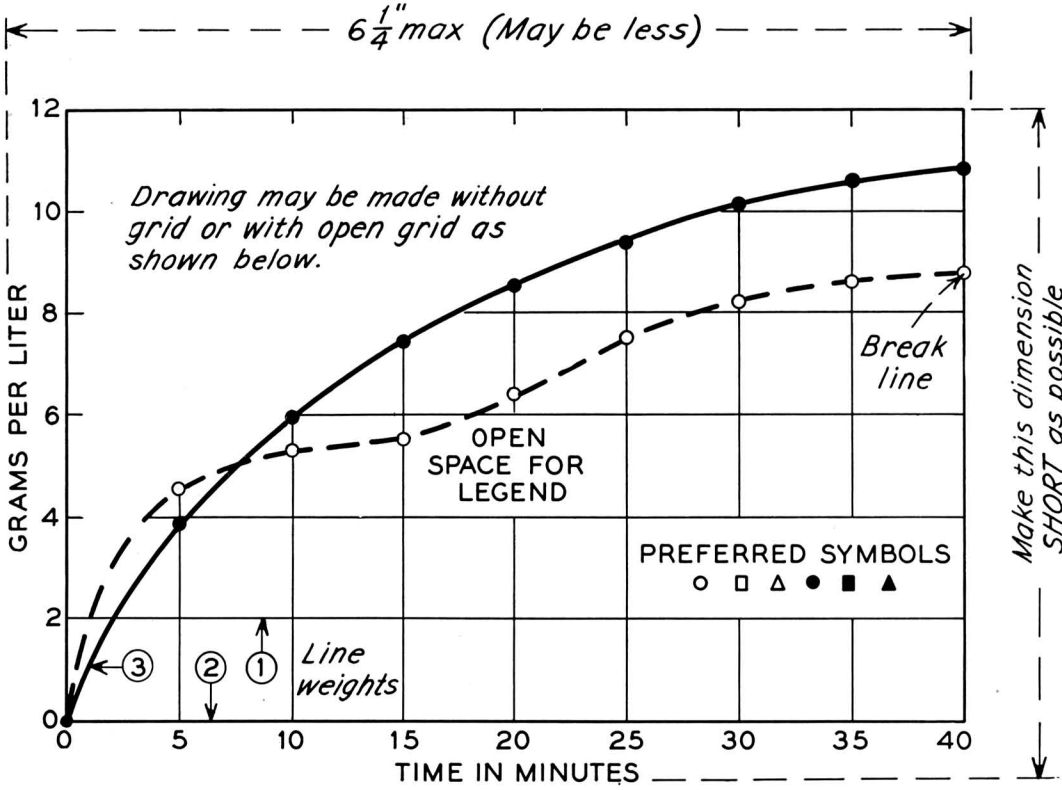

Remarks: Line weight ② is used for borders and zero lines. When several curves are shown, each may be numbered and described in the caption. Lettering is approx. 1/8".

SAMPLE CURVE DRAWING FOR REDUCTION TO $\frac{1}{2}$ SIZE

The Electrochemical Society

Patron Members

Aluminum Co. of Canada, Ltd., Montreal, Que., Canada
International Nickel Co., Inc., New York, N. Y.
Union Carbide Corp.
Divisions:
Electro Metallurgical Co., New York, N. Y.
National Carbon Co., New York, N. Y.
Westinghouse Electric Corp., Pittsburgh, Pa.

Sustaining Members

Air Reduction Co., Inc., New York, N. Y.
Ajax Electro Metallurgical Corp., Philadelphia, Pa.
Allied Chemical & Dye Corp.
General Chemical Div., Morristown, N. J.
Solvay Process Div., Syracuse, N. Y. (3 memberships)
Alloy Steel Products Co., Inc., Linden, N. J.
Aluminum Co. of America, New Kensington, Pa.
American Machine & Foundry Co., Raleigh, N. C.
American Metal Co., Ltd., New York, N. Y.
American Platinum Works, Newark, N. J. (2 memberships)
American Potash & Chemical Corp., Los Angeles, Calif. (2 memberships)
American Zinc Co. of Illinois, East St. Louis, Ill.
American Zinc, Lead & Smelting Co., St. Louis, Mo.
American Zinc Oxide Co., Columbus, Ohio
Auto City Plating Co. Foundation, Detroit, Mich.
Bart Manufacturing Co., Bellville, N. J.
Bell Telephone Laboratories, Inc., New York, N. Y. (2 memberships)
Bethlehem Steel Co., Bethlehem, Pa. (2 memberships)
Boeing Airplane Co., Seattle, Wash.
Burgess Battery Co., Freeport, Ill. (4 memberships)
Canadian Industries Ltd., Montreal, Que., Canada
Carborundum Co., Niagara Falls, N. Y.
Chrysler Corp., Detroit, Mich.
Columbia-Southern Chemical Corp., Pittsburgh, Pa.
Consolidated Mining & Smelting Co. of Canada, Ltd., Trail, B. C., Canada (2 memberships)
Corning Glass Works, Corning, N. Y.
Cramet, Inc., Chattanooga, Tenn.
Crane Co., Chicago, Ill.
Diamond Alkali Co., Painesville, Ohio (2 memberships)
Dow Chemical Co., Midland, Mich.
Wilbur B. Driver Co., Newark, N. J. (2 memberships)
E. I. du Pont de Nemours & Co., Inc., Wilmington, Del.
Eagle-Picher Co., Chemical Div., Joplin, Mo.
Eaton Manufacturing Co., Stamping Div., Cleveland, Ohio
Electric Auto-Lite Co., Toledo, Ohio
Electric Storage Battery Co., Philadelphia, Pa.
The Eppley Laboratory, Inc., Newport, R. I. (2 memberships)
Food Machinery & Chemical Corp.
Becco Chemical Div., Buffalo, N. Y.
Westvaco Chlor-Alkali Div., South Charleston, W. Va.
Ford Motor Co., Dearborn, Mich.
General Electric Co., Schenectady, N. Y.
Chemistry & Chemical Engineering Component, General Engineering Lab.
Chemistry Research Dept.
Metallurgy & Ceramics Research Dept.
General Motors Corp.
Brown-Lipe-Chapin Div., Syracuse, N. Y. (2 memberships)
Guide Lamp Div., Anderson, Ind.
Research Laboratories Div., Detroit, Mich.
Gillette Safety Razor Co., Boston, Mass.
Gould-National Batteries, Inc., Depew, N. Y.
Graham, Crowley & Associates, Inc., Chicago, Ill.
Great Lakes Carbon Corp., New York, N. Y.
Hanson-Van Winkle-Munning Co., Matawan, N. J. (3 memberships)
Harshaw Chemical Co., Cleveland, Ohio (2 memberships)
Hercules Powder Co., Wilmington, Del.
Hooker Electrochemical Co., Niagara Falls, N. Y. (3 memberships)
Houdaille-Hershey Corp., Detroit, Mich.
International Minerals & Chemical Corp., Chicago, Ill.
Jones & Laughlin Steel Corp., Pittsburgh, Pa.
Kaiser Aluminum & Chemical Corp.
Chemical Research Dept., Permanente, Calif.
Div. of Metallurgical Research, Spokane, Wash.
P. R. Mallory & Co., Indianapolis, Ind.
McGean Chemical Co., Cleveland, Ohio
Merck & Co., Inc., Rahway, N. J.
Metal & Thermit Corp., Detroit, Mich.
Minnesota Mining & Mfg. Co., St. Paul, Minn.
Monsanto Chemical Co., St. Louis, Mo.
National Cash Register Co., Dayton, Ohio
National Lead Co., New York, N. Y.
National Research Corp., Cambridge, Mass.
Norton Co., Worcester, Mass.
Olin Mathieson Chemical Corp., Niagara Falls, N. Y.
Aviation Div. (2 memberships)
Industrial Chemicals Div. (2 memberships)
Pennsylvania Salt Manufacturing Co., Philadelphia, Pa.
Philips Laboratories, Inc., Irvington-on-Hudson, N. Y.
Poor & Co.
Promat Div., Waukegan, Ill.
Potash Co. of America, Carlsbad, N. Mex.
Radio Corp. of America, Harrison, N. J.
Ray-O-Vac Co., Madison, Wis.
Reynolds Metals Co., Richmond, Va.
Shawinigan Chemicals Ltd., Montreal, Que., Canada
Speer Carbon Co.
International Graphite & Electrode Div., St. Marys, Pa. (2 memberships)
Sprague Electric Co., North Adams, Mass.
Stackpole Carbon Co., St. Marys, Pa. (2 memberships)
Stauffer Chemical Co., Henderson, Nev., and New York, N. Y. (2 memberships)
Sylvania Electric Products Inc., Bayside, N. Y. (2 memberships)
Sarkes Tarzian, Inc., Bloomington, Ind.
Tennessee Products & Chemical Corp., Nashville, Tenn.
Texas Instruments, Inc., Dallas Texas
Titanium Metals Corp. of America, Henderson, Nev.
Udylite Corp., Detroit, Mich. (4 memberships)
Vanadium Corp. of America, New York, N. Y.
Victor Chemical Works, Chicago, Ill.
Wagner Brothers, Inc., Detroit, Mich.
Weirton Steel Co., Weirton, W. Va.
Western Electric Co., Inc., Chicago, Ill.
Wyandotte Chemicals Corp., Wyandotte, Mich.
Yardney Electric Corp., New York, N. Y.

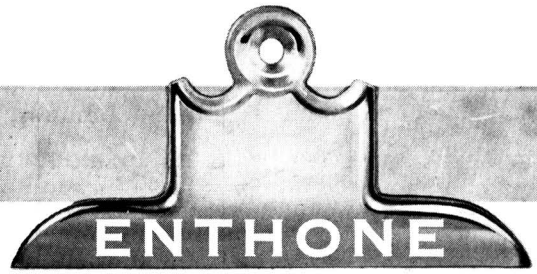

Which of ENTHONE's metal-finishing developments do you need?

- ☐ **ENSTRIP METAL STRIPPERS**—Products for quickly and economically stripping defective plated coatings, coatings from plating racks, excess solder, silver brazing metal and metal smuts, without attacking base metals in any way.
- ☐ **ENAMEL STRIPPERS**—A wide variety of strippers are maintained "in stock". In addition, Enthone will be glad to study your requirements and develop the precise stripper you need to meet your requirements.
- ☐ **"ALUMON"**—A product of highest-purity chemicals for preparing aluminum for plating. Used successfully for over 13 years by hundreds of manufacturers, Alumon is economical and easy to use.
- ☐ **EBONOL® METAL BLACKENERS**—Products for blackening copper, brass and other copper alloys; iron and steel; zinc plate and zinc castings.
- ☐ **RUST REMOVERS**—A complete line of chemicals for the removal of rust and scale. Both alkaline and acid compounds are available.
- ☐ **CLEANERS & DEGREASERS**—New alkaline and emulsion-type cleaners for removing grease, oil, and solid dirt from metals.
- ☐ **RUSTPROOFING COMPOUNDS**—Rustproofing oils, waxes and chemical compounds for protecting steel against rust in salt spray, high humidity and outdoors.
- ☐ **ZINC & CADMIUM CONVERSION COATINGS**—Enthox® salts produce iridescent, gold colored chromate coatings with high salt-spray resistance. Very simple and economical to use.

Remember — your metal finishing problem is our business! Since Enthone has been studying these problems, and developing their solutions, for 20 years, chances are we have the answer to your problem in stock. On the other hand, if yours is an unusual requirement, we will be glad to study your needs and develop the precise chemical for the purpose. Just send us a letter, outlining the problem or process—and enclose a sample of the metal concerned, if possible.

Write to Dept. J-11.

DISTRIBUTION AND SERVICE THROUGHOUT THE UNITED STATES, CANADA, MEXICO, BRAZIL AND EUROPE

PRODUCTS OF *Enthonics* THE SCIENTIFIC SOLUTION OF METAL FINISHING PROBLEMS

ENTHONE

ENTHONE
INCORPORATED
442 ELM STREET. NEW HAVEN 11, CONN.
Metal Finishing Processes • Electroplating Chemicals

SUBSIDIARY OF AMERICAN SMELTING AND REFINING COMPANY